EXPERIMENTAL INVESTIGATION ON THERMOPHYSICAL PROPERTIES OF NANOFLUIDS

A thesis submitted
in partial fulfilment of the requirements for
the award of degree of

Masters of Engineering
in
Thermal Engineering

Submitted by

Mahesh Juneja
Regd. No. 801083013

Under the guidance of

Dr. D. Gangacharyulu
Professor
Department of Chemical Engineering

DEPARTMENT OF MECHANICAL ENGINEERING

THAPAR UNIVERSITY

(Established under section 3 of UGC Act, 1956)

PATIALA -147001, INDIA

July, 2012

DECLARATION

I hereby declare that the work being presented in the thesis report entitled **Experimental Investigation on Thermophysical Properties of Nanofluids** by me in partial fulfillment of the requirements for the award of degree of Masters of Engineering in Thermal Engineering, from Department of Mechanical Engineering, Thapar University, Patiala is an authentic record of my own work carried under the supervision of Dr. D. Gangacharyulu, Professor, Department of Chemical Engineering, Thapar University, Patiala. The matter presented in this report has not been submitted in any other University/Institute for the award of Masters of Engineering or any other degree.

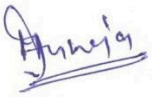

(Mahesh Juneja)
Regd. No. 801083013

CERTIFICATE

This is to certify that the thesis report entitled **Experimental Investigation on Thermophysical Properties of Nanofluids** being submitted by **Mr. Mahesh Juneja** in partial fulfillment of the requirements for the award of degree of **Master of Engineering** in **Thermal Engineering** in the **Department of Mechanical Engineering, Thapar University, Patiala**, is a record of candidate's own work carried out by him under my supervision. To the best of our knowledge, the content of this thesis does not form a basis for the award of any other degree.

D. Gangacharyulu 13/7/12

(D. GANGACHARYULU)
Professor
Department of Chemical Engineering
Thapar University, Patiala

(Countersigned by)

(Ajay Batish)
Professor & Head
Department of Mechanical Engineering
Thapar University, Patiala

(S.K. Mohapatra)
Dean of Academics Affairs
Thapar University, Patiala

ACKNOWLEDGEMENTS

I would like to express my deep sense of gratitude to Dr. D. Gangacharyulu, Professor, Department of Chemical Engineering, Thapar University, Patiala for his invaluable suggestions, excellent supervision, constant encouragement, thought provoking discussions and unabashed inspiration in nurturing the work and during the preparation of manuscript throughout the research work.

I take my opportunity to express my heartfelt adulation and gratitude to Dr. Bhupendrakumar Chudasama, Assistant Professor, School of Physics & Materials Science, Thapar University, Patiala for his unreserved guidance, constructive suggestion and carrying out all particle size measurement with his expert guidance of using Origin Pro Software during the preparation of manuscript.

My sincere thanks to Dr. Ajay Batish, Professor & Head, Department of Mechanical Engineering, Thapar University, Patiala and Dr. S.K. Mohapatra, Dean of Academic Affairs, Thapar University, Patiala for providing me with the opportunity to conduct this work and bring it out in the present form.

I offer special regards to Ms. Harkirat, Mr. Toyesh Upriti, Research Scholars, Department of Chemical Engineering, Thapar University, Patiala and Mr. Bhupender Pal, Ms. Pankil Singla, Research Scholars, School of Chemistry and Biochemistry, Thapar University, Patiala for providing their immense support in performing the experimental work throughout my research work.

I am grateful to Mr. Jaswinder Singh, Laboratory Technician of Centre of Information and Technology Management, Mr. Amit Kamboj, Laboratory Attendant and Mr. Shubham Kaushal, Laboratory Technician of Department of Chemical Engineering, Thapar University, Patiala for providing me all the lab facilities for successful completion of the work.

I would also like to thank my friends (Ms. Arshdeep Kaur, Mr. Pankaj Sharma, Mr. Sandeep Kharb and Mr. Jaggi Dhiman) for their kind support and encouragement.

The greatest thanks go to my family members; Sh. Yashpal Juneja (father), Smt. Sarla Juneja (mother) and Ms. Archna Juneja (sister) for their infinite support at each and every part of my life. Above all, I express my indebtedness to the "ALMIGHTY" for all His blessing and kindness.

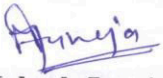

(Mahesh Juneja)

ABSTRACT

Heat transfer fluids have inherently low thermal conductivity that greatly limits the heat exchange efficiency. While the effectiveness of extending surfaces and redesigning heat exchange equipment to increase the heat transfer rate has reached a limit, many researchers made an attempt to improve the thermal transport properties of the fluids by adding more thermally conductive solids into liquids. Liquid dispersions of nanoparticles, which have been termed "nanofluids", exhibit substantially higher thermal conductivities than those of the corresponding base fluids.

Various aspects of nanofluids including synthesis, potential applications, experimental and analytical studies on the thermal conductivity, viscosity and density, particle size analysis have been carried out. For nanofluids, nanoparticles of Alumina (Al_2O_3) and the base fluids, such as, distilled water, ethylene glycol, and a mixture of distilled water & ethylene glycol are used. The volume fractions of nanoparticles used are 0.1%, 0.25%, 0.50% and 1.0%. Thermal conductivity is measured by 'KD2 pro thermal property analyzer'. Viscosity and density are measured by Ubbelohde viscometer and pycnometer, respectively. Particle size analysis of nanofluids is characterized by using Brookhaven particle size analyzer.

Results show that thermal conductivity increases with nanoparticles concentration as well as with the temperature. Whereas, viscosity and density decreases with temperature and increases with nanoparticles concentration. The particle size analysis shows that agglomeration increases with diluting the sample. It means, towards higher concentration, agglomeration decreases. In the following table, the percentage increase in density, viscosity and thermal conductivity and variation in mean diameter for different volume fraction is given.

Sr. No.	Alumina and distilled water based nanofluids				Alumina and ethylene glycol based nanofluids				Alumina and distilled water (75%) and ethylene glycol (25%) based nanofluids			
	0.1%	0.25%	0.50%	1.0%	0.1%	0.25%	0.50%	1.0%	0.1%	0.25%	0.50%	1.0%
Percentage increase in density	0.9	1.52	2.47	4.0	0.75	1.47	2.94	5.6	0.76	1.62	2.53	4.04
Percentage increase in viscosity	4.09	18	27.9	60	7.89	17.04	26.30	40.30	4.96	8.78	13.21	21.33
Percentage increase in thermal conductivity	0.65	2.1	3.27	5.0	0.40	1.19	3.47	6.72	0.42	0.82	2.02	3.76
Increase in mean diameter, nm	146	160	136	106	144	141	131	100	889	641	442	468

More theoretical and experimental studies are needed to understand the thermophysical properties and heat transfer characteristics of nanofluids and identify new applications of these fields.

CONTENTS

List of Figures

List of Tables

Nomenclature

Acronyms and abbreviations:	
CHF	Critical heat flux
CNTs	Carbon nanotubes
CVD	Chemical vapour deposition
CTAB	Cetyltrimethylammoniumbromide
DIW	De-ionized water
DW	Distilled water
EG	Ethylene glycol
EO	Engine oil
IGC	Inert-gas condensation
MWNTs	Multi walled carbon nanotubes
PO	Pump oil
SANSS	Submerged arc nanoparticles synthesis system
SDS	Sodium dodecyl sulphate
VEROS	Vacuum evaporation on to running oil substrate

Symbols

Symbols	**Item description**	**Dimensions**
β_{eff}	Thermal expansion coefficient of nanofluids	K^{-1}
C_{eff}	Specific heat of nanofluids	kJ/ (kg-K)
ρ	Density	kg/m^3
k	Thermal conductivity	W/(m-K)
k_p	Particle thermal conductivity	W/(m-K)
k_b	Base fluid thermal conductivity	W/(m-K)
k_{eff}	Effective thermal conductivity	W/(m-K)
h	Convective heat transfer coefficient	$W/(m^2K)$
α	Thermal diffusivity	m^2/sec
μ	Viscosity	cP

t	Time	seconds
T	Temperature	°C
Hz	Frequency	hertz
W	Energy	Watt
K_B	Boltzmann constant	J/K
K	Temperature	Kelvin
ml	Volume	Millilitre
lph	Volume flow rate	Litre per hour
gm.	Grams	Dimensionless
kg	Kilogram	Dimensionless
m	Metre	Dimensionless
cm	Centimetre	Dimensionless
mm	Millimetre	Dimensionless
µm	Micrometer	Dimensionless
nm	Nanometer	Dimensionless
%	Percentage	Dimensionless
∅	Volume fraction	Dimensionless
s^{-1}	Shear rate	Dimensionless
ppm	Parts per million	Dimensionless
Nu	Nussult number	Dimensionless
Pr	Prandtl number	Dimensionless
Re	Reynolds number	Dimensionless
nf	Nanofluid	Dimensionless
bf	Basefluid	Dimensionless
pH	Potential of Hydrogen	Dimensionless

Chemical formulae

Symbols	Item description
Ag	Silver
Au	Gold
Al_2O_3	Aluminium oxide
AlN	Aluminium nitride
Cu	Copper
CuO	Copper oxide
$CuSO_4.5H_2O$	Sulphate pentahydrate
H_2O	Water
Fe	Iron
$NaH_2PO_2.H_2O$	Sodium hypophosphite
Si	Silicon
SiC	Silicon carbide
SiN	Silicon nitride
SiO_2	Silicon di-oxide
TiC	Titanium carbide
TiO_2	Titanium oxide
ZnO	Zinc oxide

Chapter – 1
Introduction

1.1 Introduction

The main objective of this introductory chapter is to sketch out a big picture of the small world of nanofluids through a brief review of some historically major milestones such as development and concept of nanofluids, the production and performance of nanofluids, applications and benefits of nanofluids. Ultrahigh performance cooling is one of the most vital needs of the many industrial technologies. However, inherently low thermal conductivity is a primary limitation in developing energy efficient heat transfer fluids that are required for ultrahigh performance cooling. Nanofluids are being developed to achieve ultrahigh performance cooling and have the potential to be next generation coolants, thus representing a very significant and far reaching cooling technology for cross-cutting applications.

1.2 Why nanofluids

With ever increasing thermal loads due to smaller features of microelectronic devices and higher power outputs, thermal management of such devices to maintain their desired performance and durability is one of the most important technical issues in many high-technology industries such as microelectronics, transportations and manufacturing.

The conventional methods of increasing the cooling rate are to use extended heat transfer surfaces for exchanging heat with a heat transfer fluid. However, this approach requires an undesirable increase in the size of the thermal management systems. In addition, the inherently poor thermo physical properties of conventional heat transfer fluids such as water, ethylene glycol and engine oil greatly limit the cooling performance. Thus, conventional methods for increasing heat dissipation are not suitable to meet the demand of these high technology industries. So, there is need to develop advanced cooling techniques and innovative heat transfer fluids with better heat transfer performance than those presently available [1].

1.3 Development and concept of nanofluids

It is well known that at room temperature, metallic solids possess an order-of-magnitude higher thermal conductivity than fluids. The thermal conductivity of various materials is given by Table 1.1. The thermal conductivity of copper at room temperature is about 700 times greater than that of water and about 3000 times greater than that of engine oil. Therefore, the thermal conductivities of fluids containing suspended solid metallic or non-metallic (metallic oxide) particles would be expected to be significantly higher than those of conventional heat transfer fluids. The main problems of using such suspensions are the rapid setting of particles, clogging of flow channels and

increased pressure drop in the fluid. In contrast, nanoparticles due to their high surface to volume ratio can remain in suspension and thereby reduce erosion and clogging.

Table 1.1: Thermal conductivity of various materials [2] (At 300K)

Sr. No.	Item description	Material	Thermal conductivity, W/(m-k)
1.	Metallic solids	Silver	429
		Copper	401
		Aluminum	237
2.	Non metallic solids	Diamond	3300
		Carbon nanotubes	3000
		Silicon	148
		Alumina (Al_2O_3)	40
3.	Metallic liquids	Sodium at 644 K	72.3
4.	Non metallic liquids	Water	0.613
		Ethylene glycol	0.253
		Engine oil	0.145

Nanomaterials have unique mechanical, optical, electrical, magnetic and thermal properties. Nanofluids are engineered by suspending nanoparticles with average size below 100 nm in traditional heat transfer fluids such as water, oil and ethylene glycol. A very small amount of guest nanoparticles when dispersed uniformly and suspended stably in host fluids can provide dramatic improvements in the thermal properties of the host fluids.

Nanofluids (nanoparticles fluid suspension) is the term coined by Stephen U. S. Choi (1995) to describe this new class of nanotechnology based heat transfer fluids that exhibit thermal properties superior to those of their host fluids. Nanofluid technology, a new interdisciplinary field of great importance where nanoscience, nanotechnology and thermal engineering meet. The goal of Nanofluids is to achieve the highest possible thermal properties at the small possible concentration (preferably less than 1% by volume) by uniform dispersion and stable suspension of nanoparticles (preferably less than 10 nm) in host fluids [2]. The brief introduction of Prof. S.U.S. Choi has given in Annexure – 1.

1.4 Why nanofluids is better than microfluids

The basic concept of dispersing solids in fluids to enhance thermal conductivity is not new; it can be traced back to Maxwell [2]. Solid particles are added because they conduct heat much better than do liquids. The major problem with the use of large particles is the rapid settling of these particles in fluids. Other problems are abrasion and clogging. These problems are highly undesirable for many practical cooling applications. Nanofluids have pioneered in overcoming these problems by stably suspending in fluids nanometer-sized particles instead of millimetre- or micrometer-sized particles.

Compared with microparticles, nanoparticles stay suspended much longer and possess a much high surface area [2]. The surface/volume ratio of nanoparticles is 1000 times larger than that of microparticles. The high surface area of nanoparticles enhances the heat conduction of nanofluids since heat transfer occurs on the surface of the particle. The number of atoms present on the surface of nanoparticles, as opposed to the interior, is very large. Therefore, these unique properties of nanoparticles can be exploited to develop nanofluids with an unprecedented combination of the two features most highly desired for heat transfer systems: extreme stability and ultrahigh thermal conductivity.

Furthermore, because nanoparticles are so small, they may reduce erosion and clogging dramatically. Other benefits include decreased demand for pumping power, reduced inventory of heat transfer fluid, and significant energy saving. Stable suspension of small quantities of tiny particles makes conventional heat transfer fluids cool faster and thermal management systems smaller and lighter. The comparisons of microparticles and nanoparticles is given by Table 1.2 and shown by Fig. 1.1.

Table 1.2: Comparisons of microparticles and nanoparticles [2] (* at the same volume fraction)

Sr. No.	Characteristics	Microparticles	Nanoparticles
1.	Stability	Settle	Stable (remain in suspension almost indefinitely)
2.	Surface/volume ratio	1	1000 times larger than that of microparticles
3.	Conductivity*	Low	High
4.	Clog on micro channel	Yes	No
5.	Erosion	Yes	No
6.	Pumping power	Large	Small
7.	Nanoscale phenomenon	No	Yes

1.5 Nanoparticles and base fluids

Modern fabrication technology provides great opportunity to process materials actively at nanometer scales. Nanostructured or Nanophase materials are made of nanometer-sized substances engineered on the atomic or molecular scale. All physical mechanisms have a critical length scale below which the physical properties of materials are changed. Therefore, particles smaller than 100 nm exhibits properties different from those of conventional solids. The thermal, mechanical, optical, magnetic and electrical properties of nanophase materials are superior to those of conventional materials with coarse grain structures [4]. The material for nanoparticles and base fluids is given by Table 1.3.

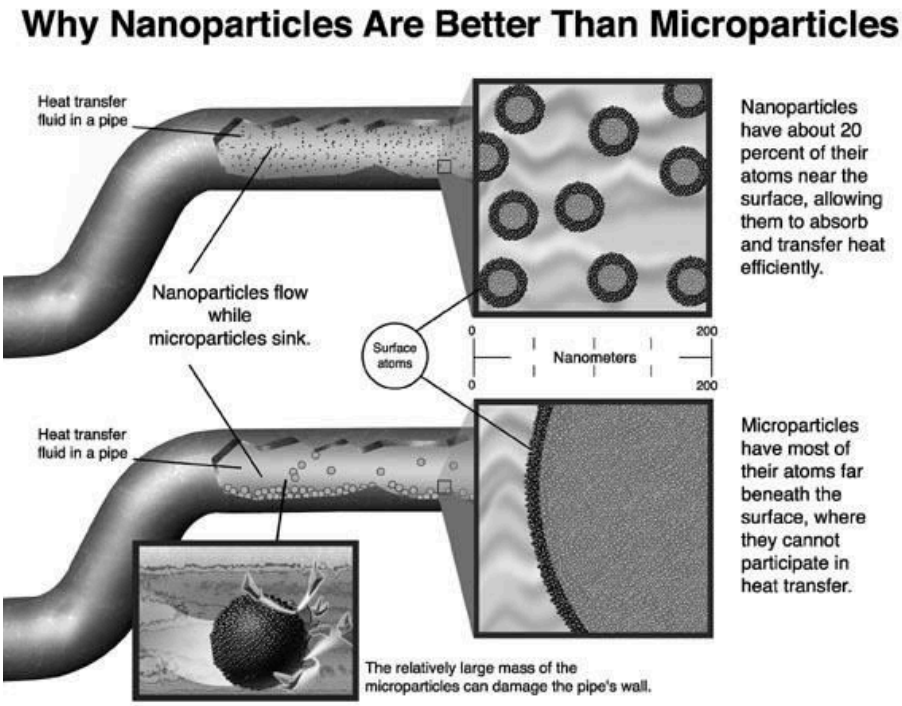

Fig. 1.1: Why nanoparticles are better than microparticles [3]

Table 1.3: Material for nanoparticles and base fluids

Sr. No.	Nanoparticles	Base fluids
1.	Oxide ceramics – Al_2O_3, CuO	Water
2.	Carbide ceramics – SiC, TiC	Ethylene or Tri-ethylene glycol
3.	Nitride ceramics – AlN, SiN	Oil and other lubricants
4.	Metals – Cu, Ag, Au	Bio-fluids
5.	Semiconductors – TiO_2 , SiC	Polymer solutions
6.	Non-metals – Graphite, Carbon nanotubes	Other coolants
7.	Layered – Al + Al_2O_3, Cu + C	Other common fluids

1.6 Thermophysical properties enhancement by nanofluids

During the past decade, a series of pioneering experiments have discovered that nanofluids, when prepared properly, exhibit a number of novel thermal transport phenomena. For example, Eastman et al. [5] found that copper nanofluids show a 40% increase in the thermal conductivity of ethylene glycol at a very low concentration (0.3% by volume) of copper nanoparticles coated with thioglycolic acid. Choi et al. [6], Hong et al. [7], and Murshed et al. [8] discovered that nanofluids containing extremely elongated multiwalled nanotubes or even spherical nanoparticles have a non-linear relationship between thermal conductivity and concentration. Das et al. [9] discovered probably one of the most fantastic features of nanofluids—the thermal conductivity of nanofluids is strongly temperature-dependent, that is, the thermal conductivity enhancement of Al_2O_3 or CuO nanofluids is two to four times that of the base fluid over a small temperature range between 20 °C and 50 °C. Chon et al. [10] and Chopkar et al. [11] found that nanofluids have strongly size-dependent thermal conductivity.

Ding et al. [12] showed that nanofluids made with carbon nanotubes have a more than two-fold increase in laminar convection heat transfer coefficient, and Xuan and Li [13] showed that water-based nanofluids containing 2 volume % of copper nanoparticles have a nearly 40% increase in turbulent convection heat transfer coefficient compared to base fluids.

Kang et al. [14] measured the viscosities of UDD (ultradispersed diamond)/ethylene glycol, silver/water, and silica/ water nanofluids and found the viscosity increment of 50%, 30% and 20% for UDD/EG, silver/water and silica/water nanofluids at volume concentrations of 1%, 2% and 3%, respectively. Murshed et al. [15] measured relative viscosity data for TiO_2 and Al_2O_3/water-based nanofluids, and reported a maximum increase of 80% at 4% and 5% particle volume fraction, respectively. Similar increments in viscosity were reported earlier by Masuda et al. [16] and Wang et al. [17]. Xie et al. [18] ran experiments for nanoparticles dispersed in organic fluids like EG and showed that the increase for the viscosity of Al_2O_3/EG nanofluids is smaller than those of water based suspensions, indicating the important effect of the base fluid on nanofluid viscosity.

1.7 Benefits of nanofluids

When the nanoparticles are properly dispersed, nanofluids can offer numerous benefits [19, 20] besides the anomalously high effective thermal conductivity. These benefits include:

a) Improved heat transfer and stability

Because heat transfer takes place at the surface of the particles, it is desirable to use particles with larger surface area. The relatively larger surface areas of nanoparticles compared to microparticles, provide significantly improved heat transfer capabilities. Because the nanoparticles are small, gravity becomes less important and thus chances of sedimentation are also less, making nanofluids more stable.

b) Microchannel cooling without clogging

Nanofluids will not only be a better medium for heat transfer in general, but they will also be ideal for Microchannel applications where high heat loads are encountered.

c) Reduction in pumping power

To increase the heat transfer of conventional fluids by a factor of two, the pumping power must usually be increased by a factor of 10. It was shown that by multiplying the thermal conductivity by a factor of three, the heat transfer in the same apparatus was doubled [21]. Thus, very large savings in pumping power can be achieved if a large thermal conductivity increase can be achieved with a small volume fraction of nanoparticles.

d) **Miniaturized systems**

Nanofluid technology will support the current industrial trend toward component and system miniaturization by enabling the design of smaller and lighter heat exchanger systems. Miniaturized systems will reduce the inventory of heat transfer fluid and will result in cost savings.

1.8 Applications of nanofluids

Nanofluids can be used to improve heat transfer and energy efficiency in thermal systems. Much of the work in the field of nanofluids is being done in national laboratories and academia [22].

a) Transportation

The addition of nanoparticles to the standard engine coolant has the potential to improve automotive and heavy-duty engine cooling rates. Such improvement can be used to remove engine heat with a reduced-size coolant system. Smaller coolant systems result in smaller and lighter radiators, which in turn benefit almost every aspect of car and truck performance and lead to increased fuel economy. Alternatively, improved cooling rates for automotive engines can be used to remove more heat from higher horsepower engines with the same size of coolant system.

b) Electronics cooling

The power density of integrated circuits and microprocessors has increased dramatically in recent years. Future processors for high-performance computers and servers have been projected to dissipate higher power, in the range of 100-300 W/cm^2. Whether these values actually become reality is not as significant as the projection that the general trend to higher power density electronics will continue. Existing air cooling techniques for removing this heat are already reaching their limits, and liquid cooling technologies are being, and have been, developed for replacing them. Single-phase fluids, two-phase fluids, and nanofluids are candidate replacements for air. All have increased heat transfer capabilities over air systems.

c) Defence

A number of military devices and systems require high-heat-flux cooling to the level of tens of MW/m^2. At this level, cooling with conventional fluids is challenging. Examples of military applications include cooling of power electronics and directed-energy weapons. Directed-energy weapons involve high heat fluxes ($> 500 - 1000$ W/cm^2), and providing adequate cooling of them and the associated power electronics is a critical need. Nanofluids have the potential to provide the required cooling in such applications as well as in other military systems, including military vehicles, submarines, and high-power laser diodes.

d) Biomedical

Nanofluids and nanoparticles have many applications in the biomedical industry. For example, to circumvent some side effects of traditional cancer treatment methods, iron-based nanoparticles could be used as delivery vehicles for drugs or radiation without damaging nearby healthy tissue. Nanofluids could also be used for safer surgery by producing effective cooling around the surgical region and thereby enhancing the patient's chance of survival and reducing the risk of organ damage.

1.9 Conclusion

It is expected that the Nanofluids will be the next generation of heat transfer fluids due to their unique thermal properties. At Present, research work on the concept, its thermo-physical properties, heat transfer enhancement, mechanism, and application of the nanofluids is still in its infancy.

The scope of the work:

1. To find thermal conductivity of distilled water, ethylene glycol and distilled water and ethylene glycol based nanofluids having alumina nanoparticles for different volume fractions and at different temperatures.
2. To find viscosity and density for the same as above.
3. To analyze the particle size distribution.

References

1. Murshed, S. M. S., Leong, K. C., and Yang, C., Thermophysical and electrokinetic properties of Nanofluids – A critical review, Applied Thermal Engineering, vol. 28, pp. 2109–2125, 2008.
2. Das, S. K., Choi, S. U. S., Wenhua, Y., and Pradeep, T., Nanofluids: Science and Technology, John Wiley & Sons, Inc. New Jersey, 2007.
3. Choi, S., Nanofluids could make cool work of hot truck engines, Research article, Argonne National laboratory, Centre for nanoscale materials, 2005.
4. Duncan M. A., Rouvray D.H., Microclusters, Sci. Am., pp. 110-115, 1989.
5. Eastman, J. A., Choi, S. U. S., Li, S., Yu,W., and Thompson, L. J., Anomalously Increased Effective Thermal Conductivity of Ethylene Glycol-Based Nanofluids Containing Copper Nanoparticles, Applied Physics Letters, vol. 78, pp. 718–720, 2001.
6. Choi, S. U. S., Zhang, Z. G., Yu,W., Lockwood, F. E., and Grulke, E. A., Anomalously Thermal Conductivity Enhancement in Nanotube Suspensions, Applied Physics Letters, vol. 79, pp. 2252– 2254, 2001.
7. Hong, T.-K., Yang, H.-S., and Choi, C. J., Study of the Enhanced Thermal Conductivity of Fe Nanofluids, Journal of Applied Physics, vol. 97, Paper 064311, pp. 4, 2005.
8. Murshed, S. M. S., Leong, K. C., and Yang, C., Enhanced Thermal Conductivity of TiO_2-Water Based Nanofluids, International Journal of Thermal Sciences, vol. 44, pp. 367–373, 2005.
9. Das, S. K., Putra, N., Thiesen, P., and Roetzel, W., Temperature Dependence of Thermal Conductivity Enhancement for Nanofluids, Transactions of the ASME, Journal of Heat Transfer, vol. 125, pp. 567–574, 2003.

10. Chon, C. H., Kihm, K. D., Lee, S. P., and Choi, S. U. S., Empirical Correlation Finding the Role of Temperature and Particle Size for Nanofluid (Al_2O_3) Thermal Conductivity Enhancement, Applied Physics Letters, vol. 87, Paper 153107, 2005.
11. Chopkar, M., Das, P. K., and Manna, I., Synthesis and Characterization of a Nanofluid for Advanced Heat Transfer Applications, Scripta Materialia, vol. 55, pp. 549–552, 2006.
12. Ding, Y., Alias, H., Wen, D., and Williams, R. A., Heat Transfer of Aqueous Suspensions of Carbon Nanotubes (CNT Nanofluids), International Journal of Heat and Mass Transfer, vol. 49, pp. 240– 250, 2006.
13. Xuan, Y., and Li, Q., Investigation on Convective Heat Transfer and Flow Features of Nanofluids, Transactions of the ASME, Journal of Heat Transfer, vol. 125, pp. 151–155, 2003.
14. Kang, H.U., Kim, S.H., and Oh, J.M., Estimation of thermal conductivity of nanofluid using experimental effective particle volume, Exp. Heat Transfer, vol. 19, pp. 181–191, 2006.
15. Murshed, S .M. S., Leong, K. C., and Yang, C., Investigations of thermal conductivity and viscosity of nanofluids, Int. J. Therm. Sci., vol. 47, pp. 560–568, 2008.
16. Masuda, H., Ebata, A., Teramae, K., and Hishinuma, N., Alteration of thermal conductivity and viscosity of liquid by dispersing ultra-fine particles (dispersion of Al_2O_3, SiO_2 and TiO_2 ultra-fine particles), Netsu Bussei (Japan),vol. 7, pp. 227–233, 1993.
17. Wang, X., Xu, X., and Choi, S. U. S., Thermal conductivity of nanoparticles–fluid mixture, J. Thermophys. Heat Transfer, vol. 4, pp. 474–480, 1999.
18. Xie, H., Chen, L., and Wu, Q., Measurements of the viscosity of suspensions (nanofluids) containing nanosized Al_2O_3 particles, High Temp. – High Press., vol. 37, pp. 127–135, 2008.
19. Choi, S. U. S., Zhang, Z. G., and Keblinski, P., Nanofluids, Encyclopedia of Nanoscience and Nanotechnology, vol. 6, pp. 757–773, 2004.
20. Zussman, S., New nanofluids increase heat transfer capability, Technology Transfer Highlights, Argonne National Laboratory, USA ,vol.8, pp. 4, 1997.
21. Choi, S. U. S., Enhancing thermal conductivity of fluids with nanoparticles, in: D.A. Siginer, H.P. Wang (Eds.), Developments and Applications of Non-Newtonian Flows, ASME, New York, FED-vol. 231/MD-vol. 66, pp. 99–105, 1995.
22. Wang, X. Q., and Mujumdar, A. S., A review on nanofluids - part II: Experiments and applications, Brazilian Journal of Chemical Engineering, vol. 25, no. 04, pp. 631 - 648, 2008.

Chapter – 2
Literature review

2.1 Introduction

Various studies on nanofluids were carried out by many researchers in the past. This chapter reviews the previous published literatures, which lays foundation and basis for further work. This helps to give a better understanding about the topic and also acts as a guideline for this thesis. In this chapter, experimental and theoretical efforts on synthesis process, theoretical models and experimental measurements of Thermophysical properties and convection heat transfer and detailed proposed theories for explaining the experimental results will be reviewed and discussed.

2.2 About nanofluids

One of the most significant scientific challenges in the industrial area is cooling, which applies to many diverse productions, including microelectronics, transportation and manufacturing. The conventional method for increasing heat dissipation is to increase the area available for exchanging heat to use a better heat conductive fluid. However, this approach involves an undesirable increase in the size of a thermal management system; therefore, there is an urgent need for new and novel coolants with improved performance. The innovative concept of 'nanofluids' – heat transfer fluids consisting of suspension of nanoparticles – has been proposed as a prospect for these challenges [1].

Choi and Eastman [2] introduced the novel concept of nanofluids by applying the unique properties of nanofluids at the annual Mechanical Engineering meeting of American Society at 1995. Goldstein et al. [3] added the condition that the particles must be in colloidal suspension. Choi and his colleagues have carried out experiments on heat transport in systems with CuO nanoparticles in water and Al_2O_3 particles in ethylene glycol and water. They found that the particles improve the heat transport by as much as 20%, and they interpreted their result in terms of an improved thermal conductivity k/k_0 which they named the effective thermal conductivity [3].

About a decade ago, some researchers reported the heat transfer and flow characteristics of the different nanofluids namely: Trisaksri and Wongwises [4], Beck [5], Wang and Mujumdar [6], Duangthongsuk and Wongwises [7], Godson et al. [8], Li et al. [9] and Wen et al. [10], Leong et al. [11]. However, prior to use nanofluids for heat transfer, significant knowledge about their thermophysical properties is required, especially their thermal conductivity and viscosity. Many researchers have measured the thermophysical properties of nanofluids while many others used well-known predictive correlations. Their works have been both experimental and theoretical [12].

2.3 Preparation of nanofluids

This includes methods of nanoparticles manufacture and dispersion of nanoparticles in liquids. Modern fabrication technology provides great opportunity to process materials actively at nanometer scales. Nanostructured or Nanophase materials are made of nanometer-sized substances engineered on the atomic or molecular scale.

2.3.1 Methods of nanoparticles manufacture

Fabrication of nanoparticles can be classified into two broad categories: physical processes and chemical processes [13, 14 &15]. Typical physical methods include inert-gas condensation (IGC), developed by [14], mechanical grinding and milling. Chemical methods include chemical vapor deposition (CVD), chemical precipitation, micro emulsions, thermal sprays and spray pyrolysis. A sonochemical method has been developed to make suspensions of iron nanoparticles stabilized by oleic acid [16]. Recently, Chopkar et al. [17] produced alloyed nanoparticles $Al_{70}Cu_{30}$ using ball milling. These nanosized materials are most commonly produced in the form of powders.

2.3.2 Dispersion of nanoparticles in liquids

Stable suspensions of nanoparticles in conventional heat transfer fluids are produced by two methods: the two-step technique and single-step technique. The two-step method first makes nanoparticles using one of the methods discussed in section 2.3.1 and then disperses them into base fluids. The single-step method simultaneously makes and then disperses nanoparticles directly into base fluids. In either case, a well-mixed and uniformly dispersed nanofluid is needed for successful production of enhanced properties.

The single-step direct evaporation approach was developed by Akoh et al. [18] and is called the VEROS (Vacuum Evaporation onto a Running Oil Substrate) technique. The original idea of this method was to produce nanoparticles, but it is difficult to subsequently separate the particles from the fluids to produce dry nanoparticles. A modified VEROS process was proposed by Wagener et al. [19]. They employed high pressure magnetron sputtering for the preparation of suspensions with metal nanoparticles such as Ag and Fe. Eastman et al. [20] developed a modified VEROS technique, in which Cu vapor is directly condensed into nanoparticles by contact with a flowing low-vapor-pressure liquid (EG).

Zhu et al. [21] presented a novel one-step chemical method for preparing copper nanofluids by reducing $CuSO_4.5H_2O$ with $NaH_2PO_2.H_2O$ in ethylene glycol under microwave irradiation. Results showed that the addition of $NaH_2PO_2.H_2O$ and the addition of microwave irradiation are two significant factors which affect radiation rate and properties of Cu nanofluids. A vacuum-SANSS (submerged arc nanoparticles synthesis system) method has been employed by Lo et al. [22] to

prepare Cu-based nanofluids with different dielectric liquids such as de-ionized water, with 30%, 50%, 70% volume solutions of ethylene glycol and pure ethylene glycol. An advantage of the one step technique is that nanoparticle agglomeration is minimized, while the disadvantage is that only low vapor pressure fluids are compatible with such a process.

The two-step method is extensively used in the synthesis of nanofluids considering the available commercial nanopowders supplied by several companies. Generally, ultrasonic equipment is used to intensively disperse the particles and reduce the agglomeration of particles. For example, Eastman et al. [20], Lee et al. [23], and Wang et al. [15] used this method to produce Al_2O_3 nanofluids. Also, Murshed et al. [25] prepared TiO_2 suspension in water using the two-step method. Other nanoparticles reported in literature are gold (Au), silver (Ag), silica and carbon nanotubes. As compared to the single-step method, the two-step technique works well for oxide nanoparticles, while it is less successful with metallic particles. The first-ever nanofluids with carbon nanotubes, nanotubes in synthetic oil, were produced by a two-step method by Choi et al. [26].

Xuan and Li [27] choose salt and oleic acid as the dispersant to enhance the stability of transformer oil-Cu and water-Cu nanofluids, respectively. Oleic acid and cetyltrimethylammonium bromide (CTAB) surfactants were used by Murshed et al. [25] to ensure better stability and proper dispersion of TiO_2- water nanofluids. Sodium dodecyl sulfate (SDS) was used by Hwang et al. [28] during the preparation of water-based multi-walled carbon nanotubes (MWCNT) nanofluids since the fibers are entangled in the aqueous suspension.

Li et al. [29] prepared Cu/water nanofluids with nanoparticle sizes typically of 1-100 nm using the two-step method. Results showed that zeta potential and absorbency are important bases for selecting conditions for dispersing particles. Furthermore, the observed sediment photographs and particle size distribution showed better dispersion behaviour in the suspension with the addition of dispersant. The effect of pH on the stability of the copper suspension was critical.

Hwang et al. [30] prepared various nanofluids (nanoparticle: MWCNT, CuO, and SiO_2; base fluid: DIW, EG and oil) and examined their stability using UV-vis spectral analysis. They claimed that the stability of nanofluid is strongly affected by the characteristics of the suspended particle and base fluids such as the particle morphology, the chemical structure of the particles and base fluid. Furthermore, addition of surfactant can improve the stability of the suspensions.

In general, methods such as change of pH value, addition of dispersant and ultrasonic vibration aim at changing the surface properties of suspended particles and suppressing formation of particle clusters to obtain stable suspensions.

2.4 Theoretical investigations

In this section we will discuss mechanisms of nanofluids and various models for thermophysical properties like thermal conductivity, viscosity, density, specific heat and convective heat transfer.

2.4.1 Mechanisms of nanofluids

From the experimental results of many researches, it is known that the thermal conductivity of nanofluids depends on many factors including the volume fraction, the size, the shape, clustering of the nanoparticles, and the temperature. However, the influences of the above factors are not clear at present. To seek the mechanism responsible for the so-called anomalous increase in thermal conductivity, many theories have been proposed.

The large enhancement of thermal conductivity in nanofluids cannot be interpreted with the traditional theories, such as Maxwell model [31], Hamilton and Crosser model [32], which explained the thermal conductivity enhancement of usual suspensions containing large particles (micro- or mini-size) quite well. Keblinski [33] and Eastman [34] proposed a comprehensive explanation of four possible factors to understand the mechanism of heat conduction in nanofluids. They were the Brownian motion of particles, liquid nanolayering at liquid/particle interface, the nature of heat transport in the nanoparticle, and the effects of nanoparticle clustering.

Wang et al. [24] argued that the thermal conductivities of nanofluids should be dependent on the microscopic motion (Brownian motion and inter-particle forces) and particle structure. Xuan and Li [35] also discussed four possible reasons for the improved effective thermal conductivity of nanofluids: the increased surface area due to suspended nanoparticles, the increased thermal conductivity of the fluid, the interaction and collision among particles, the intensified mixing fluctuation and turbulence of the fluid, and the dispersion of nanoparticles.

Many researchers used the concept of liquid/solid interfacial layer to explain the anomalous improvement of the thermal conductivity of nanofluids. Yu and Choi [36] & Yu and Choi [37] suggested models, based on conventional theory, which consider a liquid molecular layer around the nanoparticles. However, a study of Xue et al. [38] using molecular dynamics simulation showed that simple monatomic liquids had no effect on the heat transfer characteristics both normal and parallel to the surface. This means that thermal transport in a layered liquid may not be adequate to explain the increased the thermal conductivity of suspensions of nanoparticles.

Khaled and Vafai [39] investigated the effect of thermal dispersion on heat transfer enhancement of nanofluids. These results showed that the presence of dispersive elements in the core region did not affect the heat transfer rate. Koo and Kleinstreuer [40] discussed the effects of Brownian, thermo-

phoretic, and osmo-phoretic motions on the effective thermal conductivities. They found that the role of Brownian motion is much more important than the thermo-phoretic and osmo-phoretic motions.

Tillman and Hill [41] attempted to find a more systematic procedure to determine the nanolayer thickness and the thermal conductivity profile within the nanolayer. Three basic heat conduction regions were used to derive the expression for the nanolayer thickness. Evans et al. [42] suggested that the contribution of Brownian motion to the thermal conductivity of the nanofluid is very small and cannot be responsible for the extraordinary thermal transport properties of nanofluids.

2.4.2 Models for effective thermal conductivity of nanofluids

There are no theoretical formulas currently available to predict the thermal conductivity of nanofluids satisfactorily. However, there exist several semi-empirical correlations for calculating the apparent conductivity of two-phase mixtures.

For particle-fluid mixtures, numerous theoretical studies have been conducted dating back to the classical work of Maxwell [31]. The effective thermal conductivity, k_{eff} , is given by

$$k_{eff} = \frac{k_p + 2\,k_b + 2\,(k_p - k_b)\,\emptyset}{k_p + 2\,k_b - (k_p - k_b)\,\emptyset}\,k_b \tag{2.1}$$

Where $k_p\ is$ the thermal conductivity of the particle is k_b is the thermal conductivity of the base fluid and $\emptyset$ is the particle volume fraction in the suspension.

Bruggeman [43] proposed a model to analyze the interactions among randomly distributed particles. For a binary mixture of homogeneous spherical inclusions, the Bruggeman model gives

$$\emptyset\left(\frac{k_p - k_{eff}}{k_p + 2\,k_{eff}}\right) + (1-\emptyset)\left(\frac{k_b - k_{eff}}{k_b + 2\,k_{eff}}\right) = 0 \tag{2.2}$$

Hamilton and Crosser [32] proposed a model for liquid-solid mixtures of non-spherical particles. They introduced a shape factor, n, to account for the effect of the shape of the particles. The thermal conductivity, in which the ratio of conductivity of the solid and fluid phases is larger than 100 $(k_p/k_b > 100)$, can be expressed as follows:

$$k_{eff} = \frac{k_p + (n-1)k_b - (n-1)(k_b - k_p)\emptyset}{k_p + (n-1)k_b + (k_b - k_p)\emptyset}\,k_b \tag{2.3}$$

Where n is the empirical shape factor given by $n = 3/\psi$, and ψ is the particle sphericity, defined as the ratio of the surface area of a sphere with volume equal to that of the particle, to the surface

area of the particle. Comparison between equation (2.3) and equation (2.1) reveals that Maxwell's model is a special case of Hamilton and Crosser's model for sphericity equal to one.

Yu and Choi [36] proposed a modified Maxwell model to account for the effect of the nanolayer by replacing the thermal conductivity of solid particles k_p in equation (2.1) with the modified thermal conductivity of particles, k_{pe}, which is based on the so-called effective medium theory given by Schwartz et al. [44]:

$$k_{pe} = \frac{[2\,(1-\gamma)+(1+\beta)^3\,(1+2\gamma)\gamma]}{-(1-\gamma)+(1+\beta)^3\,(1+2\gamma)}\;k_p \tag{2.4}$$

Where $\gamma = k_{layer}/k_p$ is the ratio of nano-layer thermal conductivity to particle thermal conductivity and $\beta = h/r$ is the ratio of the nano-layer thickness to the original particle radius. Hence, the Maxwell equation (2.1) can be re-cast as follows:

$$k_{eff} = \frac{k_{pe} + 2k_b + 2\,(k_{pe} - k_b)(1-\beta)^3\emptyset}{k_{pe} + 2\,k_b - (k_{pe} - k_b)(1+\beta)^3\emptyset}\;k_b \tag{2.5}$$

Yu and Choi [37] proposed a modified Hamilton-Crosser model to include the particle-liquid interfacial layer for non-spherical particles. The effective thermal conductivity was expressed as

$$k_{eff} = \left(1 + \frac{n\,\emptyset_{eff}\,A}{1-\emptyset_{eff}\,A}\right) k_b \tag{2.6}$$

Where A is defined by

$$A = \frac{1}{3}\sum\nolimits_{j=a,b,c} (k_{pj} - k_b)/[k_{pj} + (n-1)k_b]$$

$$\text{And}\quad \emptyset_{eff} = \emptyset\sqrt{(a^2+t)\,(b^2+t)(c^2+t)}\,/\sqrt{abc}$$

Where, $\emptyset_{eff}$ is the equivalent volume concentration of complex ellipsoids, which is an imaged structure of elliptical particles $(a > b > c)$ with surrounding nano layers.

Xue and Xu [45] obtained an equation for the effective thermal conductivity according to Bruggeman`s model [43]. Their model takes into account the effect of interfacial shells by replacing the thermal conductivity of nanoparticles with the assumed thermal conductivity of the so-called "complex nanoparticles", which included the interfacial shells between the nanoparticles and the base fluids.

$$\left(1-\frac{\emptyset}{\alpha}\right)\frac{k_{eff}-k_b}{2k_{eff}+k_b} + \frac{\emptyset}{\alpha}\left(\frac{(k_{eff}-k_2)\,(2k_2+k_1) - \alpha(k_1-k_2)\,(2k_2+k_{eff})}{(2k_{eff}+k_2)\,(2k_2+k_1) + 2\alpha(k_1-k_2)\,(k_2-k_{eff})}\right) = 0 \tag{2.7}$$

Where α is the volume ratio of spherical nanoparticle and complex nanoparticle, and k_1 and k_2 are the thermal conductivity of the nanoparticle and interfacial shell, respectively.

Xie et al. [46] considered the interfacial nanolayer with linear thermal conductivity distribution and proposed an effective thermal conductivity model to account for the effects of nano-layer thickness, nanoparticle size, volume fraction, and thermal conductivities of fluid, nanoparticles, and nano-layer. Their formula is

$$k_{eff} = \left(1 + 3\,\theta\,\emptyset_T + \frac{3\,\theta^2\,\emptyset_T^2}{1 - \theta\,\emptyset_T}\right) \tag{2.8}$$

With $\theta = \{\beta_{lb}[(1+\gamma)^3 - \beta_{pl}/\beta_{bl}]\}/[(1+\gamma)^3 + 2\beta_{lb}\,\beta_{pl}]$,

Where $\beta_{lb} = (k_1 - k_b)/(k_1 + 2k_b)$,
$\beta_{pl} = (k_p - k_1)/(k_p + 2k_1)$ *and*
$\beta_{bl} = (k_b - k_1)/(k_b + 2k_1)$,

And $\gamma = \delta/r_p$ is the thickness ratio of nano-layer and nanoparticle. $\emptyset_T$ is the modified total volume fraction of the original nanoparticle and nano-layer, $\emptyset_T = \emptyset(1+\gamma)^3$.

Xuan et al. [47] considered the random motion of suspended nanoparticles (Brownian motion) based on the Maxwell model and proposed a modified formula for the effective thermal conductivity as follows:

$$k_{eff} = \frac{k_P + 2k_b - 2(k_b - k_P)\,\emptyset}{k_P + 2k_b + (k_b - k_P)\,\emptyset}\,k_b + \frac{\rho_P\,\emptyset\,c_P}{2}\sqrt{\frac{k_B\,T}{3\,\pi\,r_c\,\mu}} \tag{2.9}$$

Where the Boltzmann constant is $K_B = 1.381 \times 10^{-23}\ J/K$;
r_c is the apparent radius of clusters and depends on the fractal dimensions of the cluster structure.

Wang et al. [48], who developed a fractal model based on the multi-component Maxwell model by substituting the effective thermal conductivity of the particle clusters, $k_{cl}(r)$, and the radius distribution function, $n(r)$, as follows:

$$k_{eff} = \frac{(1-\emptyset) + 3\emptyset\int_0^\infty k_{cl}(r)\,n(r)/[k_{cl}(r) + 2k_b]\,dr}{(1-\emptyset) + 3\emptyset\int_0^\infty k_b(r)\,n(r)/[k_{cl}(r) + 2k_b]\,dr}\,k_b \tag{2.10}$$

Kumar et al. [49] proposed a comprehensive model to account for the large enhancement of thermal conductivity in nanofluids and its strong temperature dependence, which was deduced from the Stokes-Einstein formula. The thermal conductivity enhancement taking account of the Brownian motion of particles can be expressed as:

$$k_{eff} = k_b + c \frac{2k_B T \quad \emptyset \quad r_b}{(\pi \vartheta d_P^2) k_b (1 - \emptyset) r_P} k_b \tag{2.11}$$

Where c is a constant, ϑ is the dynamic viscosity of the base fluid, and d_P is the diameter of the particles. However, the validity of the model has got to be established; it may not be suitable for high concentrations of particles.

Bhattacharya et al. [50] developed a technique to compute the effective thermal conductivity of a nanofluid using Brownian motion simulation. They combined the liquid conductivity and particle conductivity as follows:

$$k_{eff} = \emptyset k_p + (1 - \emptyset) k_b \tag{2.12}$$

Where k_p is replaced by the effective contribution of the particles towards the overall thermal conductivity of the system,

$$k_p = \frac{1}{k_B T^2 V} \sum_{j=0}^{n} \langle Q(0) Q(j\Delta t) \rangle \Delta t. \tag{2.12.1}$$

Koo and Kleinstreuer [51, 52] developed a new model for nanofluids, which includes the effects of particle size, particle volume fraction and temperature dependence as well as properties of the base fluid and the particle subject to Brownian motion. The resulting formula is:

$$k_{eff} = \frac{k_p + 2k_b + 2(k_p - k_b)\emptyset}{k_p + 2k_b - (k_p - k_b)\emptyset} k_b + 5 \times 10^4 \beta \emptyset \rho_P c_P \sqrt{\frac{k_B T}{\rho_P D}} f(T, \emptyset) \tag{2.13}$$

Note that the first part of equation (13) is obtained directly from the Maxwell model while the second part accounts for Brownian motion, which causes the temperature dependence of the effective thermal conductivity. The function $f(T, \emptyset)$ can be assumed to vary continuously with the particle volume fraction,

$$f(T, \emptyset) = (-6.04\emptyset + 0.4705)\mathrm{T} + (1722.3\emptyset - 134.63) \tag{2.14}$$

While, β is related to particle motion.

2.4.3 Models for effective viscosity of nanofluids

Different models of viscosity have been used by researchers to model the effective viscosity of nanofluid as a function of volume fraction. Einstein [53] was the first to calculate the effective viscosity of a suspension of spherical solids using the phenomenological hydrodynamic equations. He derived the following equation:

$$\mu_{eff} = (1 + 2.5\emptyset_P)\mu_b \tag{2.15}$$

Experimental data for the effective viscosity of nanofluids are limited to certain nanofluids. The ranges of the parameters (the particle volume concentration, temperature, etc.) are also limited. Still, the experimental data show the trend that the effective viscosities of nanofluids are higher than the existing theoretical predictions. In an attempt to rectify this situation, researchers proposed equations applied to specific applications, e.g., Al_2O_3 in water by Maiga et al. [63], Al_2O_3 in ethylene glycol by Maiga et al. [64], TiO_2 in water by Tseng and Lin [62], and CuO in water with temperature change by Kulkarni et al. [66]. The problem with these equations is that they do not reduce to the Einstein equation at very low particle volume concentrations and, hence, lack a sound physical basis. Brinkmen [55] presented a viscosity correlation that extended Einstein's equation to concentrated suspension. The effect of Brownian Motion on the effective viscosity in a suspension of rigid spherical particles was studied by Batchelor [59]. Lundgren [58] proposed equation for effective viscosity in the form of a Taylor series in $\emptyset_P$. Some of these equations are included in Table 2.1.

Table 2.1: Models for effective viscosity

Sr. No.	Investigator	Equation
1.	Einstein [53]	$\mu_{eff} = (1 + 2.5\emptyset_P)\mu_b$
2.	Satio [54]	$\mu_{eff} = \left(1 + \frac{2.5}{1 - \emptyset_P}\,\emptyset_P\right)\mu_b = (1 + 2.5\emptyset_P + 2.5\emptyset_P^2 + \cdots)\mu_b$
3.	Brinkman [55]	$\mu_{eff} = \frac{1}{(1 - \emptyset_P)^{2.5}}\,\mu_b = (1 + 2.5\emptyset_P + 4.375\emptyset_P^2 + \cdots)\mu_b$
4.	Simha [56]	$\mu_{eff} = \{1 + 2.5\emptyset_P + [125/(64\,\emptyset_{P\,max})]\emptyset_P^2 + \cdots\}\mu_b$
5.	Krieger [57]	$\mu_{eff} = \frac{1}{[1 - (\emptyset_P/\emptyset_{P\,max})]^{1.82}}\,\mu_b = [1 + (1.82/\emptyset_{P\,max})\emptyset_P + (2.5662/\emptyset_{P\,max}^2)\emptyset_P^2 + \cdots]\mu_b$
6.	Lundgren [58]	$\mu_{eff} = \frac{1}{1 - 2.5\,\emptyset_P}\,\mu_b = (1 + 2.5\emptyset_P + 6.25\emptyset_P^2 + \cdots)\mu_b$
7.	Batchelor [59]	$\mu_{eff} = (1 + 2.5\emptyset_P + 6.2\emptyset_P^2)\mu_b$
8.	Tseng and Lin [60]	$\mu_{eff} = 13.47\exp(35.98\emptyset_P)\mu_b$
9.	Maiga et al. [61]	$\mu_{eff} = (1 + 7.3\emptyset_P + 123\emptyset_P^2)\mu_b$
10.	Maiga et al. [62]	$\mu_{eff} = (1 - 0.19\emptyset_P + 306\,\emptyset_P^2)\mu_b$
11.	Koo and Kleinstreuer [63]	$\mu_{Brownian} = 5 \times 10^4\,\beta\,\rho_b\,\emptyset_P\sqrt{\frac{k_B\,T}{2\rho_P\,r_P}}[(-134.63 + 1722.3\emptyset_P) + (0.4705 - 6.04\emptyset_P)\,T]$, Where the particle motion related parameter $\beta = 0.0137(100\emptyset_P)^{-0.8229}$ $\emptyset_P < 0.01$; $\beta = 0.0011(100\emptyset_P)^{-0.7272}$ $\emptyset_P > 0.01$
12.	Kulkarni et al. [64]	$\ln\mu_{eff} = -(2.8751 + 753.548\emptyset_P - 107.12\emptyset_P^2) + (1078.3 + 15857\emptyset_P + 20587\emptyset_P^2)\,(1/T)$

2.4.4 Analytical models for physical properties of nanofluids

Physical properties include density, specific heat and thermal expansion coefficient. Their models are given below:

2.4.4.1 Density

The density of nanofluid is based on the physical principle of the mixture rule. As such it can be represented as [65]:

$$\rho_{eff} = \left(\frac{m}{V}\right)_{eff} = \frac{m_f + m_P}{V_f + V_P} = \frac{\rho_f V_f + \rho_P V_P}{V_f + V_P} = (1 - \emptyset_P)\rho_f + \emptyset_P \rho_P \quad (2.16)$$

Where f and P refer to the fluid and nanoparticle respectively and

$\emptyset_P = \frac{V_P}{V_f + V_P}$ is the volume fraction of the nanoparticles.

2.4.4.2 Specific heat of nanofluids

The specific heat of nanofluid can be determined by assuming thermal equilibrium between the nanoparticles and the base fluid phase as follows [65]:

$$(\rho\, C)_{eff} = \rho_{eff} \left(\frac{Q}{m\, \Delta T}\right)_{eff} = \rho_{eff} \frac{Q_f + Q_p}{(m_f + m_p)\, \Delta T} = \rho_{eff} \frac{(m\, C)_f\, \Delta T + (m\, C)_p\, \Delta T}{(m_f + m_p)\, \Delta T} =$$

$$= \rho_{eff} \frac{(\rho\, C)_f\, V_f + (\rho\, C)_p\, V_p}{\rho_f V_f + \rho_p V_p} \Rightarrow C_{eff} = \frac{(1 - \emptyset_P)\, \rho_f\, C_f + \emptyset_P \rho_P C_P}{\rho_{eff}} \quad (2.17)$$

Where ρ_P is the density of the nanoparticle, ρ_f is the density of the base fluid, ρ_{eff} is the density of the nanofluid, and C_P and C_f are the heat capacities of the nanoparticle and the base fluid, respectively. However, some authors prefer to use a simpler expression given as:

$$C_{eff} = (1 - \emptyset_P)\, C_f + \emptyset_P C_P \quad (2.18)$$

2.4.4.3 Thermal expansion coefficient of nanofluids

The thermal expansion coefficient of nanofluids can be estimated utilizing the volume fraction of the nanoparticles on a weight basis as follows [66]:

$$\beta_{eff} = \frac{(1 - \emptyset_P)\, (\rho\, \beta)_f + \emptyset_P\, (\rho\, \beta)_p}{\rho_{eff}} \quad (2.19)$$

Where β_f and β_p are the thermal expansion coefficient of the base fluid and the nanoparticle, respectively. A simpler model for the thermal expansion coefficient of the nanofluid is suggested as:

$$\beta_{eff} = (1 - \emptyset_P)\, \beta_f + \emptyset_p\, \beta_p \quad (2.20)$$

2.4.5 Models for convective heat transfer

Since the heat transfer performance is a better indicator than the effective thermal conductivity for nanofluids used as coolants in transportation and other industries, the modelling of nanofluid heat transfer coefficients is gaining attention from researchers. However, it is still at an early stage, and the theoretical models for nanofluid heat transfer coefficients are quite limited. All the equations are modified from traditional equations such as the Dittus-Boelter equation (Dittus and Boelter, [67]) or the Gnielinski equation (Gnielinski, [68]) with empirical parameters added. Therefore, these equations are only valid for certain nanofluids over small parameter ranges. More experimental and theoretical studies are needed before general models can be developed and verified. Various models of heat transfer coefficients are given in Table 2.2.

Table 2.2: Models for effective heat transfer coefficient

Sr. No.	Investigator	Nanofluids	Correlation
1.	Pak and Cho, [69]	Al_2O_3-water, TiO_2-water, turbulent	$Nu = 0.021\, Re^{0.8}\, Pr^{0.5}$
2.	Das et al., [70]	Al_2O_3-water, pool boiling	$Nu = c\, Nu_b^m\, Pr^{0.4}$ Where, 'c' and 'm' are particle volume concentration dependent parameters.
3.	Xuan and Li, [71]	CuO-water, turbulent	$Nu = 0.0059\left(1.0 + 7.6286\emptyset_p^{0.6886}\, Pe_p^{0.001}\right)Re^{0.9238}Pr^{0.4}$
4.	Yang et al., [72]	Graphite-in transmission fluid, graphite-synthetic oil mixture,laminar	$Nu = c\, Re^m\, Pr^{1/3}\, (D/L)^{1/3}\, (\mu_b/\mu_\infty)^{0.14}$ Where, 'c' and 'm' are nanofluid and temperature dependent empirical parameters.
5.	Buongiorno [73]	Turbulent	$Nu = \frac{(f/8)\ (Re - 1000)\, Pr}{1 + \delta_\emptyset^+\, (f/8)^{1/2}\left(Pr_\emptyset^{2/3} - 1\right)}$ where the dimensionless thickness of the laminar sub layer $\delta_\emptyset^+$ is an empirical parameter.

2.5 Experiments cited in literature

In this section, various experimental set-ups for the measurement of thermal conductivity, viscosity and convective heat transfer, used by many researchers are discussed.

2.5.1 Thermal conductivity

There are two types of methods of measuring thermal conductivity of liquids: steady-state methods and transient methods. The disadvantages of steady-state methods are that

- Heat lost cannot be quantified and may give considerable inaccuracy, and
- Natural convection may set in,
- This gives higher apparent values of conductivity.

Therefore, to measure thermal conductivity accurately it is best to use transient methods.

Transient hot-wire method used by [74, 75, 76, 77 & 78] to measure the thermal conductivity of nanofluids is shown in Fig. 2.1.

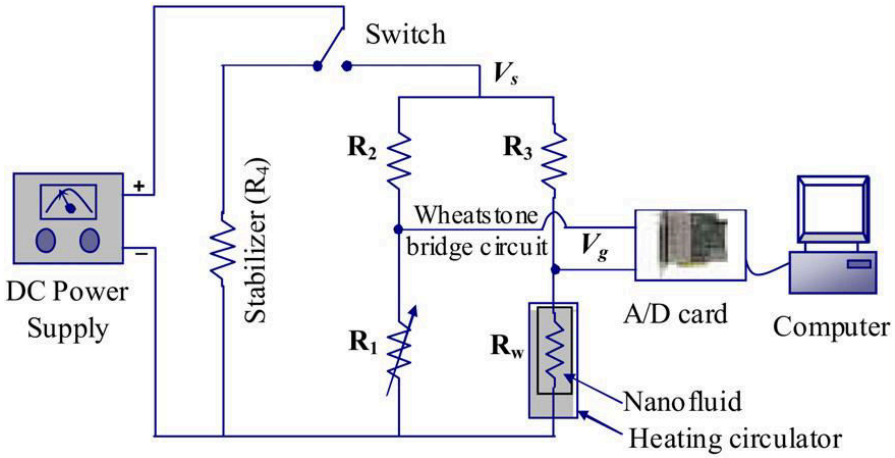

Fig. 2.1: Transient hot-wire

Temperature oscillation method used by [79] to measure the thermal conductivity of nanofluids is shown in Fig. 2.2.

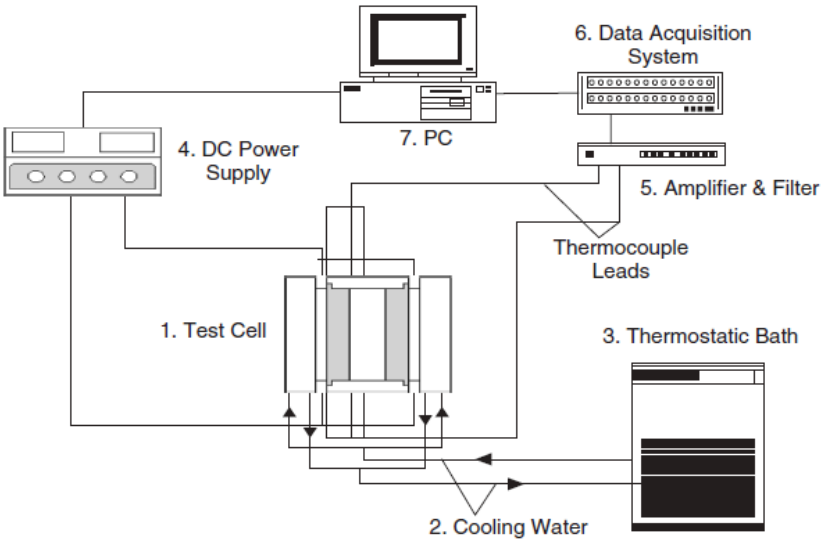

Fig. 2.2: Temperature oscillation

The Decagon devices KD2 Pro Thermal property analyzer used by [80] to measure thermal conductivity of water based nanofluids. As the determination of temperature-dependent values of thermal conductivity of nanofluids, they placed fluid specimen inside a heated, insulated enclosure, as shown in Fig. 2.3.

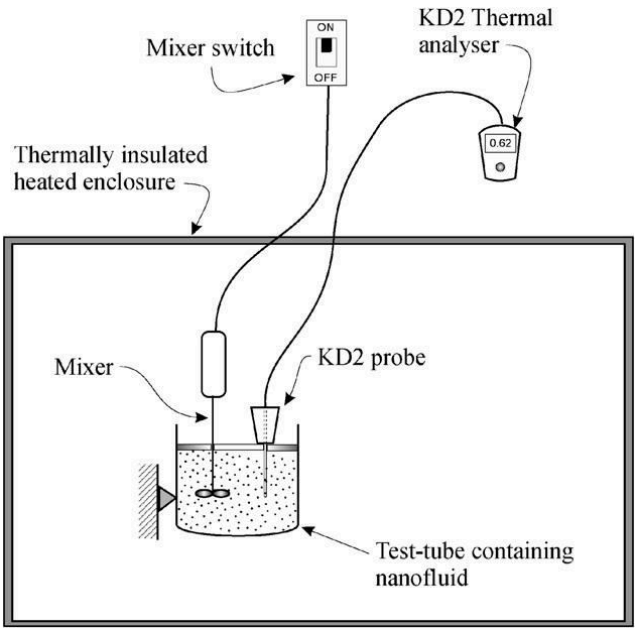

Fig. 2.3: KD2 Pro Thermal property analyzer for temperature dependent measurement

2.5.2 Viscosity

The set-up used by [81] for the viscosity measurements of the copper oxide nanoparticles suspended in an ethylene glycol–water mixture is shown by Fig. 2.4. It consists of an LVDV-II+ Brookfield programmable viscometer and Julabo temperature-controlled bath with a computer to control temperature.

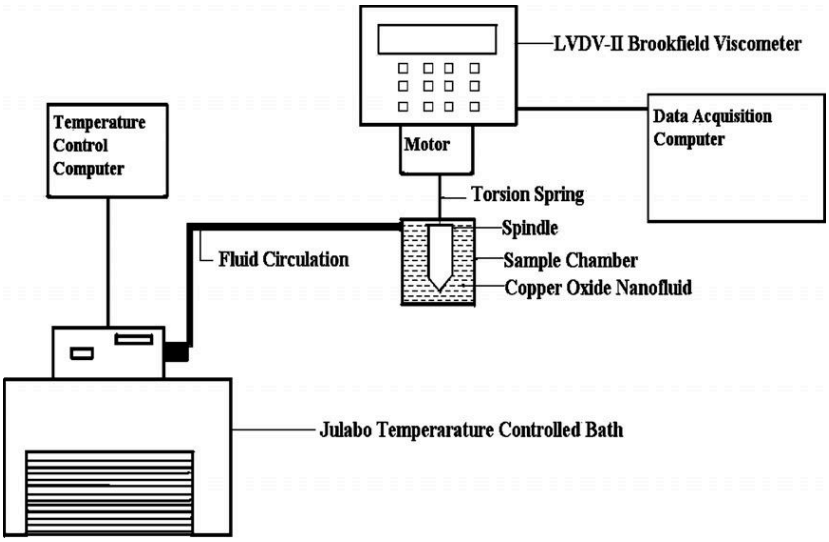

Fig. 2.4: Experimental setup for viscosity measurement of nanofluids.

2.5.3 Convective heat transfer coefficient

The experimental investigation of convective heat transfer coefficient of Al_2O_3 nanofluids at the entrance region under laminar flow conditions is done by [82]. The experimental set up used by them is shown in Fig. 2.5.

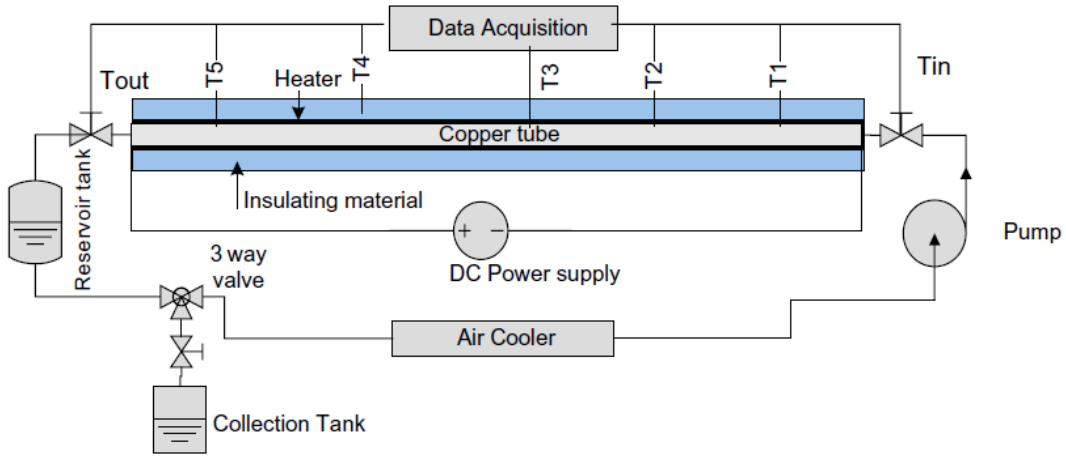

Fig. 2.5: Experimental System for convective heat transfer coefficient of Al_2O_3 nanofluids

The work on the heat transfer characteristics of γ-Al_2O_3/water and TiO_2/water nanofluids in a shell and tube heat exchanger under turbulent flow condition is done by [83]. The flow loop of constructed system used by them is shown by Fig. 2.6.

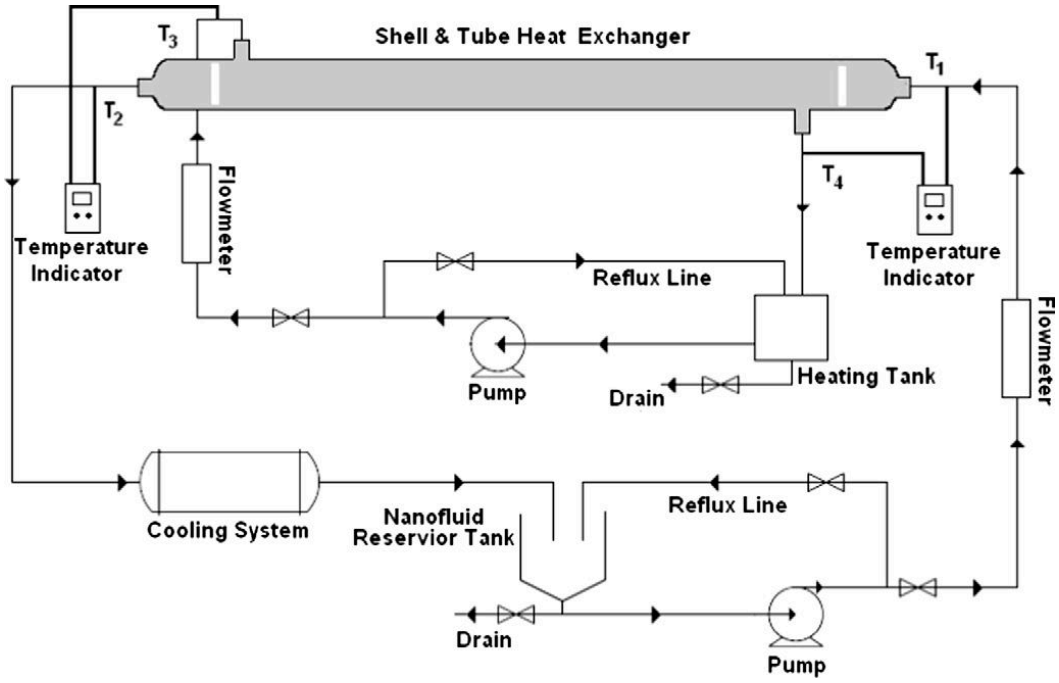

Fig. 2.6: Experimental setup for heat transfer characteristics of γ-Al_2O_3/water and TiO_2/water nanofluids

The formulation of nanofluids for natural convective heat transfer applications is done by [84]. The experimental system used by them, is shown schematically in Fig. 2.7.

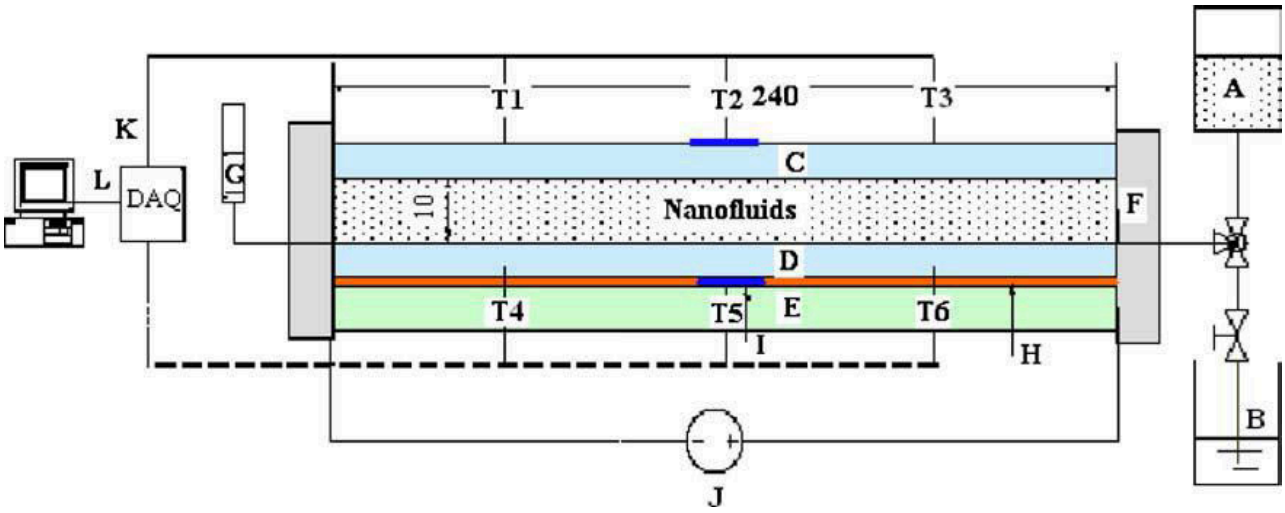

Fig. 2.7: Experimental setup for natural convective heat transfer

2.6 Experimental investigation

In this section, the experimental results for thermal conductivity, viscosity and other physical properties done by many researchers are discussed.

2.6.1 Measurement of thermal conductivity

Several experimental studies were conducted in the literature to measure the thermal conductivity of nanofluids using different techniques such as transient hot wire, steady-state parallel plates, and temperature oscillation. Among these the Transient hot-wire method has been used most extensively. A comparison of the experimental thermal conductivity enhancements of Al_2O_3 nanofluids cited in the literature [65] is given by Table 2.3. Al_2O_3 and CuO are the most common nanoparticles used in the literature.

A general correlation for the effective thermal conductivity of Al_2O_3–water and CuO–water nanofluids at ambient temperature accounting for various volume fractions and nanoparticles diameters is obtained by the [65] using the available experimental data in the literature. This model can be expressed as:

$$\frac{k_{eff}}{k_f} = 1.0 + 1.0112\ \emptyset_P + \ 2.4375\ \emptyset_P \left(\frac{47}{d_p\ (nm)}\right) - \ 0.0248\ \emptyset_P \left(\frac{k_P}{0.613}\right) \qquad (2.21)$$

Where k_f is the thermal conductivity of water.

Thermal conductivity measurements at different temperatures are essential because the measurements at ambient temperature are not adequate for estimating the heat transfer characteristics.

Table 2.3: Comparison of the experimental thermal conductivity enhancements of Al_2O_3 nanofluids cited in the literature [65]

Sr. No.	Base fluid	D_p (nm)	$\emptyset_p$ (%)	% Thermal conductivity enhancement	Method
1.	Water	38.4	4	9.4% (21 °C) , 24.3% (51 °C)	Temperature oscillation
2.	Water	131	4	24.0% (51 °C)	Steady-state parallel plates
3.	Water	13	4.4	33%	Transient hot wire
4.	Water	38.4	4.3	11%	Transient hot wire
5.	EG	38.4	5	19%	Transient hot wire
6.	Water	28	5.5	16%	Steady-state parallel plates
7.	EG	28	5	24.5%	Steady-state parallel plates
8.	Water	11	1	14.8% (70 °C)	Transient hot wire
9.	Water	47	1	10.2% (70 °C)	Transient hot wire
10.	Water	150	1	4.8% (60 °C)	Transient hot wire
11.	Water	47	4	28.8% (70 °C)	Transient hot wire
12.	Water	36	6	28.2%	Steady-state parallel plates
13.	Water	47	6	26.1%	Steady-state parallel plates
14.	Water	20	5	15%	Transient hot wire
15.	Water	11	5	8%	Transient hot wire
16.	Water	20	5	7%	Transient hot wire
17.	Water	40	5	10%	Transient hot wire

A general correlation is developed for Al_2O_3 water nanofluid by the [65] using the available experimental data at various temperatures, nanoparticle's diameter, and volume fraction. The developed correlation is expressed in terms of nanoparticle's diameter, volume fraction, dynamic viscosity of water, effective dynamic viscosity of the nanofluid, and temperature as follows:

$$\frac{k_{eff}}{k_f} = 0.9843 + 0.398\,{\emptyset_P}^{0.7383}\left(\frac{1}{d_P\,(nm)}\right)^{0.2246}\left(\frac{\mu_{eff}\,(T)}{\mu_f\,(T)}\right)^{0.0235} - 3.9517\,\frac{\emptyset_P}{T} + 34.034\,\frac{\emptyset_p^2}{T^3} + 32.509\,\frac{\emptyset_P}{T^2} \quad (2.22)$$

$$0 \le \emptyset_P \le 10\%, \quad 11nm \le d \le 150nm, \quad 20°C \le T \le 70°C\%,$$

Where the dynamic viscosity (Pa-sec) of water at different temperatures can be expressed as:

$$\mu_f\,(T) = 2.414 \times 10^{-5} \times 10^{247.8/(T-140)} \quad (2.23)$$

2.6.1.1 Effect of Volume fraction and particle size

In the past few years, many experimental investigations on the thermal conductivity of nanofluids have been reported. The effective thermal conductivities of nanofluids containing different concentrations, materials and sizes of nanoparticles dispersed in different base fluids have been experimentally investigated. The published results on the thermal conductivity of nanofluids at room temperature are summarized in Table 2.4.

Table 2.4: Summary of volume fraction/particle size dependent thermal conductivity of nanofluids.

Sr. No.	Researchers	Nanofluids [Particle (Size in nm) / base fluid]	Observations
1.	Eastman et al. [20]	Al_2O_3/CuO/Cu (33/36/18) / Water, HE-200 oil	60% improvement for 5 vol% CuO particles in water
2.	Lee et al. [23]	Al_2O_3/CuO, (24.4/18.6/23.6) / Water, EG	20% improvement for 4 vol% CuO/EG mixture
3.	Wang et al. [24]	Al_2O_3/CuO (28/23) / Water, EG,PO,EO	12% improvement for 3 vol% Al_2O_3/water nanofluids
4.	Das et al. [85]	Al_2O_3/CuO (38.4/28.6) / Water	2-4 fold increase over range of 21°C to 52 °C
5.	Xie et al. [86]	Al_2O_3 (12.2 – 30.2) / Water, EG, PO	pH value, SSA, crystalline phase
6.	Li and Peterson [87]	Al_2O_3/CuO (36/29) / Water	enhancement with volume fraction and temperature
7.	Xuan and Li [35]	Cu (100) / Water, Oil	successful suspension of relatively big metallic nanoparticles
8.	Eastman et al. [88]	Cu (< 10) / EG	40% increase for 0.3 vol% Cu-based nanofluids
9.	Hong et al. [89]	Fe (10) / EG	18% increase for 0.55 vol% Fe/EG nanofluids.
10.	Patel et al. [90]	Au, Ag (4, 15/70) / Water, Toluene	Size, temperature and chemical characteristics
11.	Murshed et al. [25]	TiO_2 $(\emptyset\ 10 \times 40, \emptyset\ 15)$ / DW	33% and 30% increase at 5 vol% for $\emptyset\ 10 \times 40$ and $\emptyset\ 15$, respectively.
12.	Xie et al. [91,92]	SiC $(\emptyset\ 26, 600)$ / Water, EG	15.8% increase at 4.2 vol% for $\emptyset\ 26$ SiC-H_2O and 22.9% at 4 vol% for $\emptyset\ 600$ SiC-H_2O
13.	Choi et al. [26]	MWNTs $(\emptyset\ 25 \times 50\ \mu m)$/Oil	exceed 250% at 1.0 vol%
14.	Biercuk et al. [93]	SWNTs $(\emptyset\ 3 - 30)$ / Epoxy	125% at 1.0 wt%
15.	Xie et al. [94]	TCNTs $(\emptyset\ 15 \times 30\ \mu m)$/ DW, EG, DE	19.6%, 12.7% and 7.0% increase at 1.0 vol% for TCNT/DE, EG and DW respectively
16.	Choi et al. [95]	SWNTs $(\emptyset\ 20 - 30 \times 200)$/Epoxy	300% at 3 wt% SWNT loading.
17.	Assael et al. [96,97 & 98]	MWNTs, DWNTs $(\emptyset\ 130 \times 10\ \mu m)$/Water	34% increase for 0.6 vol% suspension.
18.	Liu et al. [99]	CNTs $(\emptyset\ 20 - 30\ \mu m)$/EG, EO	12.4% for EG at 1 vol%, 30% for EO at 2 vol%

2.6.1.2 Effect of fluid temperature

Fluid temperature may play an important role in enhancing the effective thermal conductivity of nanofluids. Despite the fact that nanofluids may be used under various temperatures, very few studies were performed to investigate the temperature effect on the effective thermal conductivity of nanofluids. A summary of the published results on temperature-dependent thermal conductivity of various nanofluids is provided in Table 2.5.

Table 2.5: Summary of temperature-dependent thermal conductivity of nanofluids

Sr. No.	Researchers	Nanofluids [particle (size in nm) / base fluid]	Observation
1.	Das et al. [100]	Al_2O_3 (38.4) / water CuO (28.6) / water	for 4 vol%: 16% at 36°C & 25% at 51°C for 1 vol%: 22% at 36°C & 30% at 51°C
2.	Patel et al. [101]	Au (10-20) / water	for 0.00026 vol%: 5-21% at temp range of 30-60°C
3.	Chon and kihm [102]	Al_2O_3 (47) / water Al_2O_3 (150) / water	6% at 31°C & 11% at 51°C 3% at 31°C & 8.5% at 51°C [for 1 vol%]
4.	Li and Peterson [103]	Al_2O_3 (36) / water	for 2 vol%: 7% at 27.5°C and 23% at 36°C
5.	Yang and Han [104]	Bi_2Te_3 (20*70) / FC 72 / oil	For Bi_2Te_3 / FC 72 at 0.8 vol%: 8% at 10°C and 7% at 40°C
6.	Venerus et al. [105]	Au(22) / water , Al_2O_3 (30) / petroleum oil	No enhancement but slight decrease with the temperature in the range of 25-75°C
7.	Murshed et al. [106]	Al_2O_3 (80) / EG Al_2O_3 (80) / DIW Al_2O_3 (150) / DIW Al_2O_3 (80) / EO	1 vol%: 11.4% at 60°C 1 vol%: 12.1% at 60°C 1 vol%: 10.3% at 60°C 3 vol%: 37.0% at 60°C

2.6.2 Measurement of viscosity

Most published studies have focused on the heat transfer behavior and stability of nanofluids in the past 10years. In fact, viscosity is one of the key properties of nanofluids. It is believed that viscosity is as critical as thermal conductivity in engineering systems because the nanofluid was expected to show an increase in thermal conductivity without an increase in pressure drop, which in turn is related to fluid viscosity. Among the few studies about viscosity of nanofluids, the problems concerned by investigators are mainly focused on the factors influencing the viscosity of nanofluids. These factors include concentration and size of nanoparticles, temperature of nanofluids and shear rate etc.

Prasher et al. [107] investigated the viscosity of alumina-based nanofluids. The experimental results showed that the relative viscosity of alumina-based nanofluids was not a strong function of temperature and nanoparticle diameter, but is a strong function of nanoparticle volume fraction. Li et al. [108] measured the viscosity of water with CuO nanoparticle suspensions using a capillary viscometer. Results showed that the apparent viscosity of nanofluids decreased with increasing

temperature and increased somewhat with increasing concentration of the nanoparticles, the effect of concentration was not as obvious as the effect of temperature. However, as they pointed out, the capillary tube diameter may influence the apparent viscosity for higher nanoparticle mass fractions, especially at lower temperatures.

Chen et al. [109] investigated ethylene glycol based titania nanofluids and found that the nanofluids showed Newtonian behavior over a shear rate range of 0.5–10^4 s^{-1} at 293 – 333 K. The shear viscosity of the nanofluids depends strongly on temperature and the particle's concentration. Guo [110] measured the viscosity of copper oxide dispersed in ethylene glycol and water mixture and got the similar results. Nguyen et al. [111] investigated experimentally the influence of both the particle size and the temperature on dynamic viscosities of water-based nanofluids, namely Al_2O_3–water and CuO–water mixtures.

Wang et al. [112] also measured the relative viscosity of Al_2O_3-water and Al_2O_3-ethylene glycol nanofluids. Results showed a similar trend of increase of relative viscosity with increasing solid volume fraction for the two nanofluids. That means that the desirable heat transfer increase may be offset by the undesirable increase in pressure drop. Das et al. [113] also measured the viscosity of Al_2O_3-water nanofluids against shear rate. Their results showed an increase of viscosity with increased particle concentrations. There is a strong possibility that nanofluids may be non-Newtonian, even viscoelastic in some cases. Further experimental studies are needed to define the viscosity models of nanofluids so they can be used in simulation studies.

The viscosity of CNT-water nanofluids as a function of shear rate was measured by Ding et al. [114] recently. They observed that the viscosity of nanofluids increased with increasing CNT concentration and decreasing temperature. Also, the shear thinning behavior was found by the authors. That means the nanofluids can provide better fluid flow performance due to the higher shear rate at the wall, which results in low viscosity there.

2.6.3 Measurement of density

Vajjha et al. [115] measured the density of three different nanofluids containing aluminium oxide, antimony-tin oxide and zinc oxide nanoparticles in a base fluid of 60:40 EG/W, using the Anton Paar digital density meter. These measurements were compared with the theoretical equation given by Pak and Cho.

$$\rho_{nf} = \rho_p \emptyset + \rho_{bf} (1 - \emptyset) \tag{2.24}$$

The density of nanofluid increases with an increase in the volumetric concentration of the particles as their densities are higher than that of the base fluid. The density of nanofluid decreases very

modestly with temperature mostly due to the effect on the fluid. To compare the increase in densities, we calculate using equation (2.24) the values for CuO, Al_2O_3 and SiO_2 nanofluids. By the addition of 2% volume of nanoparticles at 323 K, the densities of CuO, Al_2O_3 and SiO_2 nanofluids increases by 10.14, 4.73, 2.15 % respectively in comparison to the base fluid. This is due to the higher densities of nanoparticles (CuO = 6500 kg/m^3, Al_2O_3 = 6500 kg/m^3, SiO_2 = 2200 kg/m^3) compared to the base fluid.

2.6.4 Measurement of specific heat

Vajjha and Das [116] carried out measurements of specific heat of three different nanofluids (Al_2O_3, SiO_2 and ZnO) to develop appropriate correlations. From their experimental data, they developed a general correlation given by equation (2.25), where the values of A, B and C are given in Table 2.6.

$$\frac{C_{pnf}}{C_{pbf}} = \frac{\left(A\,(T/T_o) + B\left(C_{pp}/C_{pbf}\right)\right)}{(C + \emptyset)} \tag{2.25}$$

Table 2.6: Curve-fit coefficients for specific heat of different nanofluids.

Sr. No.	Nanofluid	A	B	C
1.	Al_2O_3	0.24327	0.5179	0.4250
2.	SiO_2	0.48294	1.1937	0.8021
3.	ZnO	0.12569	0.9855	0.299

As the temperature of nanofluid increases, the effective specific heat also increases very modestly indicating that nanofluid possess slightly better thermal capacity at higher temperature.

2.6.5 Measurement of thermal diffusivity

While the determination and prediction of the effective thermal conductivity of nanofluids have attracted much attention in recent years, very little work has been performed on the thermal diffusivity of nanofluids, which is especially important in convective heat transfer applications. Xuan and Roetzel [117] discussed the effective thermal diffusivity tensor for flowing fluids under both laminar and turbulent flow conditions. However, neither experimental nor theoretical result for the effective thermal diffusivity of nanofluids was provided in their paper. Wang et al. [118] measured the thermal conductivity and specific heat of some nanofluids and thereby calculated their effective thermal diffusivity. Their calculated results were also found to fluctuate severely with volume fraction.

Murshed et al. [119] studied the effective thermal diffusivity of several types of nanofluids at different volume percentages (1–5%) of titanium dioxide (TiO_2), aluminium oxide (Al_2O_3) and aluminium (Al) nanoparticles in ethylene glycol and engine oil. The thermal diffusivities of these

nanofluids measured directly by a novel transient double hot-wire technique were found to increase substantially with increased volume fraction of nanoparticles in base fluids. For example, for maximum 5% volumetric loading of TiO_2 nanoparticles of 15 nm and 10*40 nm in ethylene glycol, the maximum increase was observed to be 25% and 29%, respectively. Nanofluids with aluminium nanoparticles in ethylene glycol and engine oil showed substantial enhancement of thermal diffusivity i.e. maximum 49% and 36%, respectively compared to their base fluids.

2.6.6 Measurement of surface tension

Studies on surface tension of nanofluids are limited in the literature [120–124]. Golubovic et al. [120] showed experimentally that the surface tension of Al_2O_3–water nanofluid does not change for concentrations of nanoparticles considered in their work (0 – 0.01 g/l) and the surface tension is approximately equal to surface tension of pure water at T = 24 °C. Xue et al. [121] showed insignificant effect of carbon nanotube nanofluid on surface tension compared with pure water. Similarly, Kim et al. [122] found that the surface tension of Al_2O_3–water nanofluids (0.1% volume fraction) differed negligibly from those of pure water.

The effect of temperature on the surface tension of nanofluids was studied by Murshed et al. [123]. Their experimental results showed that nanofluids having TiO_2 nanoparticles of 15 nm diameter in deionized water exhibit substantially lower surface tension than those of the base fluid (i.e. deionized water). Similarly, Zhu et al. [124] showed that the surface tension of nanofluids was highly dependent on the temperature. One can note from the above that as expected temperature plays a significant role on the surface tension of nanofluids.

2.6.7 Measurement of convective heat transfer

The past decade has seen many research activities in the experimental heat transfer characteristics of various nanofluids. As there is a considerable enhancement of thermal conductivity, it is expected that the convective heat transfer in nanofluids will also be enhanced. A brief summary of experiments on convective heat transfer of nanofluids is given in Table 2.7.

2.7 Application of nanofluids

Experimentally and theoretically nanofluids have been shown to possess improved heat transport properties and higher energy efficiency in a variety of thermal exchange systems for different industrial applications, such as transportation, electronic cooling, military, nuclear energy, aerospace etc. Nanofluid research could lead to a major impact in developing next generation coolants for numerous engineering and medical applications. The above applications are stated and briefly discussed.

Table 2.7: Summary of experiments on convective heat transfer of nanofluids.

Sr. No.	Investigator	Geometry	Nanofluids	Findings
	Forced convective heat transfer:			
1.	Lee and Choi [125]	Parallel channels	Unspecified	Reduction in thermal resistance by a factor of 2
2.	Xuan and Li [126]	Tube (D = 10, L = 800 mm)	Cu/water	Turbulent, large enhancement of heat transfer coefficient $Nu_{nf} = c_1 (1.0 + c2\,\emptyset m1 . Pedm2\, Renfm3.$
3.	Wen and Ding [127]	Tube (D = 4.5, L = 970 mm)	Al_2O_3/water (27-56 nm)	Laminar, enhancement increases with Reynolds No. & particle concentration
4.	Chien et al. [128]	Disk-shaped heat pipe (D = 9, H = 2 mm)	Au/water (17 nm)	Significant reduction of thermal resistance
5.	Tsai et al.[129]	Heat pipe (D = 6, L = 170 mm)	Au/water (2-35, 15-75 nm)	High potential to take place conventional fluids in heat pipe applications
6.	Ding et al. [130]	Tube (D = 4.5, L = 970 mm)	CNT/water	Significant enhancement of convective heat transfer, which depends on the flow condition, CNT concentration & pH level.
7.	Pak and Cho [69]	Tube	Al_2O_3 (13 nm), TiO_2 (27 nm)/water	h with $\emptyset$ = 0.03 vol% was 12% lower than that of pure water for a given average fluid velocity.
8.	Yang et al. [72]	Tube (D = 4.57, L = 457 mm)	Graphite Nanofluid	The enhancement of h is lower than the increase of the effective thermal conductivity.
9.	Heris et al. [131]	Annular tube (D_{in} =11 mm, D_{out} = 32 mm, L = 1 m)	Al_2O_3 (20 nm), CuO (50-60 nm) /water	Enhancement of h with $\emptyset$ and Pe. Al_2O_3 showed more enhancement than CuO
	Natural convective heat transfer:			
1.	Putra et al. [132]	Horizontal Cylinder	CuO (87.3nm), Al_2O_3(11.2nm) /water	A systematic and significant deterioration in natural convection heat transfer
2.	Wen and Ding [133]	Two horizontal discs (H = 10, D = 240 mm)	TiO_2/water (30-40 nm)	Deterioration increases with particle concentrations

2.7.1 Heat transportation

The mixture of ethylene glycol and water is almost a universally used vehicle coolant due to its lowered freezing point as well as its elevated boiling point. The thermal conductivity of ethylene glycol is relatively low compared to that of water, while the engine oils are much worse heat transfer fluids than ethylene glycol in thermal transport performance. The addition of nanoparticles

and nanotubes to these coolants and lubricants to form nanofluids can increase their thermal conductivity, and give the potential to improve the heat exchange rates and fuel efficiency. The above improvements can be used to reduce the size of the cooling systems or remove the heat from the vehicle engine exhaust in the same cooling system.

Tzeng et al. [135] have conducted research to study the effects of nanofluids in the cooling of automatic transmission. They dispersed CuO & Al_2O_3 nanoparticles and antifoam agents in the transmission fluid, and then, the transmission fluid was used in real time four wheel automatic transmissions. The results show that CuO nanofluids have the lowest temperature distribution at both high and low rotating speed and accordingly the best heat transfer effect.

2.7.2 Electronics cooling

The power dissipation of IC (Integrated Circuits) and microelectronic components has dramatically increased due to their size reduction. Better thermal management and cooling fluids with improved thermal transport properties are needed for safe operation. Nanofluids have been considered as working fluids in heat pipes for electronic cooling application.

Tsai et al. [136] were probably the first to show experimentally that the thermal performance of the heat pipe can be enhanced when nanofluids are used. Gold nanoparticles with a particle size of 17nm dispersed in water were used as a working fluid in a disk shaped miniature heat pipe. The result shows that the thermal resistance of the disk shaped miniature heat pipe is reduced by nearly 40% when nanofluids are used instead of de-ionized (DI) water.

Kang et al. [137] measured the temperature distribution and thermal resistance of a conventional grooved circular heat pipe with water based nanofluids containing 1 to 50 ppm of 35nm silver nanoparticles. The result shows that at the same charge volume, the thermal resistance of the heat pipe with nanofluids is reduced by 10% to 80% compared with that of DI water at an input power of 30 to 60 W. The results are compared with those of Wei et.al [138]. They show that the maximum reduction in the thermal resistance of the heat pipe is 50% for 10nm silver nanoparticles and 80% for 35nm silver nanoparticles.

Chein and Huang [134] numerically tested the performance of nanofluids as coolants in silicon micro channels. The nanofluids they used were water suspensions of Cu nanoparticles at various particle loadings. They found that the performance of the micro channel heat sink was greatly improved due to the increased thermal conductivity and thermal dispersion effects, as well as that the presence of the nanoparticles in water did not cause much pressure drop due to the small volume fraction of the solid particles.

Ma et al. [139] were the first to develop an ultrahigh performance chip cooling device called the nanofluid oscillating heat pipe. The conventional heat pipe with an oscillating motion generated by the variable frequency shaker dramatically increased the heat removal rate in capillary tubes. However, the use of the mechanically driven shaker limits these applications to chip cooling in practice.

2.7.3 Military applications

Military hardware both mechanical and electrical devices dissipates a large amount of heat and consequently requires high heat flux cooling fluids having sufficient cooling capacity. Nanofluids have the capability to provide the required cooling capacity in such applications, as well as in other military applications, including submarines and high power laser.

2.7.4 Medical application

Nanofluids are now being developed for medical applications, including cancer therapy. Iron based nanoparticles can be used as delivery vehicle for drugs or radiation without damaging the neighbouring healthy tissues by guiding the particles up the blood stream to the tumor locations with magnets. Nanofluids could be used to produce higher temperatures around tumors, to kill cancerous cells without affecting the nearby healthy cells [140]. Nanofluids could also be used for safer surgery by cooling around the surgical region, thereby enhancing the patient's health and reducing the risk of organ damage.

2.8 Conclusions

This chapter presents an overview of the recent developments in the study on heat transfer using nanofluids. Many important, complex and interesting phenomena involving nanofluids have been reported in literature. Researchers investigate have given much attention on the thermal conductivity rather than heat transfer characteristics. The use of nanofluids in a wide range of applications appears promising, but the development of the field faces several challenges: 1). The lack of agreement between experimental results from different groups; 2). The often poor performance of suspension; and 3). Lack of theoretical understanding of the mechanisms. Further theoretical and experimental research investigations are needed to understand the heat transfer characteristics of nanofluids and identify new and unique applications of these fields.

Gaps identified from the literature survey

Very few have found thermal conductivity of fluid mixture and compare their values at different temperatures. Limited work has been reported on the density of nanofluids at different temperatures. No work has been reported in Viscosity measurement by Ubbelohde viscometer at different temperatures.

Therefore, the aim of present work is to study the:

1. The thermal conductivity of distilled water (DW), ethylene glycol (EG) and fluid mixture distilled water and ethylene glycol based nanofluids and its variation with temperature.
2. The density and viscosity of distilled water (DW), ethylene glycol (EG) and fluid mixture distilled water and ethylene glycol based nanofluids and its variation with temperature.
3. The particle size distribution of various concentrations of nanofluids.

References

1. Keblinski, P., Eastman, J.A., and Cahill, D.G., Nanofluids for thermal transport, Mater. Today, vol. 8, no. 6, pp. 36–44, 2005.
2. Choi, S. U. S., and Eastman, J. A., Enhancing thermal conductivity of fluids with nanoparticles, in: Conference: 1995 International Mechanical Engineering Congress and Exhibition, San Francisco, CA (United States), 12-17 Nov 1995, ASME, San Francisco, pp. 99–105, 1995.
3. Goldstein, R. J., Joseph, D. D., and Pui, D. H., Convective Heat Transport in Nanofluids, proposal, Faculty of Aerospace Engineering and Mechanics, University of Minnesota, Minnesota, September 2000.
4. Trisaksri, V. and Wongwises, S., Critical review of heat transfer characteristics of the nanofluids, Renew. Sustain. Energy Rev, vol. 11, pp. 512–523, 2007.
5. Beck, M. P., Thermal Conductivity of Metal Oxide Nanofluids, Georgia Institute of Technology, Georgia, 2008.
6. Wang, X.-Q., Mujumdar, A.S., Heat transfer characteristics of nanofluids: a review, Int. J. Therm. Sci., vol. 46, no. 1, pp. 1–19, 2007.
7. Duangthongsuk, W., and Wongwises, S., A critical review of convective heat transfer of nanofluids, Renew. Sustain. Energy Rev., vol. 11, pp. 797–817, 2007.
8. Godson, L., Raja, B., Lal, D. M., and Wongwises, S., Enhancement of heat transfer using nanofluids – an overview, Renew. Sustain. Energy Rev., vol. 14, no. 2, pp. 629–641, 2010..
9. Li, Y., Zhou, J.E., Tung, S., Schneider, E., and Xi, S., A review on development of nanofluid preparation and characterization, Powder Technol., vol. 196, no. 2, pp. 89–101, 2009.
10. Wen, D., Lin, G., Vafaei, S., and Zhang, K., Review of nanofluids for heat transfer applications, Particuology, vol. 7, no. 2, pp. 141–150, 2009.
11. Leong, K. Y., Saidur, R., Kazi, S. N., and Mamun, A. H., Performance investigation of an automotive car radiator operated with nanofluid-based coolants (nanofluid as a coolant in a radiator), Appl. Therm. Eng., vol. 30, no. 17-18, pp. 2685–2692, 2010.
12. Duangthongsuk, W., and Wongwises, S., Comparison of the effects of measured and computed thermophysical properties of nanofluids on heat transfer performance, Exp. Therm. Fluid Sci,. vol. 34, no. 5, pp. 616–624, 2010.

13. Kimoto K. , Kamiliya, Nonoyama M., and Uyeda R., An electron microscope study on fine metal particles prepared by evaporation in argon gas at low pressure, Jpn. J. Appl. Phys., vol. 2, pp. 702, 1963.
14. Granqvist C. G., and Buhrman R. A., Ultrafine metal particles, J. Appl. Phys., vol. 47, pp. 2200, 1976.
15. Gleiter H., Nanocrystalline materials, Prog. Mater. Sci., vol. 33, pp. 223 – 315, 1989.
16. Suslick K. S., Fang M., and Hyeon T., J. Am. Chem. Soc., vol. 118, pp. 11960, 1996.
17. Chopkar M., Das P.K., and Manna I., Synthesis and Characterization of nanofluids for heat transfer applications, Scr. Mater., vol. 55, pp. 549-552, 2006.
18. Akoh, H., Tsukasaki, Y., S.Yatsuya, and Tasaki, A., Magnetic properties of ferromagnetic ultrafine particles prepared by vacuum evaporation on running oil substrate, Journal of Crystal Growth, vol. 45, pp. 495–500, 1978.
19. Wagener, M., Murty, B. S., and Gunther, B., Preparation of metal nanosuspensions by high pressure DC-sputtering on running liquids, In Komarnenl, S., Parker, J. C., and Wollenberger, H. J. (Editors), Nanocrystalline and Nano composite Materials II, Materials Research Society, Pittsburgh, PA, vol. 457, pp. 149–154, 1997. .
20. Eastman, J. A., Choi, S. U. S., Li, S., Thompson, L. J., and Lee, S., Enhanced thermal conductivity through the development of nanofluids, Volume 457 of Materials Research Society Symposium - Proceedings, 3–11. Materials Research Society, Pittsburgh, PA, USA, Boston, MA, USA, 1997.
21. Zhu, H., Lin, Y., and Yin, Y., A novel one-step chemical method for preparation of copper nanofluids, Journal of Colloid and Interface Science, vol. 227, pp. 100–103, 2004.
22. Lo, C.-H., Tsung, T.-T., and Chen, L.-C., Shape controlled synthesis of Cu-based nanofluid using submerged arc nanoparticle synthesis system (SANSS). Journal of Crystal Growth, vol. 277, no. 1-4, pp. 636–642, 2005.
23. Lee, S., Choi, S. U. S., Li, S., and Eastman, J. A., Measuring thermal conductivity of fluids containing oxide nanoparticles, Journal of Heat Transfer, vol. 121, pp. 280–289, 1999.
24. Wang, X., Xu, X., and Choi, S. U. S., Thermal conductivity of nanoparticle-fluid mixture. Journal of Thermophysics and Heat Transfer, vol. 13, no. 4, pp. 474–480, 1999.
25. Murshed, S. M. S., Leong, K. C., and Yang, C., Enhanced thermal conductivity of TiO_2 – Water based nanofluids, International Journal of Thermal Sciences, vol. 44, no. 4, pp. 367–373, 2005.
26. Choi S.U.S., Zhang Z.G., Yu W., Lockwood F.E., and Grulke E. A., Anomalous thermal conductivity enhancement in nanotubes suspensions, Appl. Phys. Lett., vol. 79, pp. 2252-2254, 2001.
27. Xuan, Y., and Li, Q., Heat transfer enhancement of nanofluids, International Journal of Heat and Fluid Transfer, vol. 21, pp. 58–64, 2000.
28. Hwang, Y. J., Ahn, Y. C., Shin, H. S., Lee, C. G., Kim, G. T., Park, H. S., and Lee, J. K., Investigation on characteristics of thermal conductivity enhancement of nanofluids. Current Applied Physics, vol. 6, no. 6, pp. 1068–1071, 2005.
29. Li, X., Zhu, D., and Wang, X., Evaluation on dispersion behavior of the aqueous copper nanosuspensions. Journal of Colloid and Interface Science, vol. 310, no. 2, pp. 456–463, 2007.
30. Hwang, Y. J., Lee, J. K., Lee, C. H., Jung, Y. M., Cheong, S. I., Lee, C. G., Ku, B. C., and Jang, S. P., Stability and thermal conductivity characteristics of nanofluids. Thermochimica Acta, vol. 455, no. 1-2, pp. 70–74, 2007.
31. Maxwell, J. C., A Treatise on Electricity and Magnetism, 2nd ed., Clarendon Press: Oxford, UK, 1881.
32. Hamilton, R. L., and Crosser, O. K., Thermal conductivity of heterogeneous two component systems, I&EC Fundam., vol. 1, pp. 182, 1962.
33. Keblinski, P., Phillpot, S. R., Choi, S. U. S., and Eastman, J. A., Mechanisms of heat flow in suspensions of nano-sized particles (nanofluids), Int. J. Heat Mass Transfer, vol. 45, pp. 855, 1962.

34. Eastman, J. A., Phillpot, S. R., Choi, S. U. S., and Keblinski, P.. Thermal transport in nanofluids, Annu. Rev. Mater. Res., vol. 34, pp. 219, 2004.
35. Xuan, Y. and Li, Q., Heat transfer enhancement of nanofluids, International Journal of Heat and Fluid Transfer, vol. 21, pp. 58–64, 2000.
36. Yu, W. and Choi, S. U. S., The role of interfacial layers in the enhanced thermal of nanofluids: a renovated Maxwell model, Journal of Nanoparticle Research, vol. 5, no. 1-2, pp. 167–171, 2003.
37. Yu, W. and Choi, S. U. S., The role of interfacial layers in the enhanced thermal conductivity of nanofluids: A renovated Hamilton-Crosser model. Journal of Nanoparticle Research, vol. 6, no. 4, pp. 355– 361,2004.
38. Xue, L., Keblinski, P., Phillpot, S. R., Choi, S. U. S., and Eastman, J. A., Effect of liquid layering at the liquid-solid interface on thermal transport, International Journal of Heat and Mass Transfer, vol. 47, no. 19-20, pp. 4277–4284, 2004.
39. Khaled, A. R. A., and Vafai, K., Heat transfer enhancement through control of thermal dispersion effects, International Journal of Heat and Mass Transfer, vol. 48, no. 11, pp. 2172, 2005.
40. Koo, J., and Kleinstreuer, C., Impact analysis of nanoparticle motion mechanisms on the thermal conductivity of nanofluids. International Communications in Heat and Mass Transfer, vol. 32, no. 9, pp. 1111–1118, 2005.
41. Tillman, P. and Hill, J. M., Determination of nanolayer thickness for a nanofluid. International Communications in Heat and Mass Transfer, In Press, Uncorrected Proof, 2007.
42. Evans, W., Fish, J., and Keblinski, P., Role of Brownian motion hydrodynamics on nanofluid thermal conductivity, Applied Physics Letters, vol. 88, no. 9, pp. 93,116–1–3, 2006.
43. Bruggeman, D. A. G., Berechnung verschiedener physikalischer konstanten von heterogenen substanzen, I. Dielektrizitatskonstanten und leitfahigkeiten der mischkorper aus isotropen substanzen. Annalen der Physik, Leipzig, vol. 24, pp. 636–679, 1935.
44. Schwartz, L., Garboczi, E., and Bentz, D., Interfacial transport in porous media: Application to DC electrical conductivity of mortars, Journal of Applied Physics, vol. 78, no. 10, pp. 5898–5908, 1995.
45. Xue, Q., and Xu, W.-M., A model of thermal conductivity of nanofluids with interfacial shells. Materials Chemistry and Physics, vol. 90, no. 2-3, pp. 298–301, 2005.
46. Xie, H., Fujii, M., and Zhang, X., Effect of interfacial nanolayer on the effective thermal conductivity of nanoparticle-fluid mixture, International Journal of Heat and Mass Transfer, vol. 48, no. 14, pp. 2926–2932, 2005.
47. Xuan, Y., Li, Q., and Hu, W., Aggregation structure and thermal conductivity of nanofluids. AIChE Journal, vol. 49, no. 4, pp. 1038–1043, 2003.
48. Wang, B.-X., Zhou, L.-P., and Peng, X.-F., A fractal model for predicting the effective thermal conductivity of liquid with suspension of nanoparticles, International Journal of Heat and Mass Transfer, vol. 46, pp. 2665–2672, 2003.
49. Kumar, D. H., Patel, H. E., Kumar, V. R. R., Sundararajan, T., Pradeep, T., and Das, S. K., Model for heat conduction in nanofluids, Physical Review Letters, vol. 93, no. 14, pp. 144,301–1–144,301–4, 2004.
50. Bhattacharya, P., Saha, S. K., Yadav, A., Phelan, P. E., and Prasher, R. S., Brownian dynamics simulation to determine the effective thermal conductivity of nanofluids, Journal of Applied Physics, vol. 95, no. 11, pp. 6492–6494, 2004.
51. Koo, J., and Kleinstreuer, C., A new thermal conductivity model for nanofluids, Journal of Nanoparticle Research, vol. 6, no. 6, pp. 577–588, 2004.
52. Koo, J. and Kleinstreuer, C., Laminar nanofluid flow in micro-heat sinks, International Journal of Heat and Mass Transfer, vol. 48, no. 13, pp. 2652–2661, 2005.
53. Einstein, A., Eine neue bestimmung der molekuldimensionen. Annalen der Physik, Leipzig, vol. 19, pp. 289–306, 1906.

54. Saito, N., Concentration dependence of the viscosity of high polymer solutions, Journal of the Physical Society of Japan, I., vol. 5, pp. 4–8, 1950.
55. Brinkman, H. C., The Viscosity of Concentrated Suspensions and Solutions, Journal of Chemical Physics, vol. 20, pp. 571, 1952.
56. Simha, R., A treatment of the viscosity of concentrated suspensions, Journal of Applied Physics, vol. 23, pp. 1020–1024, 1952.
57. Krieger, I., Rheology of monodisperse lattices, Advances in Colloid and Interface Sciences, vol. 3, pp. 111–136, 1972.
58. Lundgren, T., Slow flow through stationary random beds and suspensions of spheres, Journal of Fluid Mechanics, vol. 51, pp. 273–299, 1972.
59. Batchelor, G. The effect of Brownian motion on the bulk stress in a suspension of spherical particles, Journal of Fluid Mechanics, vol. 83, pp. 97–117, 1977.
60. Tseng, W., and Lin, K.-C., Rheology and colloidal structure of aqueous TiO_2 nanoparticle suspensions, Material Science and Engineering: A, vol. 355, pp. 186– 192, 2003.
61. Maiga, S. E. B., Nguyen, C. T., Galanis, N., and Roy, G., Heat transfer behaviours of nanofluids in a uniformly heated tube, Superlattices and Microstructures, vol. 35, pp. 543–557, 2004.
62. Maiga, S. E. B., Nguyen, C. T., Galanis, N., and Roy, G., Hydrodynamic and thermal behaviours of a nanofluid in a uniformly heated tube, WIT Press, Southampton, SO40 7AA, United Kingdom, Lisbon, Portugal, volume 5 of Computational Studies, pp. 453–462, 2004.
63. Koo, J. and Kleinstreuer, C., Impact analysis of nanoparticle motion mechanisms on the thermal conductivity of nanofluids, International Communications in Heat and Mass Transfer, vol. 32, no. 9, pp. 1111–1118, 2005.
64. Kulkarni, D. P., Das, D. K., and Chukwu, G., Temperature dependent rheological property of copper oxide nanoparticles suspension (Nanofluid), Journal of Nanoscience and Nanotechnology, vol. 6, pp. 1150–1154, 2006.
65. Khanafer, K., Vafai, K., A critical synthesis of thermophysical characteristics of nanofluids, International Journal of Heat and Mass Transfer, vol. 54, pp. 4410–4428, 2011.
66. Khanafer, K., Vafai, K., and Lightstone, M., Buoyancy-driven heat transfer enhancement in a two-dimensional enclosure utilizing nanofluids, Int. J. Heat Mass Transfer, vol. 46, pp. 3639–3653, 2003.
67. Dittus, F., and Boelter, L., Heat transfer in automobile radiators of the tubular type, University of California, Publications in Engineering, vol. 2, pp. 443–461, 1930.
68. Gnielinski, V., New equations for heat and mass transfer in turbulent pipe and channel flow, International Chemical Engineering, vol. 16, pp. 359–368, 1976.
69. Pak, B. and Cho, Y., Hydrodynamic and heat transfer study of dispersed fluids with submicron metallic oxide particles, Experimental Heat Transfer, vol. 11, no. 2, pp. 151–170, 1998.
70. Das, S. K., Putra, N., and Roetzel, W., Pool boiling characteristics of nano-fluids, International Journal of Heat and Mass Transfer, vol. 46, no. 5, pp. 851–862, 2003.
71. Xuan, Y. and Li, Q., Investigation on convective heat transfer and flow features of nanofluids, Journal of Heat Transfer, vol. 125, pp. 151–155, 2003.
72. Yang, Y., Zhang, Z. G., Grulke, E. A., Anderson, W. B., and Wu, G., Heat transfer properties of nanoparticle-in-fluid dispersions (nanofluids) in laminar flow, International Journal of Heat and Mass Transfer, vol. 48, no. 6, pp. 1107–1116, 2005.
73. Buongiorno, J., Convective transport in nanofluids, Journal of Heat Transfer, vol. 128, pp. 240–250, 2006.
74. Masuda, H., Ebata, A., Teramae, K., Hishinuma, N., Alteration of thermal conductivity and viscosity of liquid by dispersing ultra-fine particles (dispersion of Al_2O_3, SiO_2 and TiO_2 ultra-fine particles), Netsu Bussei, vol. 4, pp. 227–233, 1993.
75. Lee S., Choi S. U. S., Li S., and Eastman, J. A., Measuring thermal conductivity of fluids containing oxide nanoparticles, ASME J. Heat Transfer, vol. 121, pp. 280–289, 1999.

76. Chon C. H., Kihm, K. D., Lee, S. P., and Choi, S. U. S., Empirical correlation finding the role of temperature and particle size for nanofluid (Al_2O_3) thermal conductivity enhancement, Appl. Phys. Lett., vol. 87, pp. 153107, 2005.
77. Zhang, X., Gu, H., and Fujii, M., Effective thermal conductivity and thermal diffusivity of nanofluids containing spherical and cylindrical nanoparticles, J. Appl. Phys., vol. 100, pp. 1–5, 2006.
78. Timofeeva, E. V., Gavrilov, A. N., McCloskey, J. M., and Tolmachev, Y. V., Thermal conductivity and particle agglomeration in alumina nanofluids: experiment and theory, Phys. Rev. E, vol. 76, pp. 061203, 2007.
79. Das, S. K., Putra, N., Thiesen, P., and Roetzel, W., Temperature dependence of thermal conductivity enhancement for nanofluids, J. Heat Transfer, vol. 125, pp. 567–574, 2003.
80. Mintsa, H. A., Roy G., Nguyen, C. T., and Doucet, D., New temperature dependent thermal conductivity data for water-based nanofluids, International Journal of Thermal Sciences, vol. 48, pp. 363–371, 2009.
81. Namburu P. K., Kulkarni, D. P., Misra, D., and Das, D. K., Viscosity of copper oxide nanoparticles dispersed in ethylene glycol and water mixture, Experimental Thermal and Fluid Science, vol. 32, pp. 397–402, 2007.
82. Wen, D., and Ding, Y., Experimental investigation into convective heat transfer of nanofluids at the entrance region under laminar flow conditions, International Journal of Heat and Mass Transfer, vol. 47, pp. 5181–5188, 2004.
83. Farajollahi, B., Etemad, S.G., and Hojjat, M., Heat transfer of nanofluids in a shell and tube heat exchanger, International Journal of Heat and Mass Transfer, vol. 53, pp. 12–17, 2010..
84. Wen, D., and Ding, Y., Formulation of nanofluids for natural convective heat transfer applications, International Journal of Heat and Fluid Flow, vol. 26, pp. 855–864, 2005.
85. Das, S. K., Putta, N., Thiesen, P., and Roetzel, W., Temperature dependence of thermal conductivity enhancement for nanofluids, ASME Trans. J. Heat Transfer, vol. 125, pp. 567-574, 2003.
86. Xie, H., Wang, J., Xi, T., Liu, Y., Ai, F., and Wu, Q., Thermal conductivity enhancement of suspensions containing nanosized alumina particles, Journal of Applied Physics, vol. 91, no. 7, pp. 4568–4572, 2002.
87. Li, C. H. and Peterson, G. P., Experimental investigation of temperature and volume fraction variations on the effective thermal conductivity of nanoparticle suspensions (nanofluids), Journal of Applied Physics, vol. 99, no. 8, pp. 084,314, 2006..
88. Eastman, J. A., Choi, S. U. S., Li, S., Yu, W., and Thompson, L. J., Anomalously increased effective thermal conductivities of ethylene glycol-based nanofluids containing copper nanoparticles, Applied Physics Letters, vol. 78, no. 6, pp. 718–720, 2001.
89. Hong, T.-K., Yang, H.-S., and Choi, C. J., Study of the enhanced thermal conductivity of Fe nanofluids, Journal of Applied Physics, vol. 97, no. 6, pp. 1–4, 2005.
90. Patel, H. E., Das, S. K., Sundararagan, T., Nair, A. S., Geoge, B., and Pradeep, T., Thermal conductivities of naked and monolayer protected metal nanoparticle based nanofluids: Manifestation of anomalous enhancement and chemical effects, Applied Physics Letters, vol. 83, pp. 2931–2933, 2003.
91. Xie, H., Wang, J., Xi, T., and Liu, Y., Study on the thermal conductivity of SiC nanofluids, Journal of the Chinese Ceramic Society, vol. 29, no. 4, pp. 361– 364, 2001.
92. Xie, H., Wang, J., Xi, T., Liu, Y., Ai, F., and Wu, Q., Thermal conductivity enhancement of suspensions containing nanosized alumina particles, Journal of Applied Physics, vol. 91, no. 7, pp. 4568–4572, 2002.
93. Biercuk, M., Llaguno, M., Radosavljevic, M., Hyun, J., Johnson, A., and Fischer, J., Carbon nanotubes composites for thermal management, Applied Physics Letters, vol. 80, no. 15, pp. 2767–2769, 2002.
94. Xie, H., Lee, H., Youn, W., and Choi, M., Nanofluids containing multiwalled carbon nanotubes and their enhanced thermal conductivities, Journal of Applied Physics, vol. 94, no. 8, pp. 4967–4971, 2003.

95. Choi, E. S., Brooks, J. S., Eaton, D. L., Al-Haik, M. S., Hussaini, M. Y., Garmestani, H., Li, D., and Dahmen, K., Enhancement of thermal and electrical properties of carbon nanotube polymer composites by magnetic field processing, Journal of Applied Physics, vol. 94, no. 9, pp. 6034–6039, 2003.
96. Assael, M. J., Chen, C. F., Metaxa, I. N., and Wakeham, W. A., Thermal conductivity of suspensions of carbon nanotubes in water, In 15th Symposium on Thermophysical Properties. National Institute of Standards, University of Colorado, Boulder, USA, 2003.
97. Assael, M. J., Chen, C. F., Metaxa, I. N., and Wakeham, W. A., Thermal Conductivity of Suspensions of Carbon Nanotubes in Water, International Journal of Thermophysics, vol. 25, no. 4, pp. 971–985, 2004.
98. Assael, M. J., Metaxa, I. N., Arvanitidis, J., Christofilos, D., and Lioutas, C., Thermal conductivity enhancement in aqueous suspensions of carbon multi-walled and double-walled nanotubes in the presence of two different dispersants, International Journal of Thermophysics, vol. 26, no. 3, pp. 647–664, 2005.
99. Liu, M.-S., Ching-Cheng Lin, M., Huang, I. T., and Wang, C.-C., Enhancement of thermal conductivity with carbon nanotube for nanofluids, International Communications in Heat and Mass Transfer, vol. 32, no. 9, pp. 1202–1210, 2005.
100. Das, S.K., Putra, N., Thiesen, P., and Roetzel, W., Temperature dependence of thermal conductivity enhancement for nanofluids, Journal of Heat Transfer, vol. 125, pp. 567–574, 2003.
101. Patel, H. E., Das, S. K., Sundararajan, T., Nair, A. S., George, B., and Pradeep, T., Thermal conductivity of naked and monolayer protected metal nanoparticles based nanofluids: manifestation of anomalous enhancement and chemical effects, Applied Physics Letters, vol. 83, pp. 2931–2933, 2003.
102. Chon, C. H., and Kihm, K. D., Thermal conductivity enhancement of nanofluids by Brownian motion, Journal of Heat Transfer, vol. 127, pp. 810, 2005.
103. Li, C. H., and Peterson, G. P., Experimental investigation of temperature and volume fraction variations on the effective thermal conductivity of nanoparticle suspensions (nanofluids), Journal of Applied Physics, vol. 99, pp. 084314-1–084314-8, 2006.
104. Yang, B., and Han, Z. H., Temperature-dependent thermal conductivity of nanorod-based nanofluids, Applied Physics Letters, vol. 89, pp. 083111-1–083111-3, 2006.
105. Venerus, D. C., Kabadi, M. S., Lee, S., and Perez-Luna, V., Study of thermal transport in nanoparticle suspensions using forced Rayleigh scattering, Journal of Applied Physics, vol. 100, pp. 094310-1–094310-5, 2006.
106. Murshed, S. M. S., Leong, K. C., and Yang C., Investigations of thermal conductivity and viscosity of nanofluids, International Journal of Thermal Sciences, in press, doi:10.1016/j.ijthermalsci.2007. 05.004, 2006.
107. Prasher, R., Song, D., and Wang, J., Measurements of nanofluid viscosity and its implications for thermal applications, Appl. Phys. Lett., vol. 89, paper 133108, pp. 1–3, 2006.
108. Li, J. M., Li, Z. L., and Wang, B. X., Experimental viscosity measurements for copper oxide nanoparticle suspensions, Tsinghua Sci. Technol., vol. 7, pp. 198–201, 2002.
109. Chen, H., Ding, Y., He, Y., and Tan, C., Rheological behaviour of ethylene glycol based titania nanofluids, Chem. Phys. Lett., vol. 444, pp. 333–337, 2007.
110. Guo, S., Luo, Z., Wang, T., Zhao, J., and Cen, K., Viscosity of monodisperse silica nanofluids, Bull.Chin. Ceram. Soc., vol. 25, pp. 52–55, 2006. (In Chinese).
111. Nguyen, C. T., Desgranges, F., Roy, G., and Galanis, N., Temperature and particle size dependent viscosity data for water-based nanofluid-hysteresis phenomenon, International Journal of Heat and Fluid Flow, vol. 28, pp. 1492–1506, 2007.
112. Wang, X., Xu, X., and Choi, S. U. S., Thermal conductivity of nanoparticle-fluid mixture, Journal of Thermophysics and Heat Transfer, vol. 13, no. 4, pp. 474–480, 1999.
113. Das, S. K., Putra, N., and Roetzel, W., Pool boiling characteristics of nano-fluids, International Journal of Heat and Mass Transfer, vol. 46, no. 5, pp. 851–862, 2003.

114. Ding, Y., Alias, H., Wen, D., and Williams, R. A., Heat transfer of aqueous suspensions of carbon nanotubes (CNT nanofluids), International Journal of Heat and Mass Transfer, vol. 49, no. 1-2, pp. 240–250, 2005.
115. Vajjha, R. S., Das, D. K., Mahagaonkar, B. M., Density measurements of different nanofluids and their comparison with theory, Petro. Sci. Tech., vol. 27, no. 6, pp. 612–624, 2009.
116. Vajjha, R. S., Das, D. K., Specific heat measurement of three nanofluids and development of new correlations, J. Heat Transfer, vol. 131, pp. 071601-1 to 7, 2009.
117. Xuan, Y., and Roetzel, W., Conceptions for heat transfer correlation of nanofluid, International Journal of Heat and Mass Transfer, vol. 43, pp. 3701–3707, 2000.
118. Wang, B. X., Zhou, L. P., and Peng, X. F., Viscosity thermal diffusivity and Prandtl number of nanoparticle suspensions, Progress in Natural Science, vol. 14, pp. 922–926, 2004.
119. Murshed, S. M. S., Leong, K. C., and Yang, C., Determination of the effective thermal diffusivity of nanofluids by the double hot-wire technique, Journal of Physics D: Applied Physics, vol. 39, pp. 5316–5322, 2006.
120. Golubovic, M., Hettiarachchi, H. D. M., Worek, W. M., and Minkowycz, W. J., Nanofluids and critical heat flux, experimental and analytical study, Appl. Therm. Eng., vol. 29, pp. 1281–1288, 2009.
121. Xue, H. S., Fan, J. R., Hong, R. H., and Hu, Y. C., Characteristic boiling curve of carbon nanotube nanofluid as determined by the transient calorimeter technique, Appl. Phys. Lett., vol. 90, paper 184107, 2007.
122. Kim, H. D., Kim, J., and et al., Experimental studies on CHF characteristics of nanofluids at pool boiling, Int. J. Multiphase Flow, vol. 33, pp. 691–706, 2007.
123. Murshed, S. M. S., Tan, S. H., and Nguyen, N. T., Temperature dependence of interfacial properties and viscosity of nanofluids for droplet-based microfluidics, J. Phys. D: Appl. Phys., vol. 41, paper 085502, 2008.
124. Zhu, D. S., Wu, S.Y., and Wang, N., Surface tension and viscosity of aluminium oxide nanofluids, in: The 6th International Symposium on Multiphase Flow, Heat Mass Transfer and Energy Conversion, AIP Conference Proceedings – March 1, 2010, vol. 1207, pp. 460–464, 2010.
125. Lee, S. and Choi, S. U. S., Application of metallic nanoparticle suspensions in advanced cooling systems, In 1996 International Mechanical Engineering Congress and Exhibition. Atlanta,USA, 1996.
126. Xuan, Y. and Li, Q., Investigation on convective heat transfer and flow features of nanofluids, Journal of Heat Transfer, vol. 125, pp. 151–155, 2003.
127. Wen, D. and Ding, Y., Experimental investigation into convective heat transfer of nanofluids at the entrance region under laminar flow conditions, International Journal of Heat and Mass Transfer, vol. 47, no. 24, pp. 5181, 2004.
128. Chien, H.-T., Tsai, C.-I., Chen, P.-H., and Chen, P.-Y., Improvement on thermal performance of a disk shaped miniature heat pipe with nanofluid, ICEPT 2003. Fifth In ternational Conference on Electronic Packaging Technology. Proceedings. (IEEE Cat. No.03EX750), 389. IEEE, Shanghai, China, 2003.
129. Tsai, C. Y., Chien, H. T., Ding, P. P., Chan, B., Luh, T. Y., and Chen, P. H., Effect of structural character of gold nanoparticles in nanofluid on heat pipe thermal performance. Material Letters, vol. 58, pp. 1461–1465, 2004.
130. Ding, Y., Alias, H., Wen, D., and Williams, R. A., Heat transfer of aqueous suspensions of carbon nanotubes (CNT nanofluids). International Journal of Heat and Mass Transfer, vol. 49, no. 1-2, pp. 240–250, 2005.
131. Heris, S., Etemad, S. G., and Esfahany, M., Experimental investigation of oxide nanofluids laminar flow convective heat transfer, International Communications in Heat and Mass Transfer, vol. 33, no. 4, pp. 529–535, 2006.
132. Putra, N., Roetzel, W., and Das, S. K., Natural convection of nano-fluids. Heat and Mass Transfer, vol. 39, no. 8-9, pp. 775–784, 2003.

133. Wen, D. and Ding, Y., Formulation of nanofluids for natural convective heat transfer applications, International Journal of Heat and Fluid Flow, vol. 26, no. 6, pp. 855–864, 2005.
134. Chein, R., and Haung G., Analysis of micro channel heat sink performance using nanofluids, Applied Thermal Engineering, vol. 25, no. 17, pp. 3104-3114, 2006.
135. Tzeng, S., Lin, C., and Huang, K., Heat Transfer Enhancement of Nano Fluids in Rotary Balde Coupling of Four Wheel Drive Vehicles, Acta Mechanica, vol. 179, no. 1, pp. 11-23, 2005.
136. Tsai, C. Y., Chien, H. T., Ding, P. P., Chan, B., Luh, T. Y., and Chen, P. H., Effect of Structural Character of Gold Nanoparticles in Nanofluid on Heat Pipe Thermal Performance, Materials Letters, vol. 58, pp. 1461–1465, 2004.
137. Kang S. W., Wei, W. C., Tsai S. H., and Yang, S. Y., Experimental Investigation Of Silver Nano Fluid on Heat Pipe Thermal Performance, Applied Thermal Engineering, vol. 26, pp. 2377-2382, 2004.
138. Wei S. W., Tsai S. H., Yang, S. Y., Kang, S. W., Effect of Nano Fluid Concentration on Heat Pipe Thermal Performance, IASME Trans, vol. 2, pp. 1432-1439, 2005..
139. Ma H. B., Wilson C., Borgmeyer B., Park K., Yu Q., Choi S. U. S. and Tirumala M., Effect Of Nano Fluid on the Heat Transport Capability in An Oscillating Heat Pipe, Applied Physics Letters, vol. 88, no. 14, paper 143116, 2004.
140. Jordan, A., Scholz, R., Wust, P., Fahling, H., and Felix, R., Magnetic Fluid Hyperthermia (MFH): Cancer Treatment with AC Magnetic Field Induced Excitation of Biocompatible Super paramagnetic Nanoparticles, Journal of Magnetism and Magnetic Materials, vol. 201, pp. 413–419, 1999.

Chapter – 3
Experimentation and methodology

3.1 Introduction

The present work aims to prepare nanofluids with alumina (Al_2O_3) nanoparticles with distilled water and ethylene glycol as base fluid for improving the heat transfer characteristics of the fluid. These analyses are performed by measuring the thermo physical properties like thermal conductivity, viscosity and density at different temperatures for different volume concentrations of nanofluids.

In this chapter, the method adopted for preparation of nanofluids and various set up with their actual photographs and the methodology adopted for the measurement of thermal conductivity, viscosity and density of nanofluids at different temperatures is discussed. Firstly, for the synthesis of nanofluids, ultra sonicator is used. To measure the thermal conductivity, KD2 pro thermal property analyzer is used, for viscosity Ubbelohde viscometer is used and for density Pycnometer is used. These instruments, their working principle and their use are discussed in detail.

3.2 Synthesis of nanofluids

The present work aims at to prepare nanofluids with alumina (Al_2O_3) nanoparticles and distilled water and ethylene glycol as base fluids. Work is to be done on 4 different volume fractions i.e. 0.1%, 0.25%, 0.50% and 1.0%. First, material required and then the methodology for the preparation of nanofluids is discussed.

3.2.1 Materials required for preparing nanofluids

- Al_2O_3 nanoparticles (particle size – 40-50 nm)
- Ethylene Glycol
- Distilled water

3.2.1.1 Background of alumina (Al_2O_3)

Aluminium oxide (Al_2O_3) commonly referred to as alumina, white crystalline powder that is found as balls or lumps of various mesh sizes, possesses strong ionic interatomic bonding giving rise to its desirable material characteristics. Alumina is most cost effective and one of the most versatile of refractory ceramic oxides. The raw materials from which this high performance technical grade ceramic is made are readily available and reasonably priced, resulting in good value for the cost in fabricated alumina shapes. With an excellent combination of properties and an attractive price, it is no surprise that fine grain technical grade alumina has a very wide range of applications like gas laser tubes, wear pads, seal rings, high temperature and high voltage electrical insulators etc. The thermophysical properties [1] for different purity grades of alumina are given in Table 3.1.

Table 3.1: Thermophysical properties for different purity grades of alumina

Sr. No.	Property*	Alumina grade				
		86 %	94 %	97.5 %	**99.5 %**	99.9%
1.	Density, (gm/cm^3)	3.5	3.7	3.78	**3.89**	3.9
2.	Thermal conductivity, (W/m-K)	15	20	24	**26**	28-35
3.	Thermal expansion coefficient, (10^{-6} 1/K)	7	7.6	8.1	**8.3**	8
4.	Specific heat, (J/kg K)	920	900	872	**850**	830

* All properties are at room temperature unless otherwise noted.

3.2.1.2 Ethylene glycol

Ethylene glycol is a clear, colourless, odourless liquid with a sweet taste. Its chemical formula is $C_2H_4(OH)_2$. It is hygroscopic and completely miscible with many polar solvents such as water, alcohols, glycol ethers, and acetone. Its solubility is low however, in nonpolar solvents, such as benzene, toluene, dichloroethane, and chloroform.

Ethylene glycol water mixtures are the most common antifreeze fluid for standard heating and cooling applications. They are common in heat-transfer applications where the temperature in the heat transfer fluid can be below 0 °C. Glycol water solutions are also commonly used in heating applications that temporarily may not be operated in surroundings with freezing conditions - such as cars and machines with water cooled engines [2].

3.2.2 Methodology for the preparation of nanofluids

Aluminium oxide (Al_2O_3) nanoparticles are purchased from M/s. Alpha Aesar, A Jhonson Matthey Chemicals India Pvt. Ltd., Hyderabad. The size of nanoparticles is 40-45 nm as it was mentioned by the company. Nanofluids are prepared by two step process. The work is done on 4 different volume fractions i.e. 0.1%, 0.25%, 0.50% and 1.0%. So, for each volume fraction, the exact amount of Al_2O_3 nanoparticles is to be calculated, to disperse in the base fluids i.e. ethylene glycol and distilled water. For thermal conductivity, density and viscosity measurement, at least 50 ml nanofluids sample for each volume fraction is needed. The method adopted for calculating the mass of nanoparticles is given in annexure – II.

The samples, 12 in nos., are made as per the following composition.

- By taking **distilled water** as base fluid and 0.1%, 0.25%, 0.50% and 1.0% volume fraction, 4 samples are made, (Fig. 3.1).
- By taking **ethylene glycol** as base fluid and 0.1%, 0.25%, 0.50% and 1.0% volume fraction, 4 samples are made, (Fig. 3.2).
- By taking **ethylene glycol (25%) + distilled water (75%)** as base fluid and 0.1%, 0.25%, 0.50% and 1.0% volume fraction, 4 samples are made, (Fig. 3.3)

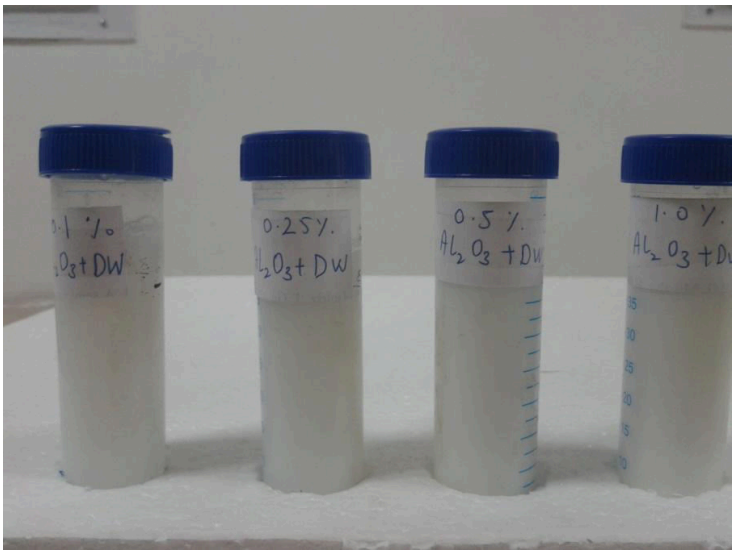

Fig. 3.1: Alumina and distilled water based nanofluids; (0.1%, 0.25%, 0.50% and 1.0%)

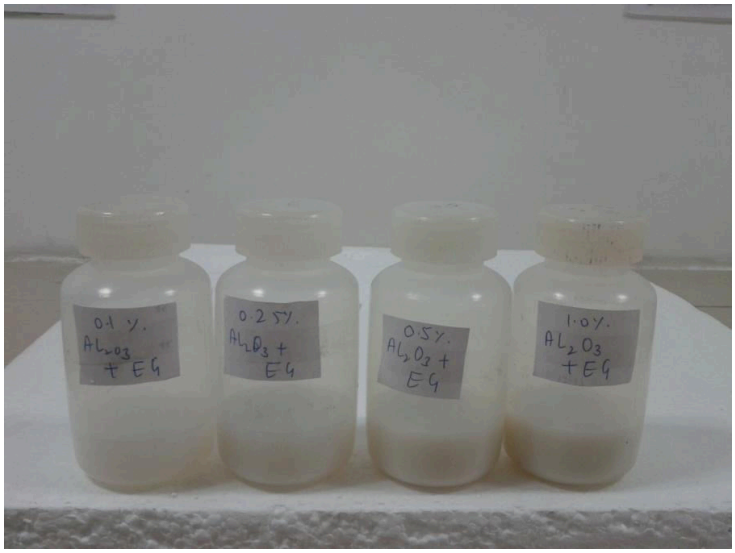

Fig. 3.2: Alumina and ethylene glycol based nanofluids; (0.1%, 0.25%, 0.50% and 1.0%)

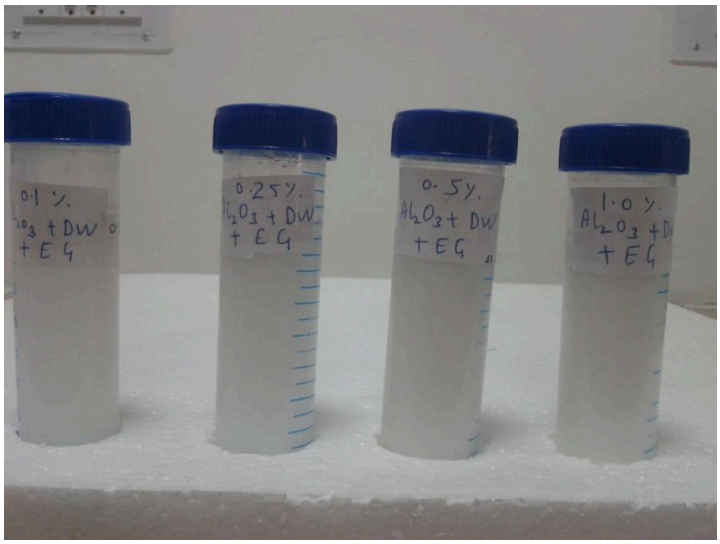

Fig. 3.3: Alumina and distilled water (75%) and ethylene glycol (25%) based nanofluids; (0.1%, 0.25%, 0.50% and 1.0%)

First of all, weigh the exact amount of alumina nanoparticles as per volume fraction calculated above with the help of digital weighing balance machine. Then, take 50 ml distilled water in a conical flask, and pour the calculated amount of alumina nanoparticles in the flask very gently, avoiding the sticking of nanoparticles on the flask wall. Then placed this conical flask on the magnetic stirrer and stir it at average speed for at least half an hour for proper mixing.

To make the nanoparticles more stable and remain more dispersed in ethylene glycol, ultra sonicator is used. Now pour the nanofluid sample in fluken tube, and put this fluken tube in the Ultra sonicator. Then Sonication is done for 4-5 hours before testing any thermo physical property of the nanofluids. Repeat the same procedure for each volume fraction and for ethylene glycol as base fluid and distilled water (75%) and ethylene glycol (25%) as base fluid. By doing so, nanoparticles become more evenly dispersed in base Fluid. The description of Ultra sonicator is given below.

3.2.3 Ultra sonicator

Sonication is the act of applying sound (usually ultrasound) energy to agitate particles in a sample, for various purposes. In the laboratory, it is usually applied using an ultrasonic bath known as a sonicator. Sonication can be used to speed dissolution, by breaking intermolecular interactions. Sonication is commonly used in nanotechnology for evenly dispersing nanoparticles in liquids.

Fig. 3.4(a): Front View of Ultra Sonicator bath

Fig. 3.4(b): Top view of Ultra Sonicator bath

The front view & top view of Ultra sonicator bath are shown, respectively, in Fig. 3.4(a) and Fig. 3.4(b). In Fig. 3.4(b), it can be clearly seen that nanofluids samples are held in clamps on stands.

3.3 Thermal conductivity measurement

In this section, thermal conductivity by 2 different methods will be discussed. One is guarded plate method and another is by using KD2 pro thermal properties analyzer.

3.3.1 Guarded plate method

The apparatus of thermal conductivity measurement of liquids by guarded plate method is shown in Fig. 3.5. This is supplied by Mass International, 93 Preet Nagar, Jagadhri Road, Ambala Cantt, 133001.

Fig. 3.5: Actual picture of thermal conductivity of liquid measuring apparatus

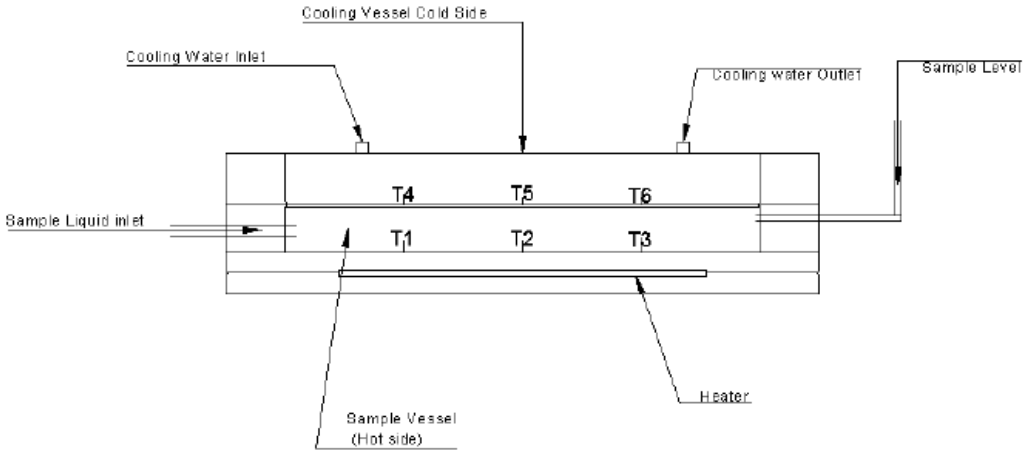

Fig. 3.6: Line diagram for the "Guarded hot plate" method

Specification:

1. Hot plate

Material = Copper, Diameter = 170 mm

2. Cold plate

Material = Aluminium, Diameter = 170 mm

3. Heater = Nichrome heater 250 Watt

A heater heats hot plate and voltage to the heater is varied with the help of variac to conduct the experiment on different voltages as well as different heat inputs. Temperatures are measured by RTD PT-100 sensors attached at three different places on the hot plate as well as on the cold plate. These sensor readings are used as T_h and T_c at steady state condition. Heat is supplied by an electric heater for which, we have to record the voltmeter reading (V) and ammeter reading (A) after attaining the steady state condition. The temperature of the cold surface (of cold plate) is maintained by circulating cold water @ 60 lph. The gap between hot plate and cold plate forms the liquid cell, in which liquid sample is filled.

Formulae: -

$$q = \frac{-k\,A}{\Delta x}\,(T_2 - T_1) \tag{3.1}$$

$$k = q\,\frac{\Delta x}{A\,(T_h - T_c)} \tag{3.2}$$

Note: All the above data is taken from "Thermal conductivity of liquid (guarded plate method)" ; Instruction Manual, supplied by Mass International, 93 Preet Nagar, Jagadhri Road, Ambala Cantt, 133001 [3].

Problem incurred

While calibrating the above apparatus with distilled water, its thermal conductivity is found to be in the range of 0.9-0.94 W/m-k; which is not accurate. Because thermal conductivity of distilled water at room temperature is 0.613 W/m-k. So, it is decided that the above apparatus is not suitable for the thermal conductivity measurement of nanofluids. Therefore, we use KD2 pro thermal properties analyzer for thermal conductivity measurement of nanofluids.

Firstly, a detailed description is given for KD2 pro and then it's working at different temperature is discussed.

3.3.2 KD2 pro thermal properties analyzer

KD2 pro is supplied by Decagon Devices, Inc. 2365 NE Hopkins Ct. Pullman, WA 99163 USA. The KD2 Pro is a battery-operated, menu-driven and handheld device used to measure thermal properties. It consists of a handheld controller and sensors that can be inserted into the medium you wish to measure. The single- needle sensors measure thermal conductivity and resistivity; while the dual-needle sensor also measures volumetric specific heat capacity and diffusivity. The KD2 Pro has been designed for ease of use and maximum functionality.

Specifications:

Operating environment:

Controller: 0 to 50 °C

Sensors: −50 to +150 °C

Power: 4 AA cells

Battery Life: At least 500 readings in constant use or 3 years with no use (battery drain in sleep mode < 50 uA)

Case Size: 15.5 cm x 9.5 cm x 3.5 cm

Display: 3 cm x 6 cm, 128 x 64 pixel graphics LCD

Keypad: 6 key, sealed membrane

Data Storage: 4095 measurements in flash memory (both raw and processed data are stored for download)

Interface: 9-pin serial

Read Modes: Manual and auto read

Fig. 3.7: KD2 pro thermal properties analyzer with sensors

Fig. 3.8 KS-1 sensor needle

Sensors: The specifications of all the 3 sensors are given below.

1. 60 mm (small) single-needle (KS-1):

Size: 1.3 mm diameter x 60 mm long

Range: 0.02 to 2.00 W/(m· K) (thermal conductivity)

50 to 5000 °C·cm/W (thermal resistivity)

Accuracy (conductivity): ± 5% from 0.2 - 2 W/(m· K) ±0.01 W/(m· K) from 0.02 - 0.2 W/(m· K)

Cable length: 0.8

2. 100 mm (large) single-needle (TR-1):

Size: 2.4 mm diameter x 100 mm long

Range: 0.10 to 4.00 W/(m· K) (thermal conductivity)

25 to 1000 °C·cm/W (thermal resistivity)

Accuracy (conductivity): ±10% from 0.2 - 4 W/(m· K) ±0.02 W/(m· K) from 0.1 - 0.2 W/(m· K)

Cable length: 0.8 m

3. 30 mm dual-needle (SH-1):

Size: 1.3 mm diameter x 30 mm long, 6 mm spacing

Range: 0.02 to 2.00 W /(m· K) (thermal conductivity)

50 to 5000 °C·cm/W (thermal resistivity)

0.1 to 1 mm^2/s (diffusivity)

0.5 to 4 $mJ/(m^3K)$ (volumetric specific heat)

Accuracy: (Conductivity) ± 10% from 0.2 - 2 W/(m· K) ±0.01 W/(m· K) from 0.02 - 0.2 W/(m· K)

(Diffusivity) ±10% at conductivities above 0.1 W/(m· K)

(Volumetric Specific Heat) ±10% at conductivities above 0.1 W/ (m· K)

Cable length: 0.8 m

3.3.2.1 Key points for KS-1 sensor

As in present work, only KS-1 sensor is used. So, some key points for the same can be discussed as:

The KD2 pro KS-1 sensor (Fig. 3.8) is specially designed to add a very small amount of heat to the sample during measurement and thereby minimize problems with free convection. In high viscosity liquids (e.g. oils, glycerine), free convection is generally not an issue. However, in low viscosity liquids like water or aqueous solutions, there are several important steps that will aid in accurate measurements.

- When dealing with low viscosity liquid samples, the duration of the read time should be minimized to minimize the amount of heat added to the sample.
- The default read time for the KS-1 sensor is 1 minute. If you are measuring in low viscosity liquids, use this read time.
- In liquid samples, the KS-1 sensor needle should be oriented vertically during the measurement to help prevent free convection.
- Never use the KS-1 sensor in high power mode in liquids. The sensor must be configured in low power mode to prevent free convection.

Note: All the above data and Fig. 3.7 is taken from KD2 pro thermal properties analyzer, Operator's Manual (Version 10), supplied by Decagon Devices, Inc., WA 99163 USA [4].

3.3.2.2 Principle of measurement

KD2 Pro has 5% accuracy over the 5 ˚C to 40 ˚C temperature range. It consists of a handheld microcontroller and sensor needles. The KD2's sensor needle contains both a heating element and a thermistor. The controller module contains a battery, a 16-bit microcontroller/AD converter, and power control circuitry. The thermal conductivity measurement assumes several things like: (i) the long heat source can be treated as an infinitely long heat source; (ii) the medium is both homogeneous and isotropic, and at uniform initial temperature. Although these assumptions are not true in the strict sense, they are adequate for accurate thermal properties measurements [5].

The KS-1 sensor needle can be used for measuring thermal conductivity of fluids in the range of 0.2–2 W/mk with accuracy of ±5%. Each measurement cycle consists of 90 s. During the first 30 s, the instrument will equilibrate which is then followed by heating and cooling of sensor needle for 30 s each. At the end of the reading, the controller computes the thermal conductivity using the change in temperature (ΔT)–time data from

$$k = \frac{q\ (\ln t_2 - \ln t_1)}{4\pi\ (\Delta T_2 - \Delta T_1)} \tag{3.3}$$

Where q is constant heat rate applied to an infinitely long and small ‘‘line" source, ΔT_1 and ΔT_2 are the changes in the temperature at times t_1 and t_2 respectively.

NOTE: Experimental results from researchers have shown that the KD2-Pro' KS-1 sensor can make accurate measurements in water and aqueous solutions up to about 50 °C. Above this temperature, the viscosity of the water becomes too low and free convection begins to affect the measurement.

3.3.2.3 Thermal conductivity measurement of nanofluids at different temperatures

Thermal conductivity of nanofluids measured by KD2 pro thermal properties analyzer at room temperature is shown in Fig. 3.9.

Fig. 3.9: KD2 Pro with nanofluid sample at room temperature

Fig. 3.10: Water bath used for heating the nanofluid sample

And for different temperature, a water bath (Fig. 3.10) is used. Firstly, the whole process is done for base fluids i.e. ethylene glycol, distilled water and distilled water (75%) and ethylene glycol (25%), then this process is repeated for all 12 samples of nanofluids. It is found that in the laboratory environment water starts boiling above 90°C. Therefore, keep the temperature of water in the water bath below it. First of all, put the sample in fluken tube, then placed it in the stand. Then with the help of cello tape, put the KD2's KS-1 sensor needle in the upper part of fluken tube. Then placed this whole arrangement in the water bath as shown in Fig. 3.11. And then wait for steady state, After this note the readings at different temperatures, starting from the higher first (say 60 °C), and as the temperature downs with the time, take another readings at lower temperatures up

to room temperature (say at 30 °C). Same experiment is repeated for the different volume fractions and different base fluids of nanofluids i.e. all the 12 samples at different temperatures. The readings are taken from 30 °C to 60 °C. Because above 60 °C, KD2 pro gives large errors.

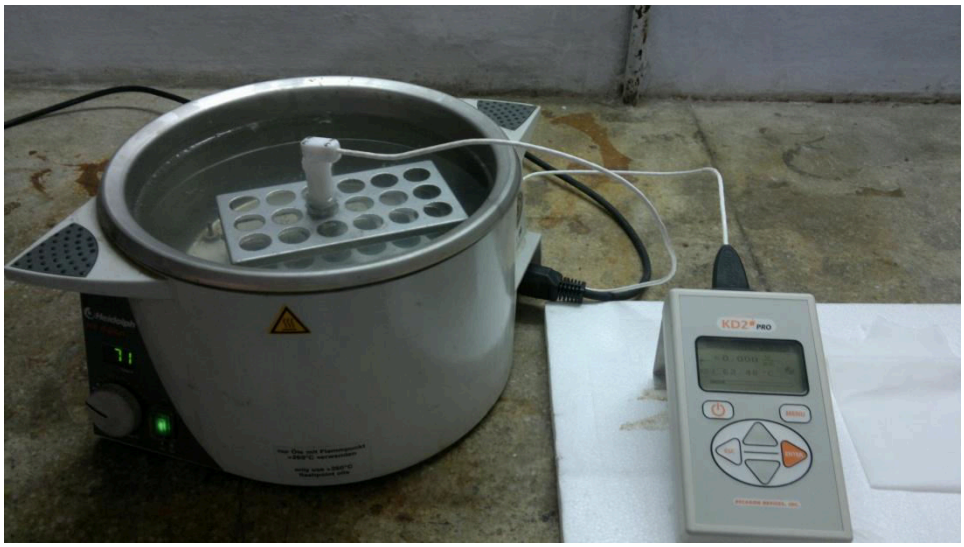

Fig. 3.11: KD2 Pro with nanofluid sample in the water bath for measurement at different temperature

3.3.2.4 Liquid sample temperature control

There are several things that should be avoided when measuring thermal properties of heated or cooled samples.

- Do not heat the sample from the bottom (e.g. on a hot plate). The temperature gradient from the heating will cause free convection.
- Do not make measurements in a conventional refrigerator or freezer. Conventional cooling devices have very large cyclical temperature cycles which can cause excessive sample temperature drift and poor measurements. Vibrations from the compressor will also cause forced convection in the sample.
- Do not measure the thermal properties of the sample while it is in a circulating water bath. The vibrations from the water bath pump and from the circulating water will cause forced convection in the sample.

According to several researchers who use the KD2 Pro with liquid samples, the best method for controlling temperature of liquid samples is as follows.

1. Heat or cool the sample (with sensor inserted) in a water bath.
2. Once the sample temperature has equilibrated to the desired water bath temperature, turn the water bath off.
3. Allow enough time for the water bath to become absolutely still, and make the measurement.

3.4 Viscosity measurement

For the measurement of viscosity of nanofluids, Ubbelohde viscometer as shown in Fig. 3.12 is used. As this apparatus is cheap and easily available, but still no one had find viscosity through this viscometer. A detailed description and use of Ubbelohde viscometer is explained below as:

3.4.1 Ubbelohde viscometer

An Ubbelohde type viscometer or suspended-level viscometer is a measuring instrument which uses a capillary based method of measuring viscosity. The advantage of this instrument is that the values obtained are independent of the total volume. The device was invented by the German chemist Leo Ubbelohde (1877-1964).

The Ubbelohde viscometer is closely related to the Ostwald viscometer. Both are u-shaped pieces of glassware with a reservoir on one side and a measuring bulb with a capillary on the other. A liquid is introduced into the reservoir then sucked through the capillary and measuring bulb. The liquid is allowed to travel back through the measuring bulb and the time it takes for the liquid to pass through two calibrated marks is a measure for viscosity. The Ubbelohde device has a third arm extending from the end of the capillary and open to the atmosphere. In this way the pressure head only depends on a fixed height and no longer on the total volume of liquid. The Ubbelohde viscometers are used for the measurement of viscosity of newtonian liquids that are sufficiently transparent to enable the meniscus of the liquid to be observed during measurement.

The viscosity of the test liquid is determined by measuring the time it takes for the sample, whose volume is defined by two ring-shaped marks to flow laminarly through a capillary under the influence of gravity. Hence, the friction within the liquid with high viscosity needs more time to pass the distance between the two measuring marks within the capillary tube. In accurate measurements these time is mostly measured by stopwatches.

The time taken for a liquid to flow between two marks is a function both of dynamic viscosity and density. The relationship between dynamic viscosity and density is called kinematic viscosity and is defined as

$$kinematic\ viscosity = \frac{Dynamic\ viscosity}{Density}$$

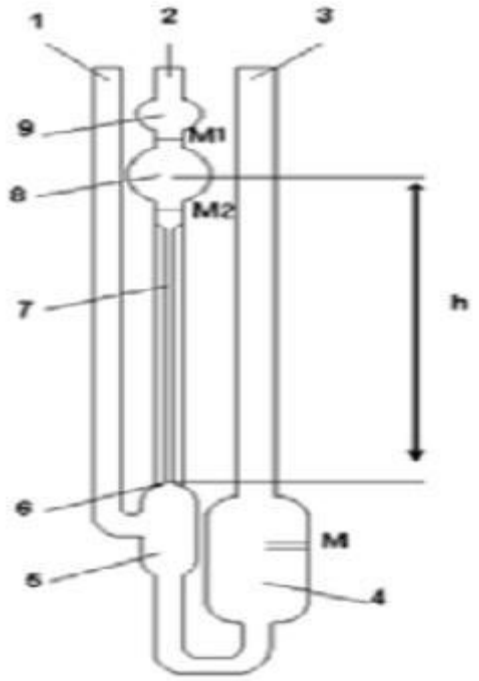

1. Ventilation tube
2. Capillary tube
3. Filling tube
4. Lower reservoir
5. Suspended level tube
6. Capillary
7. Timing bulb
8. Upper reservoir

M_1 and M_2 – measuring marks
M – filling marks
h – mean driving head

Fig. 3.12: Ubbelohde viscometer

The Ubbelohde Viscometer therefore, measure kinematic viscosity. The viscosity of nanofluid sample can be compared with the one whose viscosity is known (eg. Water) and the viscosity calculated in this way.

Thus, the viscosity of the nanofluid may be calculated from

$$\mu_{nf} = \mu_w \frac{t_{nf}\ \rho_{nf}}{t_w\ \rho_w} \tag{3.4}$$

Where μ = Dynamic Viscosity (Pa-sec)
ρ = Density (kg/m^3)
t = time (sec.)

subscripts nf and w represents nanofluid and water respectively.

3.4.1.1 Viscosity measurement by Ubbelohde viscometer at different temperature

Before doing any measurement, first of all Ubbelohde viscometer is to be filled with potassium dichromate solution for at least 12 hours. As potassium dichromate solution is good cleaning agent. So, it removes any kind of dust particles in the viscometer. Then, it is cleaned with distilled water, and then it is to be dried in Oven at above 120 °C for at least 4-5 hours. So, that no water particles left in the capillary of the Ubbelohde viscometer. Now, it is ready to use.

Measurement of viscosity of nanofluid sample by Ubbelohde viscometer at room temperature is shown in Fig. 3.13. But for different temperature, we use hot plate as shown in Fig. 3.14.

Firstly, the whole process is done for base fluids i.e. ethylene glycol, distilled water and distilled water and (75%) and ethylene glycol (25%), then the process is repeated for all 12 samples of nanofluids.

First of all, water is filled in a glass beaker and make it insulated with aluminium foil. So that heat transfer from the environment can be minimized. Then place this beaker on the hot plate. This will work as a hot water bath for the viscometer. Please ensure that the beaker should be fully filled with water. Place a thermometer inside this beaker with the help of a clamp and stand. Then with the help of another stand put the Ubbelohde viscometer in the beaker and then with the help of a flask, pour the nanofluid sample in the reservoir or filling tube.

Now, with the help of a suction pump, suck this nanofluid sample through the capillary tube. And when it comes down, then note down the time with the help of stopwatch very precisely between two ring-shaped calibrated marks. Repeat this for different temperature and different volume fraction of nanofluids. The whole arrangement is shown in Fig. 3.15. The readings are taken from 30 °C to 90 °C.

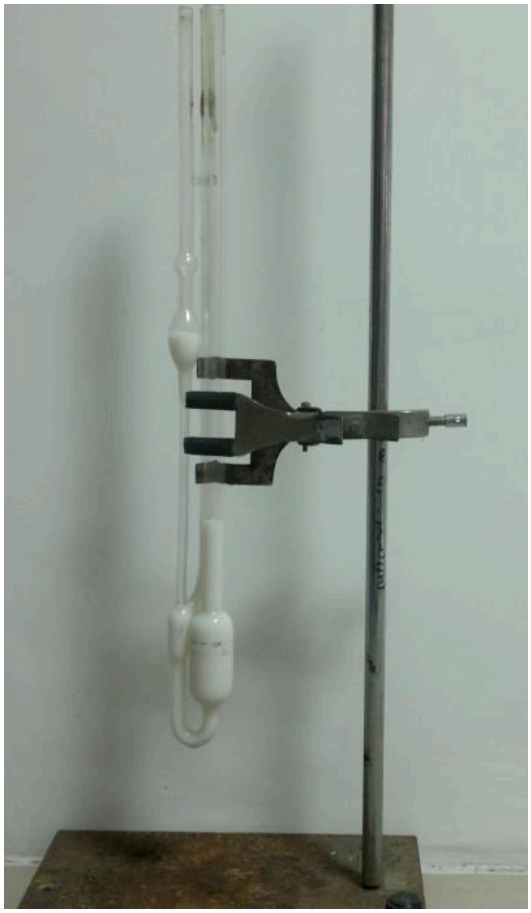

Fig. 3.13: Ubbelohde Viscometer with nanofluid sample

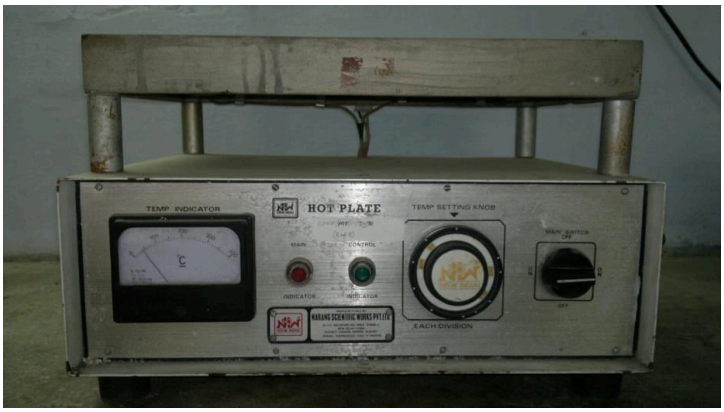

Fig. 3.14: Hot Plate

Fig. 3.15: Ubbelohde viscometer with nanofluid sample on the Hot Plate.

Fig. 3.16 (a): Pycnometer

Fig. 3.16 (b): Actual picture of pycnometer

3.5 Density measurement

For the measurement of density of nanofluids, pycnometer as shown in Fig. 3.16 (a) & Fig. 3.16 (b) is used. A detailed description and use of pycnometer is explained below as:

3.5.1 Pycnometer

Pycnometer is also known as specific gravity bottle or relative density bottle. Density determination by pycnometer is a very precise method. It uses a working liquid with well-known density, such as water. We will use distilled water, for which temperature dependent values of density is known. The pycnometer is a glass flask with a close-fitting ground glass stopper with a capillary hole through it. This fine hole releases a spare liquid after closing a top-filled pycnometer and allows for obtaining a given volume of measured and/or working liquid with a high accuracy. The actual picture of pycnometer is shown in Fig. 3.16 (b).

First of all, weigh the empty pycnometer with digital weighing balance machine. Then, fill the pycnometer with distilled water. The volume of distilled water that is filling the pycnometer and the stopper is

$$V = \frac{m_{H2O}}{\rho_{H2O}} \tag{3.5}$$

Where m_{H2O} is experimentally determined weight of water (empty pycnometer weight subtracted).

We repeat the procedure for the liquid with unknown density ρ_L and determine its weight m_L (measured weight minus weight of empty pycnometer). Volume V obtained in this measurement is the same as the volume of water determined from equation 3.5. It follows alternated equation

$$V = \frac{m_L}{\rho_L} \tag{3.6}$$

Combining equations (3.5) and (3.6)

$$\frac{m_{H2O}}{\rho_{H2O}} = \frac{m_L}{\rho_L} \tag{3.7}$$

This yields a relation that provides the density of measured liquid

$$\rho_L = \frac{m_L}{m_{H2O}} \cdot \rho_{H2O} \tag{3.8}$$

3.5.1.1 Density measurement of nanofluid by pycnometer at different temperature

Before doing any measurement, first of all, pycnometer is to be filled with potassium dichromate solution for at least 12 hours. As potassium dichromate solution is good cleaning agent. So, it removes any kind of dust particles in the pycnometer. Then, it is cleaned with distilled water, and

then it is to be dried in Oven at above 120 °C for at least 4-5 hours. So, that no water particles left in it. Now, it is ready to use.

Now, First of all, weigh the empty pycnometer with the digital weighing balance machine. Then pour the exactly 5 ml sample of nanofluid in the pycnometer by micro pipette. Then weigh the pycnometer again. Now this will give the weight of 5 ml sample of nanofluid sample by subtracting the empty pycnometer weight from the total weight. Fig. 3.17 shows digital weighing balance machine with nanofluid sample. So, density of this 5 ml sample can be found by the following equation:

$$\rho = \frac{weight\ of\ nanofluid\ sample\ (in\ gms.)}{5\ ml} = \ ----\ gm/cm^3 \qquad (3.9)$$

Fig. 3.17: Digital weighing balance machine with pycnometer filled with nanofluid sample

The above procedure is for density measurement by pycnometer at room temperature. But for different temperature, we use hot plate as shown in Fig. 3.14. Firstly, the whole process is done for base fluids i.e. ethylene glycol, distilled water and distilled water (75%) and ethylene glycol (25%), then the process is repeated for all 12 samples of nanofluids. The readings are taken from 30 °C to 90 °C.

Now for different temperature density measurement, we take a beaker, and filled the water in it up to the height a little less than the height of pycnometer. Put this beaker on the hot plate. This will work as a hot water bath for pycnometer. Also with the help of a clamp and stand, put a thermometer in the beaker for different temperature measurement. Now very gently put the pycnometer filled with nanofluid inside the beaker. And then slowly increase the temperature of hot plate. This whole arrangement is shown in Fig. 3.18. Now repeat it, at every temperature and then weigh the pycnometer on digital weighing balance machine. And the density of nanofluid sample can be found out by equation 3.9.

Fig. 3.18: Pycnometer with nanofluid sample in hot water bath.

3.6 Particle size analysis by Brookhaven particle size analyzer

Particle size analysis is done by Brookhaven particle size analyzer as shown in Fig. 3.19. It works on the principle of dynamic light scattering. A detailed description of the instrument is given as:

Fig. 3.19: Brookhaven particle size analyzer

3.6.1 Features at a glance

- Rapid and accurate particle size distributions
- Multimodal & unimodal size distribution software

- Range < 1 nm to 6 µm
- Easy to use Windows™ software
- Customizable reports, SPC charts
- Ideal for fast, routine sizing applications in research or quality control
- High power 35 mW diode laser
- Dynamic light scattering at 90° and 15°
- Compact bench top unit
- Optional zeta potential modules available
- Molecular weight determination

Specifications:

Size Range	< 1 nm to 6 µm depending on refractive index, concentration & scattering angle
Precision	± 1% typically
Sample Type	Most colloidal-sized materials, suspended in any clear liquid
Sample Volume	1 to 3 mL
Temperature Control	–5 °C to 110 °C, ± 0.1 °C, active control. No external circulator required
Laser	35 mW, solid state, standard
Scattering Angles	15° & 90°
Data Presentation	Average & width, lognormal fit, and multimodal size distribution standard
Computer	External PC; now Windows 7 compatible
Power Requirements	100/115/220/240 VAC, 50/60 Hz, 150 Watts
Dimensions	42.7 x 48.1 x 23.3 cm (HWD)
Weight	15 kg
Environmental Characteristics	Temperature 10 °C to 75 °C Humidity 0% to 95%, non-condensing

Note: All the above data is taken from [6].

3.6.2 Principles of operation

Dynamic light scattering (also known as photon correlation spectroscopy or quasi-elastic light scattering) is a technique in physics that can be used to determine the size distribution profile of small particles in suspension or polymers in solution. When light hits small particles, the light scatters in all directions (Rayleigh scattering) as long as the particles are small compared to the wavelength (below 250 nm). If the light source is a laser, and thus is monochromatic and coherent,

then one observes a time-dependent fluctuation in the scattering intensity. This fluctuation is due to the fact that the small molecules in solutions are undergoing Brownian motion, and so the distance between the scatterers in the solution is constantly changing with time. This random motion is modelled by the Stokes-Einstein equation. Below the equation is given in the form most often used for particle size analysis. The Stokes-Einstein relation that connects diffusion coefficient measured by dynamic light scattering to particle size is given by equation 3.10. The calculations are handled by instrument software.

$$D_h = \frac{K_B\, T}{3\,\pi\,\eta\, D_t} \tag{3.10}$$

Where,

- D_h is the hydrodynamic diameter (this is the goal: particle size!)
- D_t is the translational diffusion coefficient (this is find by dynamic light scattering)
- K_B is Boltzmann's constant (this is known)
- T is thermodynamic temperature (this is to be controlled)
- η is dynamic viscosity (this is known)

Dilute suspensions, on the order of 0.0001 to 1.0% v/v are prepared, using suitable wetting and/or dispersing agents. A small ultrasonicator is sometimes useful in breaking up loosely-held agglomerates. Two or three ml of suspension is required to make the measurements. Disposable, acrylic square cells are used for aqueous and simple alcohol suspensions. Disposable, glass round cells with reusable Teflon stoppers are used for aggressive solvent suspensions. Just a few minutes are required for the sample and cell to equilibrate with the actively controlled temperature environment inside the instrument.

3.6.3 Procedure

In present work, particle size analysis is done on all 12 samples of nanofluids, mentioned previously; the 3 ml sample is put in the square cell, and then put this square cell in the instrument. But, the results were not accurate, as the samples were more concentrated. So, this is limitation of the instrument. Then the samples are diluted by adding base fluids. By hit and trial, change the concentrations of samples 3-4 times and it is to be seen that if samples are made diluted by 5 times, then the results are more acceptable. Therefore, all the samples are diluted by 5 times. Take 0.5 ml of nanofluid sample and add 2.5 ml of base fluid. Then, the sonication is done for 5-7 minutes and the measurement has been carried out.

As 2.5 ml of base fluid is added in each concentration i.e. 0.15, 0.25%, 0.50% and 1.0%. So, all the concentrations' change accordingly, but there is linear variations in all concentrations. Therefore, the comparison of particle size in all samples of nanofluids can be easily done. The detailed results are discussed in the section 4.5 of the next chapter.

3.6.4 Applications

Many everyday industrial processes and products involve dispersions. The dispersed phase is often in a state of fine subdivision. The technology to produce these dispersions, to ensure that they perform according to specifications and to solve problems which may arise in production or use, requires knowledge of the particle size. This instrument can handle virtually any type of submicron sample suspended in, or dissolved in, a liquid. Some examples are:

- Polymer latexes
- Pharmaceutical preparations
- Oil/Water and Water/Oil emulsions
- Paints and pigments
- Inks and toners
- Cosmetic formulation

3.7 Conclusion

In this chapter, various instruments like KD2 pro thermal property analyzer, Ubbelohde viscometer, pycnometer and Brookhaven particle size analyzer have been discussed. Their principle of measurement and working at different temperature are discussed in detail. Also, hot plate and water bath, used for maintaining higher temperature are given. Now, in the next chapter, all the results by the measurement on these instruments are discussed thoroughly.

References

1. Alumina – Aluminium Oxide – Al_2O_3 – A Refractory Ceramic Oxide, Research article, www. Ceram.com,Queens Road, Penkhull ,Stoke-on-Trent, Staffordshire, ST4 7LQ, United Kingdom.
2. Al-Amayreh, M., Experimental Study of Thermal Conductivity of Ethylene Glycol Water Mixtures, European Journal of Scientific Research, vol. 44, no. 2, pp. 300-313, 2010.
3. Thermal conductivity of liquid (guarded plate method); Instruction Manual, supplied by MASS INTERNATIONAL, 93 Preet Nagar, Jagadhri Road, Ambala Cantt, 133001.
4. KD2 Pro Thermal Properties Analyzer, *Operator's Manual (Version 10),* supplied by Decagon Devices, Inc., WA 99163 USA.
5. Chandrasekar M., Suresh S., and Bose A. C., Experimental investigations and theoretical determination of thermal conductivity and viscosity of Al_2O_3/water nanofluid, Experimental Thermal and Fluid Science, vol. 34, pp. 210–216, 2010.
6. Operating manuals, 90 Plus Particle size analyzer, Brookhaven instruments Corporation, 750 Blue Point Road,Holtsville, NY 11742.

Chapter – 4
Results and Discussion

4.1 Introduction

The thermo-physical properties of nanofluids are evaluated by performing number of experiments by using KD2 pro thermal properties analyzer, Ubbelohde viscometer and pycnometer for thermal conductivity, viscosity and density, respectively, as mentioned in previous chapter. In this chapter, all the results are discussed from these experiments.

4.2 Density measurement

Density has been measured using pycnometer at a temperature range from 30 °C to 90 °C for all 12 samples, as mentioned in 3rd chapter.

4.2.1 Distilled water based nanofluids

The value of weight and density of 5 ml sample of distilled water, 0.1%, 0.25%, 0.50% and 1.0% volume fraction of alumina (Al_2O_3) and distilled water (DW) based nanofluids are respectively given in Table 4.1 & Table 4.2.

Table 4.1: Weight of distilled water and alumina and distilled water based nanofluids (gm.)

Sr. No.	Temperature (°C)	DW	0.1%	0.25%	0.50%	1.0%
1.	30	4.975	5.019	5.052	5.101	5.191
2.	40	4.962	5.010	5.044	5.096	5.186
3.	50	4.945	5.003	5.039	5.083	5.180
4.	60	4.921	4.992	5.032	5.069	5.172
5.	70	4.891	4.980	5.008	5.051	5.168
6.	80	4.868	4.960	4.975	5.018	5.161
7.	90	4.837	4.931	4.943	4.992	5.128

Table 4.2: Density of distilled water and alumina and distilled water based nanofluids (kg/m^3)

Sr. No.	Temperature (°C)	DW	0.1%	0.25%	0.50%	1.0%
1.	30	995.0	1003.8	1010.4	1020.2	1038.2
2.	40	992.4	1002.0	1008.8	1019.2	1037.2
3.	50	989.0	1000.6	1007.8	1016.6	1036.0
4.	60	984.2	998.4	1006.4	1013.8	1034.4
5.	70	978.2	996.0	1001.6	1010.2	1033.6
6.	80	973.6	992.0	995.0	1003.6	1032.2
7.	90	967.4	986.2	988.6	998.4	1025.6

The variation of density with temperature is shown by Fig. 4.1. And the generalized polynomial equation of density with temperature for distilled water and alumina and distilled water based nanofluids is given by equation 4.1 to equation 4.5.

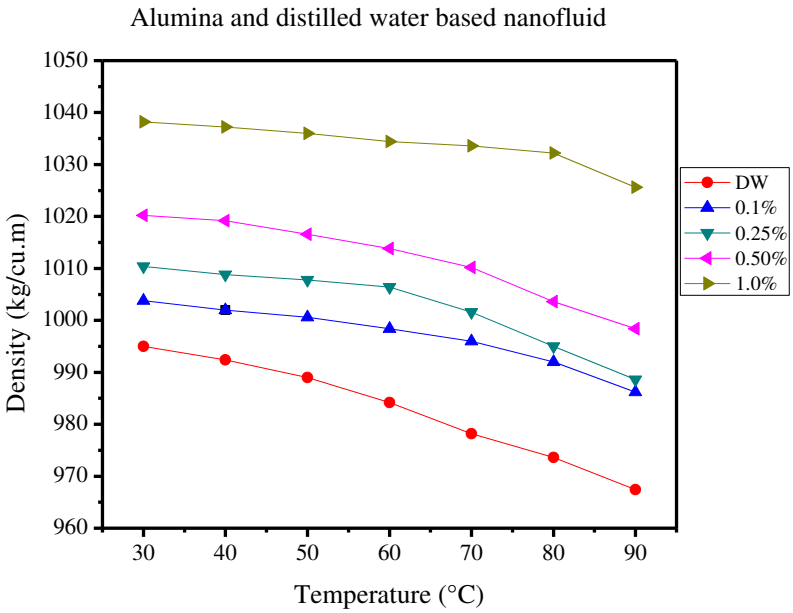

Fig 4.1: Variation of density with temperature

$$\rho = 713.6 + 34.818\ T - 1.72953\ T^2 + 0.04437\ T^3 - 6.23333\times10^{-4}\ T^4 + 4.53333\times10^{-6}\ T^5 - 1.33333\times10^{-8}\ T^6 \quad (4.1)$$

$$\rho = 1326.4 - 36.416\ T + 1.66897\ T^2 - 0.03979\ T^3 + 5.19306\times10^{-4}\ T^4 - 3.525\times10^{-6}\ T^5 + 9.72222\times10^{-9}\ T^6 \quad (4.2)$$

$$\rho = 557.8 + 53.67167\ T - 2.54552\ T^2 + 0.06183\ T^3 - 8.13333\times10^{-4}\ T^4 + 5.5\times10^{-6}\ T^5 - 1.5\times10^{-8}\ T^6 \quad (4.3)$$

$$\rho = 1179.6 - 21.27333\ T + 1.14235\ T^2 - 0.03141\ T^3 + 4.65417\times10^{-4}\ T^4 - 3.54167\times10^{-6}\ T^5 + 1.08333\times10^{-8}\ T^6 \quad (4.4)$$

$$\rho = 1242.2 - 22.95567\ T + 1.03802\ T^2 - 0.02405\ T^3 + 2.99306\times10^{-4}\ T^4 - 1.89167\times10^{-6}\ T^5 + 4.72222\times10^{-9}\ T^6 \quad (4.5)$$

It can be seen from the Fig 4.1, that at 30 °C, with the increase in the concentration of nanoparticles from 0.1% to 1.0%, density of alumina and distilled water based nanofluids increases from 0.9% to 4.0% (i.e. 0.9% for 0.1% concentration, 1.52% for 0.25% concentration, 2.47% for 0.50% concentration and 4.0% for 1.0% concentration) compared to base fluid i.e. distilled water.

And with the increase in temperature, density of alumina and distilled water based nanofluids decreases. From 30 °C to 90 °C, density decreases by 1.75% for 0.1% concentration, 2.75% for 0.25% concentration, 2.13% for 0.50% concentration and 1.21% for 1.0% concentration.

4.2.2 Ethylene glycol based nanofluids

The value of weight and density of 5 ml sample of ethylene glycol, 0.1%, 0.25%, 0.50% and 1.0% volume fraction of alumina (Al_2O_3) and ethylene glycol (EG) based nanofluids are respectively given in Table 4.3 & Table 4.4.

Table 4.3: Weight of ethylene glycol and alumina and ethylene glycol based nanofluids (gm.)

Sr. No.	Temperature (°C)	EG	0.1%	0.25%	0.50%	1.0%
1.	30	5.549	5.591	5.632	5.717	5.878
2.	40	5.512	5.585	5.617	5.711	5.862
3.	50	5.482	5.575	5.602	5.701	5.847
4.	60	5.441	5.567	5.590	5.689	5.835
5.	70	5.417	5.548	5.581	5.678	5.822
6.	80	5.377	5.531	5.568	5.662	5.810
7.	90	5.337	5.507	5.550	5.647	5.792

Table 4.4: Density of ethylene glycol and alumina and ethylene glycol based nanofluids (kg/m^3)

Sr. No.	Temperature (°C)	EG	0.1%	0.25%	0.50%	1.0%
1.	30	1109.8	1118.2	1126.4	1143.4	1175.6
2.	40	1102.4	1117.0	1123.4	1142.2	1172.4
3.	50	1096.4	1115.0	1120.4	1140.2	1169.4
4.	60	1088.2	1113.4	1118.0	1137.8	1167.0
5.	70	1083.4	1109.6	1116.2	1135.6	1164.4
6.	80	1075.4	1106.2	1113.6	1132.4	1162.0
7.	90	1067.4	1101.4	1110.0	1129.4	1158.4

The variation of density with temperature is shown by Fig. 4.2. And the generalized polynomial equation of density with temperature for ethylene glycol and alumina and ethylene glycol based nanofluids is given by equation 4.6 to equation 4.10.

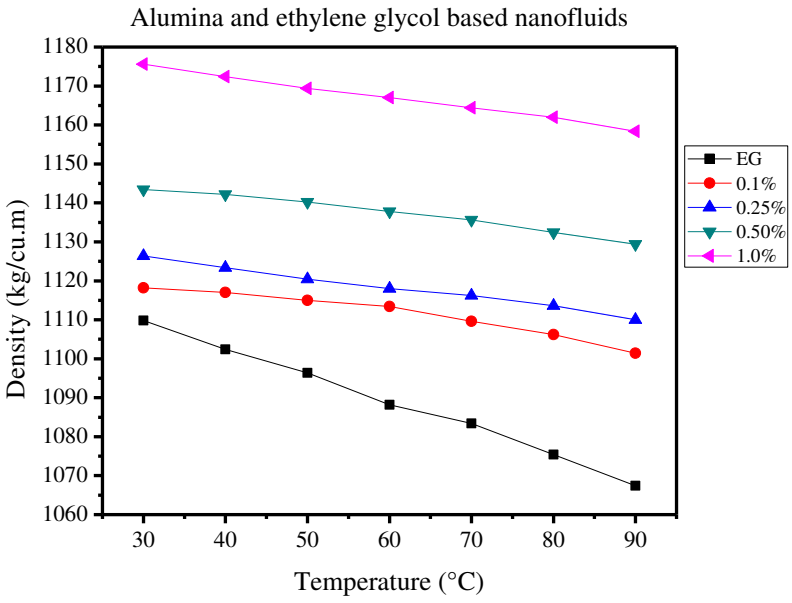

Fig 4.2: Variation of density with temperature

$$\rho = 338.2 + 90.596\ T - 4.23745\ T^2 + 0.10241\ T^3 - 0.00135\ T^4 + 9.275\times10^{-6}\ T^5 - 2.58333\times10^{-8}\ T^6 \quad (4.6)$$

$$\rho = 1232.4 - 12.405\ T + 0.61052\ T^2 - 0.01589\ T^3 + 2.24306\times10^{-4}\ T^4 - 1.625\times10^{-6}\ T^5 + 4.72222\times10^{-9}\ T^6 \quad (4.7)$$

$$\rho = 1356.8 - 25.54367\ T + 1.24034\ T^2 - 0.03116\ T^3 + 4.25694\times10^{-4}\ T^4 - 3.00833\times10^{-6}\ T^5 + 8.61111\times10^{-9}\ T^6 \quad (4.8)$$

$$\rho = 962.8 + 25.55533\ T - 1.21305\ T^2 + 0.02938\ T^3 - 3.8875\times10^{-4}\ T^4 + 2.675\times10^{-6}\ T^5 - 7.5\times10^{-9}\ T^6 \quad (4.9)$$

$$\rho = 2979 - 214.267\ T + 9.95674\ T^2 - 0.24016\ T^3 + 0.00317\ T^4 - 2.1675\times10^{-5}\ T^5 + 6.02778\times10^{-8}\ T^6 \quad (4.10)$$

It can be seen from the Fig 4.2, that at 30 °C, with the increase in the concentration of nanoparticles from 0.1% to 1.0%, density of alumina and ethylene glycol based nanofluids increases from 0.75% to 5.6% (i.e. 0.75% for 0.1% concentration, 1.47% for 0.25% concentration, 2.94% for 0.50% concentration and 5.6% for 1.0% concentration) compared to base fluid i.e. ethylene glycol.

And with the increase in temperature, density of alumina and ethylene glycol based nanofluids decreases. From 30 °C to 90 °C, density decreases by 1.5% for 0.1% concentration, 1.45% for 0.25% concentration, 1.22% for 0.50% concentration and 1.46% for 1.0% concentration.

4.2.3 Distilled water and ethylene glycol based nanofluids

The value of weight and density of 5 ml sample of distilled water (75%) and ethylene glycol (25%), 0.1%, 0.25%, 0.50% and 1.0% volume fraction of alumina and distilled water (75%) and ethylene glycol (25%) based nanofluids are respectively given in Table 4.5 & Table 4.6.

The variation of density with temperature is shown by Fig. 4.3. And the generalized polynomial equation of density with temperature for distilled water (75%) and ethylene glycol (25%) and alumina and distilled water (75%) and ethylene glycol (25%) based nanofluids is given by equation 4.11 to equation 4.15.

Table 4.5: Weight of distilled water (75%) and ethylene glycol (25%) and alumina and distilled water (75%) and ethylene glycol (25%) based nanofluids (gm.)

Sr. No.	Temperature (°C)	DW (75%) + EG (25%)	0.1%	0.25%	0.50%	1.0%
1.	30	5.171	5.211	5.256	5.305	5.389
2.	40	5.127	5.201	5.249	5.300	5.380
3.	50	5.108	5.193	5.241	5.291	5.365
4.	60	5.084	5.184	5.231	5.279	5.349
5.	70	5.047	5.173	5.219	5.264	5.337
6.	80	5.011	5.159	5.204	5.252	5.327
7.	90	4.979	5.138	5.187	5.239	5.308

Table 4.6: Density of distilled water (75%) and ethylene glycol (25%) and alumina and distilled water (75%) and ethylene glycol (25%) based nanofluids (kg/m^3)

Sr. No.	Temperature (°C)	DW (75%) + EG (25%)	0.1%	0.25%	0.50%	1.0%
1.	30	1034.2	1042.2	1051.2	1061	1077.8
2.	40	1025.4	1040.2	1049.8	1060.0	1076.0
3.	50	1021.6	1038.6	1048.2	1058.2	1073.0
4.	60	1016.8	1036.8	1046.2	1055.8	1069.8
5.	70	1009.4	1034.6	1043.8	1052.8	1067.4
6.	80	1002.2	1031.8	1040.8	1050.4	1065.4
7.	90	995.8	1027.6	1037.4	1047.8	1061.6

alumina and distilled water (75%) and ethylene glycol (25%) based nanofluids

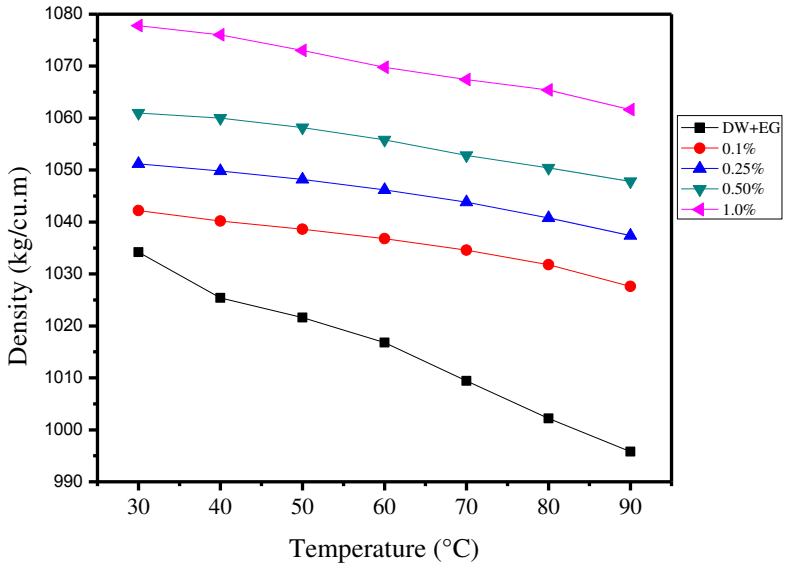

Fig 4.3: Variation of density with temperature

$$\rho = 1095.6 - 4.83967\ T + 0.22089\ T^2 - 0.00535\ T^3 + 7.09722\times10^{-5}\ T^4 - 4.91667\times10^{-7}\ T^5 + 1.38889\times10^{-9}\ T^6 \quad (4.11)$$

$$\rho = 896 + 19.52067\ T - 0.93151\ T^2 + 0.02307\ T^3 - 3.14306\times10^{-4}\ T^4 + 2.225\times10^{-6}\ T^5 - 6.38889\times10^{-9}\ T^6 \quad (4.12)$$

$$\rho = 1123.4 - 5.59967\ T + 0.27989\ T^2 - 0.00705\ T^3 + 9.09722\times10^{-5}\ T^4 - 5.75\times10^{-7}\ T^5 + 1.38889\times10^{-9}\ T^6 \quad (4.13)$$

$$\rho = 1031.8 + 8.906\ T - 0.75095\ T^2 + 0.02444\ T^3 - 3.89583\times10^{-4}\ T^4 + 3.025\times10^{-6}\ T^5 - 9.16667\times10^{-9}\ T^6 \quad (4.14)$$

$$\rho = 1065.4 - 1.616\ T + 0.03924\ T^2 - 3.45833\times10^{-4}\ T^3 - 2.36111\times10^{-6}\ T^4 + 5.83333\times10^{-8}\ T^5 - 2.77778\times10^{-10}\ T^6 \quad (4.15)$$

It can be seen from the Fig 4.3, that at 30 °C, with the increase in the concentration of nanoparticles from 0.1% to 1.0%, density of alumina and distilled water (75%) and ethylene glycol

(25%) based nanofluids increases from 0.76% to 4.04% (i.e. 0.76% for 0.1% concentration, 1.62% for 0.25% concentration, 2.53% for 0.50% concentration and 4.04% for 1.0% concentration) compared to base fluid i.e. distilled water (75%) and ethylene glycol (25%).

And with the increase in temperature, density of alumina and distilled water (75%) and ethylene glycol (25%) based nanofluids decreases. From 30 °C to 90 °C, density decreases by 1.4% for 0.1% concentration, 1.31% for 0.25% concentration, 1.24% for 0.50% concentration and 1.50% for 1.0% concentration.

4.3 Viscosity measurement

Viscosity has been measured using Ubbelohde viscometer at different temperature range from 30 °C to 90 °C for all 12 samples. In the Ubbelohde viscometer, the viscosity of any sample can be compared with the one whose viscosity is known (eg. distilled water) and then the viscosity of that sample is find out. In the present work, only the viscosity of distilled water at different temperature is taken as standard and not measured. While all other viscosities are experimentally measured, by taking distilled water as standard reference fluid by using the following:

$$\mu_{nf} = \mu_{bf} \frac{t_{nf}\ \rho_{nf}}{t_{bf}\ \rho_{bf}} \tag{4.16}$$

Where μ = Dynamic Viscosity (Pa-sec) or (cP)

ρ = Density (Kg/m^3)

t = time (sec.)

subscripts nf and bf represents nanofluid and base fluid respectively.

Also in Ubbelohde viscometer, while measuring the time taken by using stopwatch, 3-4 readings are taken for high accuracy and then the average of all these readings is taken. Therefore, the average time is taken.

4.3.1 Distilled water based nanofluids

The average time taken to cover the distance between two ring-shaped calibrated marks for the distilled water, and 0.1%, 0.25%, 0.50% and 1.0% volume fraction of alumina and distilled water based nanofluids is given by Table 4.7. And the viscosities for the same are given by Table 4.8.

The values of viscosity of distilled water at different temperatures are taken as standard for calculating the viscosities of all other samples (i.e. 0.1%, 0.25%, 0.50% and 1.0% volume fraction of alumina and distilled water based nanofluids). In equation 4.16, μ_{bf} values are taken from standard data available, while ρ_{bf} and all ρ_{nf} values are taken from Table 4.2 for their respective temperatures. While all t_{bf} and t_{nf} values at different temperatures are taken from Table 4.7.

Table 4.7: Average time taken to cover the distance between two calibrated marks (sec.)

Sr. No.	Temperature (°C)	DW	0.1%	0.25%	0.50%	1.0%
1.	30	116	120	141	157	178
2.	40	106	111	125	137	151
3.	50	92	97	107	118	133
4.	60	84	89	101	111	120
5.	70	74	77	85	92	103
6.	80	69	72	78	87	94
7.	90	64	68	71	76	84

Table 4.8: Viscosities of distilled water and alumina and distilled water based nanofluids (cP)

Sr. No.	Temperature (°C)	DW*	0.1%	0.25%	0.50%	1.0%
1.	30	0.798	0.832	0.984	1.107	1.277
2.	40	0.653	0.690	0.782	0.866	0.972
3.	50	0.547	0.583	0.648	0.721	0.828
4.	60	0.467	0.502	0.574	0.637	0.701
5.	70	0.404	0.428	0.475	0.518	0.595
6.	80	0.355	0.377	0.410	0.461	0.513
7.	90	0.315	0.341	0.357	0.386	0.438

* taken from http://www.EngineeringToolBox.com/Water-Dynamic and kinematic Viscosity/

The variation of viscosity with temperature is shown by Fig. 4.4. And the generalized polynomial equation of viscosity with temperature for distilled water and alumina and distilled water based nanofluids is given by equation 4.17 to equation 4.21.

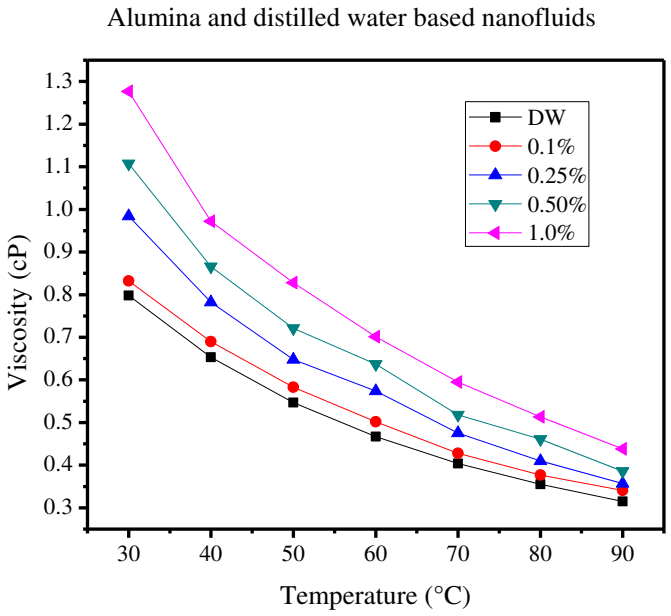

Fig 4.4: Variation of viscosity with temperature

$$\mu = -2.449 + 0.43867\ T - 0.0221\ T^2 + 5.50708\times10^{-4}\ T^3 - 7.40694\times10^{-6}\ T^4 + 5.14167\times10^{-8}\ T^5 - 1.44444\times10^{-10}\ T^6 \quad (4.17)$$

$$\mu = -16.206 + 2.08751\,T - 0.10024\,T^2 + 0.00245\,T^3 - 3.24903\times10^{-5}\,T^4 + 2.22833\times10^{-7}\,T^5 - 6.19444\times10^{-10}\,T^6 \quad (4.18)$$

$$\mu = -20.965 + 2.71258\,T - 0.13205\,T^2 + 0.00328\,T^3 - 4.41125\times10^{-5}\,T^4 + 3.07167\times10^{-7}\,T^5 - 8.66667\times10^{-10}\,T^6 \quad (4.19)$$

$$\mu = 13.587 - 1.19581\,T + 0.04756\,T^2 - 0.00101\,T^3 + 1.17556\times10^{-5}\,T^4 - 7.2\times10^{-8}\,T^5 + 1.80556\times10^{-10} \quad (4.20)$$

$$\mu = 1.335 - 0.00534\,T - 0.00123\,T^2 + 4.24583\times10^{-5}\,T^3 - 6.43056\times10^{-7}\,T^4 + 4.75\times10^{-9}\,T^5 - 1.38889\times10^{-11}\,T^6 \quad (4.21)$$

It can be seen from the Fig 4.4, that at 30 °C, with the increase in the concentration of nanoparticles from 0.1% to 1.0%, viscosity of alumina and distilled water based nanofluids increases from 4.09% to 60% (i.e. 4.09% for 0.1% concentration, 18% for 0.25% concentration, 27.9% for 0.50% concentration and 60% for 1.0% concentration) compared to base fluid i.e. distilled water.

And with the increase in temperature, viscosity of alumina and distilled water based nanofluids decreases. From 30 °C to 90 °C, viscosity decreases by 59% for 0.1% concentration, 63.7% for 0.25% concentration, 65% for 0.50% concentration and 65.7% for 1.0% concentration.

4.3.2 Ethylene Glycol based nanofluids

The Average time taken to cover the distance between two ring-shaped calibrated marks for the distilled water, and 0.1%, 0.25%, 0.50% and 1.0% volume fraction of alumina and ethylene glycol based nanofluids is shown by Table 4.9. And the viscosities for the same are given by Table 4.10.

Table 4.9: Average time taken to cover the distance between two calibrated marks (sec.)

Sr. No.	Temperature (°C)	EG	0.1%	0.25%	0.50%	1.0%
1.	30	1874	1998	2202	2442	2932
2.	40	1526	1629	1865	2138	2539
3.	50	1152	1278	1512	1778	2112
4.	60	949	1099	1329	1579	1992
5.	70	752	838	1038	1436	1666
6.	80	648	732	920	1242	1432
7.	90	534	662	835	1054	1303

The values of viscosity of ethylene glycol at different temperatures are calculated by taking distilled water as standard reference fluid. While for calculating the viscosities of all other samples (0.1%, 0.25%, 0.50% and 1.0% volume fraction of alumina and ethylene glycol based nanofluids), the Ethylene glycol is taken as standard reference fluid, as it is the base fluid. And then the comparison of base fluid and nanofluids viscosity can be easily done.

In equation 4.16, μ_{bf} values are calculated first, and then all μ_{nf} values are calculated. All ρ_{bf} and ρ_{nf} values are taken from the Table 4.4 for their respective temperatures. While all t_{bf} and t_{nf} values at different temperatures are taken from Table 4.9.

Table 4.10: Viscosities of ethylene glycol and alumina and ethylene glycol based nanofluids (cP)

Sr. No.	Temperature (°C)	EG	0.1%	0.25%	0.50%	1.0%
1.	30	14.379	15.612	17.333	19.512	24.087
2.	40	10.443	11.295	13.006	15.159	18.479
3.	50	7.593	8.566	10.183	12.187	14.848
4.	60	5.833	6.911	8.392	10.148	13.131
5.	70	4.547	5.190	6.466	9.101	10.826
6.	80	3.682	4.278	5.413	7.432	8.793
7.	90	2.899	3.709	4.716	6.056	7.681

The variation of viscosity with temperature is shown by Fig. 4.5. And the generalized polynomial equation of viscosity with temperature for ethylene glycol and alumina and ethylene glycol based nanofluids is given by equation 4.22 to equation 4.26.

$$\mu = -58.376 + 9.75704\,T - 0.48424\,T^2 + 0.01173\,T^3 - 1.52818\times10^{-4}\,T^4 + 1.02992\times10^{-6}\,T^5 - 2.82222\times10^{-9}\,T^6 \quad (4.22)$$

$$\mu = -189.536 + 26.01278\,T - 1.28374\,T^2 + 0.03189\,T^3 - 4.28277\times10^{-4}\,T^4 + 2.96871\times10^{-6}\,T^5 - 8.32917\times10^{-9}\,T^6 \quad (4.23)$$

$$\mu = -210.597 + 28.65189\,T - 1.40757\,T^2 + 0.03491\,T^3 - 4.6875\times10^{-4}\,T^4 + 3.25042\times10^{-6}\,T^5 - 9.125\times10^{-9}\,T^6 \quad (4.24)$$

$$\mu = 277.418 - 28.75778\,T + 1.33178\,T^2 - 0.03269\,T^3 + 4.41972\times10^{-4}\,T^4 - 3.10675\times10^{-6}\,T^5 + 8.86389\times10^{-9}\,T^6 \quad (4.25)$$

$$\mu = -367.475 + 47.45211\,T - 2.26019\,T^2 + 0.05448\,T^3 - 7.10382\times10^{-4} + 4.77983\times10^{-6}\,T^5 - 1.30194\times10^{-8}\,T^6 \quad (4.26)$$

It can be seen from the Fig 4.5, that at 30 °C, with the increase in the concentration of nanoparticles from 0.1% to 1.0%, viscosity of alumina and ethylene glycol based nanofluids increases from 7.89% to 40.30% (i.e. 7.89% for 0.1% concentration, 17.04% for 0.25% concentration, 26.30% for 0.50% concentration and 40.30% for 1.0% concentration) compared to base fluid i.e. ethylene glycol.

And with the increase in temperature, viscosity of alumina and ethylene glycol based nanofluids decreases. From 30 °C to 90 °C, viscosity decreases by 76.24% for 0.1% concentration, 72.79% for 0.25% concentration, 68.96% for 0.50% concentration and 68.10% for 1.0% concentration.

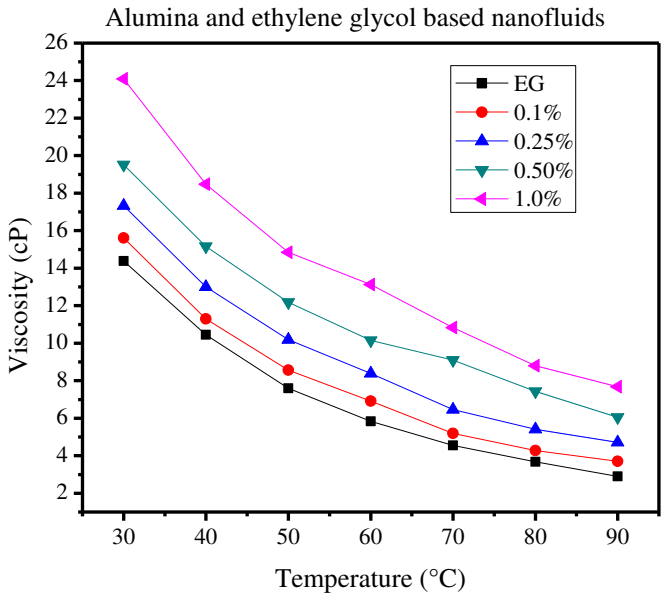

Fig 4.5: Variation of viscosity with temperature

4.3.3 Distilled water and ethylene glycol based nanofluids

The Average time taken to cover the distance between two ring-shaped calibrated marks for the distilled water (75%) and ethylene glycol (25%) and 0.1%, 0.25%, 0.50% and 1.0% volume fraction of alumina and distilled water (75%) and ethylene glycol (25%) based nanofluids is given by Table 4.11. And the viscosities for the same are given by Table 4.12.

Table 4.11: Average time taken to cover the distance between two calibrated marks (sec.)

Sr. No.	Temperature (°C)	DW (75%) + EG (25%)	0.1%	0.25%	0.50%	1.0%
1.	30	228	238	246	256	277
2.	40	201	212	229	242	255
3.	50	165	169	186	206	236
4.	60	150	157	169	185	208
5.	70	128	137	158	176	190
6.	80	118	125	138	157	177
7.	90	104	109	119	135	161

The values of viscosity of distilled water (75%) and ethylene glycol (25%) at different temperatures are calculated by taking distilled water as standard reference fluid. While for calculating the viscosities of all other samples (0.1%, 0.25%, 0.50% and 1.0% volume fraction of alumina and distilled water (75%) and ethylene glycol (25%) based nanofluids), the distilled water (75%) and ethylene glycol (25%) is taken as standard reference fluid, as it is the base fluid. And then the comparison of base fluid and nanofluids viscosity can be easily done.

In equation 4.16, μ_{bf} values are calculated first, and then all μ_{nf} values are calculated. All ρ_{bf} and ρ_{nf} values are taken from the Table 4.6 for their respective temperatures. While all t_{bf} and t_{nf} values at different temperatures are taken from Table 4.11.

Table 4.12: Viscosities of distilled water (75%) and ethylene glycol (25%) and alumina and distilled water (75%) and ethylene glycol (25%) based nanofluids (cP)

Sr. No.	Temperature (°C)	DW (75%) + EG (25%)	0.1%	0.25%	0.50%	1.0%
1.	30	1.630	1.715	1.787	1.878	2.072
2.	40	1.279	1.368	1.492	1.592	1.703
3.	50	1.013	1.055	1.172	1.310	1.522
4.	60	0.862	0.920	0.999	1.104	1.258
5.	70	0.721	0.791	0.920	1.034	1.132
6.	80	0.625	0.682	0.759	0.872	0.997
7.	90	0.526	0.569	0.627	0.718	0.868

The variation of viscosity with temperature is shown by Fig. 4.6. And the generalized polynomial equation of viscosity with temperature for distilled water (75%) and ethylene glycol (25%) and alumina and distilled water (75%) and ethylene glycol (25%) nanofluids is given by equation 4.27 to equation 4.31.

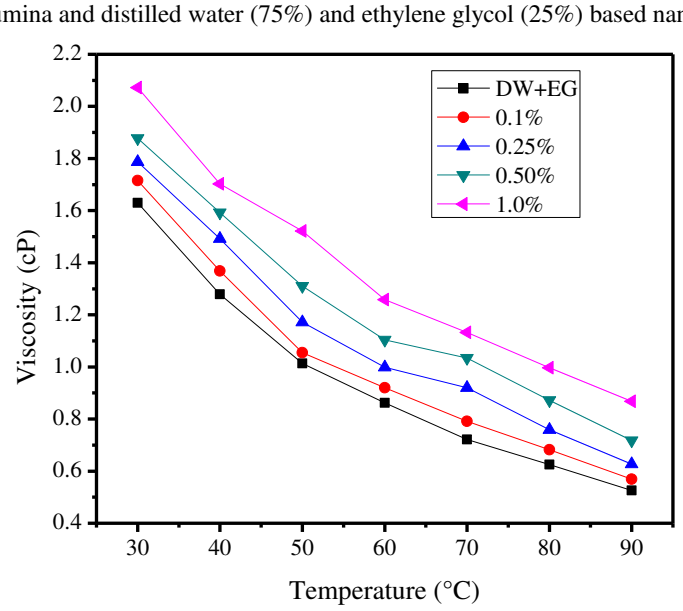

Fig 4.6: Variation of viscosity with temperature

$$\mu = 3.909 - 0.38158\ T + 0.02728\ T^2 - 9.35417\times10^{-4}\ T^3 + 1.59736\times10^{-5}\ T^4 - 1.32667\times10^{-7}\ T^5 + 4.27778\times10^{-10}\ T^6 \quad (4.27)$$

$$\mu = 32.632 - 3.63164\ T + 0.17558\ T^2 - 0.00443\ T^3 + 6.08306\times10^{-5}\ T^4 - 4.31833\times10^{-7}\ T^5 + 1.23889\times10^{-9}\ T^6 \quad (4.28)$$

$$\mu = 71.377 - 7.72968\ T + 0.3496\ T^2 - 0.00822\ T^3 + 1.05876\times10^{-4}\ T^4 - 7.0875\times10^{-7}\ T^5 + 1.93056\times10^{-9}\ T^6 \quad (4.29)$$

$$\mu = -18.851 + 2.48033\ T - 0.11786\ T^2 + 0.00284\ T^3 - 3.70708\times10^{-5}\ T^4 + 2.51167\times10^{-7}\ T^5 - 6.91667\times10^{-10}\ T^6 \quad (4.30)$$

$$\mu = -34.09 + 4.14425\ T - 0.19009\ T^2 + 0.00445\ T^3 - 5.66458\times10^{-5}\ T^4 + 3.74583\times10^{-7}\ T^5 - 1.00833\times10^{-9}\ T^6 \quad (4.31)$$

It can be seen from the Fig 4.6, that at 30 °C, with the increase in the concentration of nanoparticles from 0.1% to 1.0%, viscosity of alumina and distilled water (75%) and ethylene glycol (25%) based nanofluids increases from 4.96% to 21.33% (i.e. 4.96% for 0.1% concentration, 8.78% for 0.25% concentration, 13.21% for 0.50% concentration and 21.33% for 1.0% concentration) compared to base fluid i.e. distilled water (75%) and ethylene glycol (25%).

And with the increase in temperature, viscosity of alumina and distilled water (75%) and ethylene glycol (25%) based nanofluids decreases. From 30 °C to 90 °C, viscosity decreases by 66.82% for 0.1% concentration, 64.91% for 0.25% concentration, 61.77% for 0.50% concentration and 58.10% for 1.0% concentration.

4.4 Thermal conductivity measurement

Thermal conductivity of nanofluids can be measured by using KD2 pro thermal property analyzer. And KD2's KS-1 sensor needle is used in present work. The thermal conductivity is measured in the range 25 °C (i.e. room temperature) to 60 °C for base fluids i.e. distilled water, ethylene glycol, distilled water (75%) and ethylene glycol (25%) and for all 12 samples of nanofluids.

Table 4.13: Thermal conductivity of distilled water

Sr. No.	Temperature (°C)	Thermal conductivity (W/m-K)
1.	24.32	0.609
2.	28.24	0.619
3.	31.20	0.624
4.	35.19	0.630
5.	37.99	0.632
6.	40.52	0.633
7.	45.66	0.637
8.	49.12	0.642
9.	53.91	0.648
10.	57.11	0.653

4.4.1 Distilled water based nanofluids

The thermal conductivity of distilled water, 0.1%, 0.25%, 0.50% and 1.0% volume fractions of alumina and distilled water based nanofluids at different temperatures are given by Table 4.13 to

Table 4.17. The variation of thermal conductivity with temperature is shown by Fig. 4.7. And the generalized polynomial equation of thermal conductivity with temperature for distilled water and alumina and distilled water based nanofluids is respectively given by equation 4.32 to equation 4.36.

Table 4.14: Thermal conductivity of 0.1 % alumina and distilled water based nanofluid

Sr. No.	Temperature (°C)	Thermal conductivity (W/m-K)
1.	25.16	0.613
2.	27.12	0.621
3.	32.18	0.627
4.	36.59	0.634
5.	39.50	0.635
6.	42.56	0.640
7.	46.21	0.645
8.	50.92	0.651
9.	53.16	0.654
10.	58.02	0.659

Table 4.15: Thermal conductivity of 0.25 % alumina and distilled water based nanofluid

Sr. No.	Temperature (°C)	Thermal conductivity (W/m-K)
1.	24.18	0.622
2.	27.56	0.632
3.	30.29	0.637
4.	34.56	0.643
5.	37.57	0.653
6.	39.87	0.663
7.	44.21	0.676
8.	47.56	0.685
9.	50.29	0.697
10.	55.67	0.703

Table 4.16: Thermal conductivity of 0.50 % alumina and distilled water based nanofluid

Sr. No.	Temperature (°C)	Thermal conductivity (W/m-K)
1.	26.12	0.629
2.	30.46	0.635
3.	34.48	0.652
4.	36.24	0.663
5.	39.56	0.679
6.	42.18	0.686
7.	45.69	0.693
8.	49.27	0.699
9.	53.49	0.707
10.	57.21	0.712

Table 4.17: Thermal conductivity of 1.0% alumina and distilled water based nanofluid

Sr. No.	Temperature (°C)	Thermal conductivity (W/m-K)
1.	25.51	0.641
2.	29.46	0.650
3.	32.03	0.657
4.	35.05	0.670
5.	38.67	0.683
6.	43.79	0.699
7.	46.89	0.705
8.	49.17	0.711
9.	54.49	0.718
10.	56.21	0.722

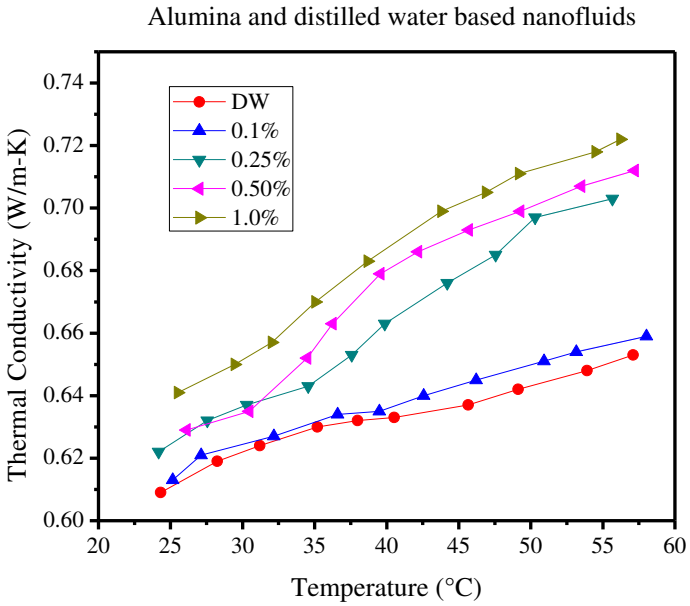

Fig 4.7: Variation of thermal conductivity with temperature

$$k = -0.33884 - 1.38085\,T + 0.30734\,T^2 - 0.02802\,T^3 + 0.00142\,T^4 - 4.42322\times10^{-5}\,T^5 + 8.66433\times10^{-7}\,T^6 - 1.04479\times10^{-8}\,T^7 + 7.098\times10^{-11}\,T^8 - 2.08184\times10^{-13}\,T^9 \quad (4.32)$$

$$k = -1.14328 - 4.73182\,T + 1.02149\,T^2 - 0.09273\,T^3 + 0.00472\,T^4 - 1.48442\times10^{-4}\,T^5 + 2.94892\times10^{-6}\,T^6 - 3.6203\times10^{-8}\,T^7 + 2.51255\times10^{-10}\,T^8 - 7.55059\times10^{-13}\,T^9 \quad (4.33)$$

$$k = 1.27644 + 5.0606\,T - 1.10996\,T^2 + 0.10369\,T^3 - 0.00543\,T^4 + 1.75023\times10^{-4}\,T^5 - 3.55203\times10^{-6}\,T^6 + 4.43836\times10^{-8}\,T^7 - 3.12373\times10^{-10}\,T^8 + 9.48616\times10^{-13}\,T^9 \quad (4.34)$$

$$k = -3.0935 - 13.22357\,T + 2.73959\,T^2 - 0.24022\,T^3 + 0.01184\,T^4 - 3.60023\times10^{-4}\,T^5 + 6.92937\times10^{-6}\,T^6 - 8.2521\times10^{-8}\,T^7 + 5.56382\times10^{-10}\,T^8 - 1.62711\times10^{-12}\,T^9 \quad (4.35)$$

$$k = -0.11871 - 0.49675\,T + 0.10059\,T^2 - 0.0076\,T^3 + 2.95289\times10^{-4}\,T^4 - 6.15529\times10^{-6}\,T^5 + 5.79058\times10^{-8}\,T^6 + 9.26029\times10^{-11}\,T^7 - 6.24187\times10^{-12}\,T^8 + 3.55242\times10^{-14}\,T^9 \quad (4.36)$$

It can be seen from the Fig 4.7, that at ambient temperature, with the increase in the concentration of nanoparticles from 0.1% to 1.0%, thermal conductivity of alumina and distilled water based nanofluids increases from 0.65% to 5.0% (i.e. 0.65% for 0.1% concentration, 2.1% for 0.25% concentration, 3.27% for 0.50% concentration and 5.0% for 1.0% concentration) compared to base fluid i.e. distilled water.

And with the increase in temperature, thermal conductivity of alumina and distilled water based nanofluids increases. From 25 °C to 60 °C, thermal conductivity increases by 6.27% for 0.1% concentration, 10.76% for 0.25% concentration, 11.03% for 0.50% concentration and 10.72% for 1.0% concentration.

4.4.2 Ethylene glycol based nanofluids

The thermal conductivity of ethylene glycol, 0.1%, 0.25%, 0.50% and 1.0% volume fractions of alumina and ethylene glycol based nanofluids at different temperatures are given by Table 4.18 to Table 4.22.

Table 4.18: Thermal conductivity of ethylene glycol

Sr. No.	Temperature (°C)	Thermal conductivity (W/m-K)
1.	24.96	0.250
2.	29.21	0.252
3.	34.69	0.255
4.	37.12	0.256
5.	40.02	0.257
6.	44.12	0.260
7.	47.22	0.261
8.	51.12	0.262
9.	53.21	0.263
10.	57.27	0.265

Table 4.19: Thermal conductivity of 0.1% alumina and ethylene glycol based nanofluid

Sr. No.	Temperature (°C)	Thermal conductivity (W/m-K)
1.	25.67	0.251
2.	28.27	0.252
3.	32.17	0.255
4.	36.93	0.256
5.	41.09	0.259
6.	45.19	0.262
7.	48.29	0.264
8.	51.67	0.264
9.	54.27	0.265
10.	58.29	0.267

Table 4.20: Thermal conductivity of 0.25% alumina and ethylene glycol based nanofluid

Sr. No.	Temperature (°C)	Thermal conductivity (W/m-K)
1.	26.72	0.253
2.	31.27	0.256
3.	35.16	0.261
4.	38.72	0.263
5.	41.63	0.265
6.	45.73	0.267
7.	49.63	0.269
8.	52.14	0.273
9.	55.24	0.274
10.	57.19	0.278

Table 4.21: Thermal conductivity of 0.50% alumina and ethylene glycol based nanofluid

Sr. No.	Temperature (°C)	Thermal conductivity (W/m-K)
1.	25.94	0.259
2.	28.27	0.262
3.	32.88	0.266
4.	36.54	0.271
5.	39.05	0.277
6.	43.15	0.279
7.	48.21	0.285
8.	52.21	0.287
9.	55.41	0.288
10.	58.49	0.290

Table 4.22: Thermal conductivity of 1.0% alumina and ethylene glycol based nanofluid

Sr. No.	Temperature (°C)	Thermal conductivity (W/m-K)
1.	24.69	0.268
2.	27.56	0.273
3.	30.16	0.276
4.	35.67	0.283
5.	39.62	0.286
6.	43.72	0.287
7.	47.16	0.290
8.	49.26	0.293
9.	53.36	0.295
10.	57.49	0.299

The variation of thermal conductivity with temperature is shown by Fig. 4.8. And the generalized polynomial equation of thermal conductivity with temperature for ethylene glycol and alumina and ethylene glycol based nanofluids is respectively given by equation 4.37 to equation 4.41.

$$k = 0.12717 + 0.54263\ T - 0.09792\ T^2 + 0.00761\ T^3 - 3.26915\times10^{-4}\ T^4 + 8.41318\times10^{-6}\ T^5 - 1.309\times10^{-7}\ T^6 + 1.17058\times10^{-9}\ T^7 - 5.16339\times10^{-12}\ T^8 + 6.85825\times10^{-15}\ T^9 \quad (4.37)$$

$$k = 0.22987 + 0.97097\ T - 0.18672\ T^2 + 0.01543\ T^3 - 7.14601\times10^{-4}\ T^4 + 2.02864\times10^{-5}\ T^5 - 3.61372\times10^{-7}\ T^6 + 3.94366\times10^{-9}\ T^7 - 2.40961\times10^{-11}\ T^8 + 6.307\times10^{-14}\ T^9 \quad (4.38)$$

$$k = 2.77597 + 12.27808\ T - 2.4993\ T^2 + 0.21706\ T^3 - 0.01063\ T^4 + 3.22018\times10^{-4}\ T^5 - 6.18304\times10^{-6}\ T^6 + 7.35362\times10^{-8}\ T^7 - 4.9549\times10^{-10}\ T^8 + 1.44865\times10^{-12}\ T^9 \quad (4.39)$$

$$k = -0.67624 - 2.88609\ T + 0.59547\ T^2 - 0.05178\ T^3 + 0.00252\ T^4 - 7.58071\times10^{-5}\ T^5 + 1.43775\times10^{-6}\ T^6 - 1.6837\times10^{-8}\ T^7 + 1.11395\times10^{-10}\ T^8 - 3.18993\times10^{-13}\ T^9 \quad (4.40)$$

$$k = 0.07321 + 0.29592\ T - 0.07731\ T^2 + 0.00875\ T^3 - 5.4491\times10^{-4}\ T^4 + 2.04503\times10^{-5}\ T^5 - 4.75899\times10^{-7}\ T^6 + 6.73033\times10^{-9}\ T^7 - 5.30396\times10^{-11}\ T^8 + 1.7875\times10^{-13}\ T^9 \quad (4.41)$$

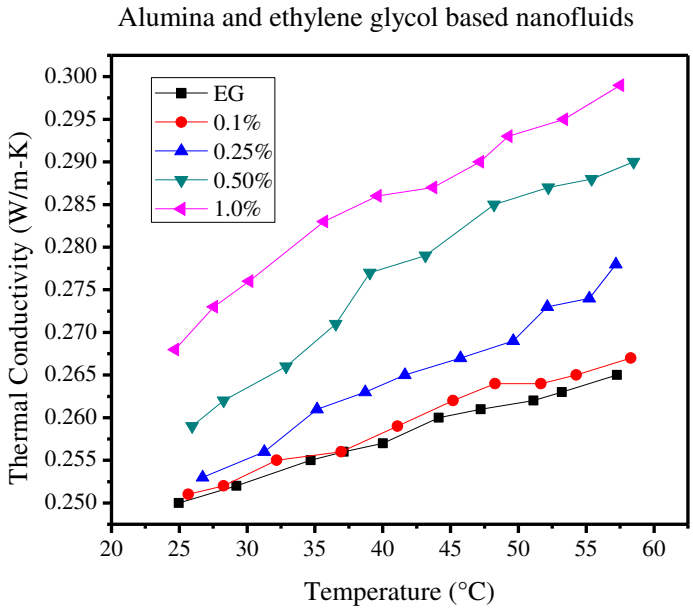

Fig 4.8: Variation of thermal conductivity with temperature

It can be seen from the Fig 4.8, that at ambient temperature, with the increase in the concentration of nanoparticles from 0.1% to 1.0%, thermal conductivity of alumina and ethylene glycol based nanofluids increases from 0.40% to 6.71% (i.e. 0.40% for 0.1% concentration, 1.19% for 0.25% concentration, 3.47% for 0.50% concentration and 6.72% for 1.0% concentration) compared to base fluid i.e. ethylene glycol.

And with the increase in temperature, thermal conductivity of alumina and ethylene glycol based nanofluids increases. From 25 °C to 60 °C, thermal conductivity increases by 6.0% for 0.1% concentration, 9.0% for 0.25% concentration, 10.69% for 0.50% concentration and 10.36% for 1.0% concentration.

4.4.3 Distilled water and ethylene glycol based nanofluids

The thermal conductivity of distilled water (75%) and ethylene glycol (25%), 0.1%, 0.25%, 0.50% and 1.0% volume fractions of alumina and distilled water (75%) and ethylene glycol (25%) based

nanofluids at different temperatures is given by Table 4.23 to Table 4.27. The variation of thermal conductivity with temperature is shown by Fig. 4.9. And the generalized polynomial equation of thermal conductivity with temperature for distilled water (75%) and ethylene glycol (25%) and alumina and distilled water (75%) and ethylene glycol (25%) based nanofluids is respectively given by equation 4.42 to equation 4.46.

Table 4.23: Thermal conductivity of distilled water (75%) and ethylene glycol (25%)

Sr. No.	Temperature (°C)	Thermal conductivity (W/m-K)
1.	25.69	0.485
2.	28.10	0.487
3.	31.16	0.490
4.	35.19	0.491
5.	38.62	0.492
6.	42.01	0.495
7.	45.11	0.496
8.	49.21	0.498
9.	55.14	0.500
10.	59.24	0.501

Table 4.24: Thermal conductivity of 0.1% alumina and distilled water (75%) and ethylene glycol (25%) based nanofluid

Sr. No.	Temperature (°C)	Thermal conductivity (W/m-K)
1.	25.64	0.487
2.	29.18	0.489
3.	32.05	0.492
4.	34.06	0.494
5.	37.16	0.497
6.	41.18	0.501
7.	46.17	0.505
8.	50.18	0.511
9.	56.28	0.521
10.	59.11	0.525

Table 4.25: Thermal conductivity of 0.25% alumina and distilled water (75%) and ethylene glycol (25%) based nanofluid

Sr. No.	Temperature (°C)	Thermal conductivity (W/m-K)
1.	25.11	0.489
2.	29.13	0.493
3.	33.06	0.497
4.	36.62	0.502
5.	38.19	0.509
6.	42.69	0.514
7.	46.18	0.520
8.	51.27	0.529
9.	56.16	0.535
10.	58.26	0.537

Table 4.26: Thermal conductivity of 0.50% alumina and distilled water (75%) and ethylene glycol (25%) based nanofluid

Sr. No.	Temperature (°C)	Thermal conductivity (W/m-K)
1.	25.29	0.495
2.	28.16	0.499
3.	31.78	0.505
4.	35.86	0.512
5.	39.68	0.519
6.	43.17	0.527
7.	47.19	0.534
8.	51.21	0.542
9.	55.17	0.556
10.	57.11	0.562

Table 4.27: Thermal conductivity of 1.0% alumina and distilled water (75%) and ethylene glycol (25%) based nanofluid

Sr. No.	Temperature (°C)	Thermal conductivity (W/m-K)
1.	25.13	0.504
2.	28.24	0.510
3.	33.29	0.514
4.	37.19	0.524
5.	40.29	0.531
6.	44.13	0.539
7.	48.23	0.548
8.	52.11	0.559
9.	57.21	0.566
10.	58.27	0.572

alumina and distilled water (75%) and ethylene glycol (25%) based nanofluids

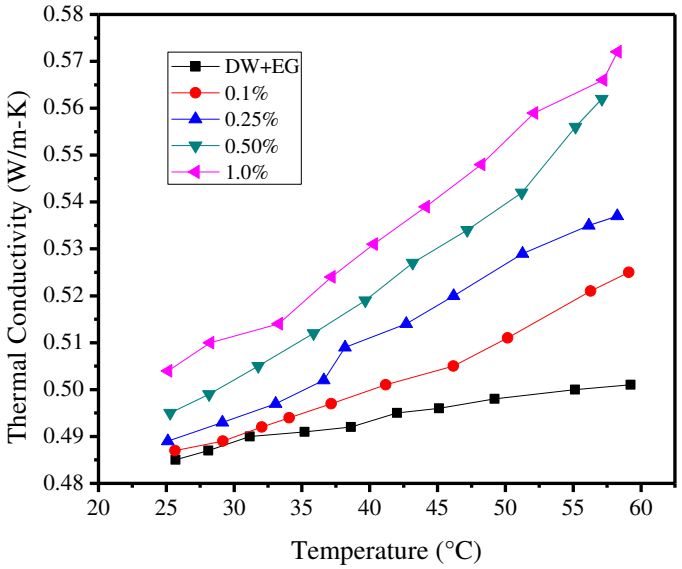

Fig 4.9: Variation of thermal conductivity with temperature

$$k = 0.42933 + 1.81151\ T - 0.37176\ T^2 + 0.0331\ T^3 - 0.00167\ T^4 + 5.19092\times10^{-5}\ T^5 - 1.02376\times10^{-6}\ T^6 + 1.24844\times10^{-8}\ T^7 - 8.60641\times10^{-11}\ T^8 + 2.56799\times10^{-13}\ T^9 \quad (4.42)$$

$$k = -0.23247 - 0.98655\,T + 0.19868\,T^2 - 0.01623\,T^3 + 7.29626\times10^{-4}\,T^4 - 1.98573\times10^{-5}\,T^5 + 3.35058\times10^{-7}\,T^6 - 3.41387\times10^{-9}\,T^7 + 1.90975\times10^{-11}\,T^8 - 4.4453\times10^{-14}\,T^9 \quad (4.43)$$

$$k = 0.0658 + 0.27712\,T - 0.03701\,T^2 + 0.00202\,T^3 - 4.0285\times10^{-5}\,T^4 - 6.87624\times10^{-7}\,T^5 + 5.31638\times10^{-8}\,T^6 - 1.1491\times10^{-9}\,T^7 + 1.14952\times10^{-11}\,T^8 - 4.52994\times10^{-14}\,T^9 \quad (4.44)$$

$$k = -0.12121 - 0.51924\,T + 0.08545\,T^2 - 0.00478\,T^3 + 8.67411\times10^{-5}\,T^4 + 2.15709\times10^{-6}\,T^5 - 1.37308\times10^{-7}\,T^6 + 2.80132\times10^{-9}\,T^7 - 2.68245\times10^{-11}\,T^8 + 1.01619\times10^{-13}\,T^9 \quad (4.45)$$

$$k = 0.73409 + 3.04022\,T - 0.63129\,T^2 + 0.05624\,T^3 - 0.00282\,T^4 + 8.74189\times10^{-5}\,T^5 - 1.71166\times10^{-6}\,T^6 + 2.07051\times10^{-8}\,T^7 - 1.41539\times10^{-10}\,T^8 + 4.18813\times10^{-13}\,T^9 \quad (4.46)$$

It can be seen from the Fig 4.9, that at ambient temperature, with the increase in the concentration of nanoparticles from 0.1% to 1.0%, thermal conductivity of alumina and distilled water (75%) and ethylene glycol (25%) based nanofluids increases from 0.42% to 3.76% (i.e. 0.42% for 0.1% concentration, 0.82% for 0.25% concentration, 2.02% for 0.50% concentration and 3.76% for 1.0% concentration) compared to base fluid i.e. alumina and distilled water (75%) and ethylene glycol (25%).

And with the increase in temperature, thermal conductivity of alumina and distilled water (75%) and ethylene glycol (25%) based nanofluids increases. From 25 °C to 60 °C, thermal conductivity increases by 7.24% for 0.1% concentration, 8.94% for 0.25% concentration, 11.92% for 0.50% concentration and 11.88% for 1.0% concentration.

Important Note:

Fig. 4.7 to Fig. 4.9 demonstrates that the experimental values of thermal conductivity of different nanofluids increases significantly with the fluid temperature. This is because the high fluid temperature intensifies the Brownian motion of nanoparticles and also decreases the viscosity of base fluid. With an intensified Brownian motion, the contribution of microconvection in heat transport increases which results in increased enhancement of the thermal conductivity of nanofluids.

4.5 Particle Size Analysis

The determination of the agglomerate size distribution is of primary importance for proper interpretation of the thermal transport data. Dynamic light scattering (DLS) is a powerful and well-established technique that can be used to determine the size distribution of small particles in solution. This is done by analyzing temporal correlation of the intensity scattered by thermal fluctuations of the particles in solution i.e. Brownian motion.

The study is on 2 parameters, one is scattering intensity also called volume distribution and other is particle size. Means how much percentage of nanoparticles lies in which range. Therefore, The graphs between scattering intensity (%age) or volume distribution and particle size are made.

Another graph is between concentration and particle size of nanofluids sample. Means, with the concentration, how the particle size is getting affected. So, first of all the mean diameter of all the concentrations i.e. 0.1%, 0.25%, 0.50% and 1.0% is found from the first graph and then the graph between concentrations and particle size has been made.

For plotting this graph between concentration and particle size, the mean diameter value of each concentration is required. Therefore, by taking lognormal as a function and doing non linear curve fitting, the mean diameter value can be found out for that particular concentration.

Table 4.28: Particle size with scattering intensity for 0.1% alumina and distilled water based nanofluids

Sr. No.	Particle size (nm)	Scattering intensity (%age)
1.	68.9	26
2.	78.9	44
3.	86.5	58
4.	93.0	70
5.	99.1	80
6.	104.8	87
7.	110.4	93
8.	116.0	97
9.	121.7	99
10.	127.6	100
11.	133.8	99
12.	140.3	97
13.	147.4	93
14.	155.3	87
15.	164.3	80
16.	174.9	70
17.	188.1	58
18.	206.3	44
19.	236.4	26

4.5.1 Distilled water based nanofluids

As discussed previously, all the samples are diluted by 5 times. And 3 ml sample of nanofluid is required. Therefore, 0.5 ml sample of alumina and distilled water based nanofluid sample is taken in the square cell and 2.5 ml of distilled water is added in it. The variation of particle size with scattering intensity for 0.1%, 0.25%, 0.50% and 1.0% volume fractions of alumina and distilled water based nanofluids are given by Table 4.28 to Table 4.31. And the graph between particle size and scattering intensity for all volume fractions is shown by Fig. 4.10.

The mean diameter of all volume fractions of alumina and distilled water based nanofluids is given by Table 4.32. And the graph between concentration and mean diameter is shown by Fig. 4.11.

Table 4.29: Particle size with scattering intensity for 0.25% alumina and distilled water based nanofluids

Sr. No.	Particle size (nm)	Scattering intensity (%age)
1.	80.2	26
2.	91.1	44
3.	99.3	58
4.	106.2	70
5.	112.7	80
6.	118.7	87
7.	124.7	93
8.	130.6	97
9.	136.5	99
10.	142.6	100
11.	149.1	99
12.	155.8	97
13.	163.2	93
14.	171.3	87
15.	180.6	80
16.	191.5	70
17.	204.9	58
18.	223.3	44
19.	253.6	26

Table 4.30: Particle size with scattering intensity for 0.50% alumina and distilled water based nanofluids

Sr. No.	Particle size (nm)	Scattering intensity (%age)
1.	59.9	26
2.	69.4	44
3.	76.7	58
4.	82.9	70
5.	88.8	80
6.	94.3	87
7.	99.8	93
8.	105.3	97
9.	110.8	99
10.	116.6	100
11.	122.7	99
12.	129.2	97
13.	136.3	93
14.	144.1	87
15.	153.2	80
16.	163.9	70
17.	177.3	58
18.	195.9	44
19.	226.9	26

Table 4.31: Particle size with scattering intensity for 1.0% alumina and distilled water based nanofluids

Sr. No.	Particle size (nm)	Scattering intensity (%age)
1.	33.7	26
2.	40.8	44
3.	46.5	58
4.	51.5	70
5.	56.3	80
6.	61.0	87
7.	65.6	93
8.	70.4	97
9.	75.3	99
10.	80.5	100
11.	86.0	99
12.	92.0	97
13.	98.7	93
14.	106.2	87
15.	115.0	80
16.	125.7	70
17.	139.3	58
18.	158.7	44
19.	192.3	26

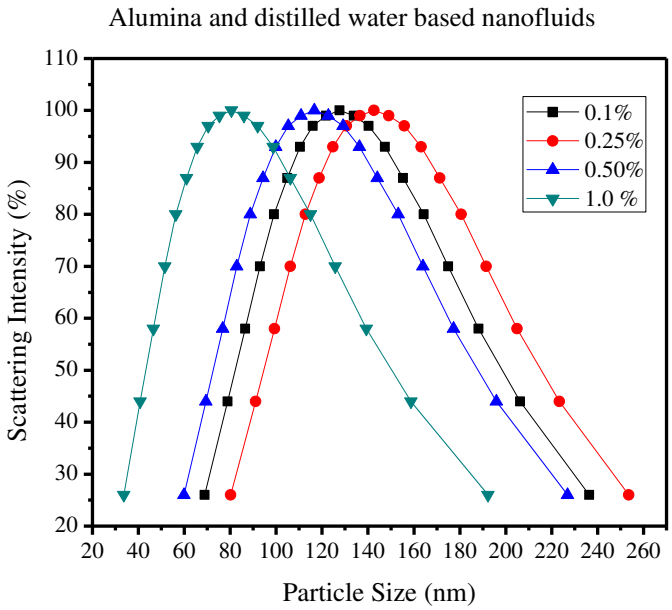

Fig. 4.10: Variation of particle size with scattering intensity

Table 4.32: Mean diameter of alumina and distilled water based nanofluids

Sr. No.	Volume fraction	Mean diameter (nm)
1.	0.1%	146.46
2.	0.25%	160.79
3.	0.5%	136.86
4.	1.0%	106.02

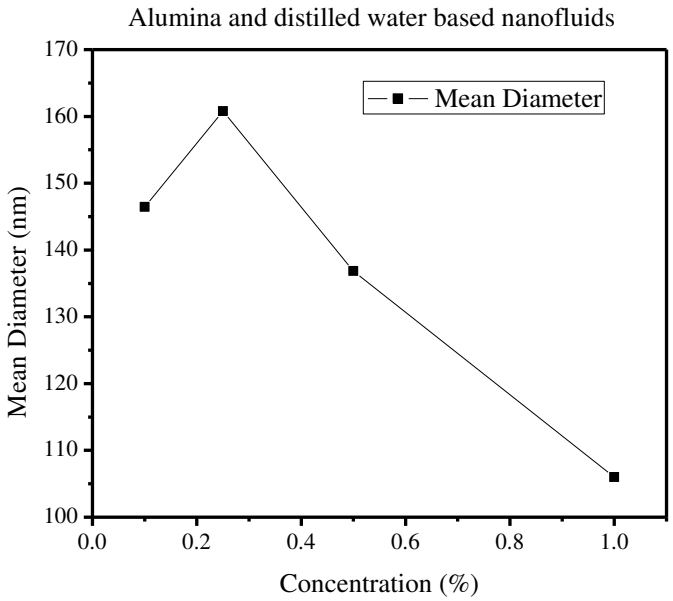

Fig. 4.11: Variation of mean diameter with concentration

4.5.2 Ethylene glycol based nanofluids

Here also 0.5 ml sample of alumina and ethylene glycol based nanofluid sample is taken in the square cell and 2.5 ml of ethylene glycol is added in it. The variation of Particle size with scattering intensity for 0.1%, 0.25%, 0.50% and 1.0% volume fractions of alumina and ethylene glycol based nanofluids are given by Table 4.33 to Table 4.36. And the graph between Particle size and scattering intensity for all volume fractions is shown by Fig. 4.12.

Table 4.33: Particle size with scattering intensity for 0.1% alumina and ethylene glycol based nanofluid

Sr. No.	Particle size (nm)	Scattering intensity (%age)
1.	74.9	26
2.	84.6	44
3.	91.8	58
4.	97.9	70
5.	103.6	80
6.	108.9	87
7.	114.1	93
8.	119.2	97
9.	124.3	99
10.	129.7	100
11.	135.2	99
12.	141.1	97
13.	147.4	93
14.	154.4	87
15.	162.3	80
16.	171.7	70
17.	183.2	58
18.	198.8	44
19.	224.4	26

Table 4.34: Particle size with scattering intensity for 0.25% alumina and ethylene glycol based nanofluid

Sr. No.	Particle size (nm)	Scattering intensity (%age)
1.	64.0	26
2.	73.7	44
3.	81.2	58
4.	87.6	70
5.	93.6	80
6.	99.3	87
7.	104.8	93
8.	110.4	97
9.	116.0	99
10.	121.9	100
11.	128.1	99
12.	134.6	97
13.	141.7	93
14.	149.7	87
15.	158.7	80
16.	169.5	70
17.	182.9	58
18.	201.4	44
19.	232.2	26

Table 4.35: Particle size with scattering intensity for 0.50% alumina and ethylene glycol based nanofluid

Sr. No.	Particle size (nm)	Scattering intensity (%age)
1.	56.0	26
2.	65.1	44
3.	72.1	58
4.	78.2	70
5.	83.8	80
6.	89.2	87
7.	94.5	93
8.	99.8	97
9.	105.2	99
10.	110.8	100
11.	116.7	99
12.	123.0	97
13.	130.0	93
14.	137.7	87
15.	146.5	80
16.	157.1	70
17.	170.2	58
18.	188.5	44
19.	219.1	26

Table 4.36: Particle size with scattering intensity for 1.0% alumina and ethylene glycol based nanofluid

Sr. No.	Particle size (nm)	Scattering intensity (%age)
1.	32.8	26
2.	39.6	44
3.	45.0	58
4.	49.8	70
5.	54.3	80
6.	58.7	87
7.	63.1	93
8.	67.5	97
9.	72.1	99
10.	77.0	100
11.	82.2	99
12.	87.8	97
13.	94.0	93
14.	101.0	87
15.	109.2	80
16.	119.1	70
17.	131.7	58
18.	149.7	44
19.	180.6	26

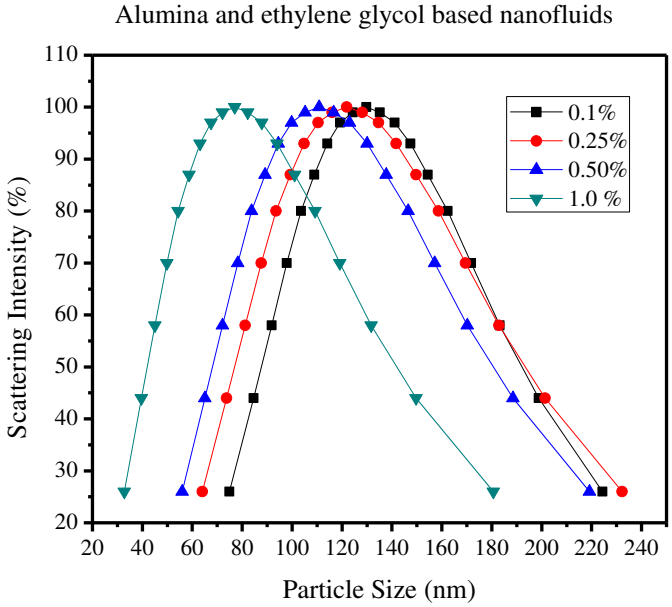

Fig. 4.12: Variation of particle size with scattering intensity

The mean diameter of all volume fractions of alumina and ethylene glycol based nanofluids is given by Table 4.37. And the graph between concentration and mean diameter is shown by Fig. 4.13.

Table 4.37: Mean diameter of alumina and ethylene glycol based nanofluids

Sr. No.	Volume fraction	Mean diameter (nm)
1.	0.1%	144.58
2.	0.25%	141.71
3.	0.5%	131.10
4.	1.0%	100.14

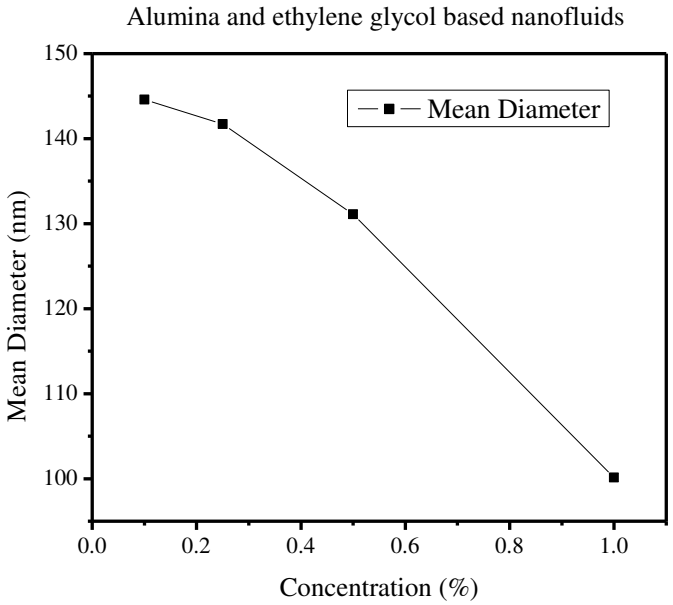

Fig. 4.13: Variation of mean diameter with concentration

4.5.3 Distilled water and ethylene glycol based nanofluids

Here also 0.5 ml sample of alumina and distilled water (75%) and ethylene glycol (25%) based nanofluid sample is taken in the square cell and 0.5 ml ethylene glycol with 2.0 ml of distilled water is added in it. The variation of particle size with scattering intensity for 0.1%, 0.25%, 0.50% and 1.0% volume fractions of alumina and distilled water (75%) and ethylene glycol (25%) based nanofluids are given by Table 4.38 to Table 4.41. And the graph between particle size and scattering intensity for all volume fractions is shown by Fig. 4.14. The mean diameter of all volume fractions of alumina and distilled water (75%) and ethylene glycol (25%) based nanofluids is given by Table 4.42. And the graph between concentration and mean diameter is shown by Fig. 4.15.

Table 4.38: Particle size with scattering intensity for 0.1% alumina and distilled water (75%) and ethylene glycol (25%) based nanofluids

Sr. No.	Particle Size (nm)	Scattering Intensity (%age)
1.	510.4	26
2.	566.7	44
3.	608.3	58
4.	643.3	70
5.	675.2	80
6.	705.0	87
7.	733.8	93
8.	762.2	97
9.	790.6	99
10.	819.9	100
11.	850.2	99
12.	881.8	97
13.	916.0	93
14.	953.4	87
15.	995.5	80
16.	1044.9	70
17.	1105.0	58
18.	1186.1	44
19.	1316.8	26

Table 4.39: Particle size with scattering intensity for 0.25% alumina and distilled water (75%) and ethylene glycol (25%) based nanofluids

Sr. No.	Particle size (nm)	Scattering intensity (%age)
1.	339.0	26
2.	381.5	44
3.	413.3	58
4.	440.2	70
5.	464.9	80
6.	488.1	87
7.	510.6	93
8.	533.0	97
9.	555.5	99
10.	578.7	100
11.	602.9	99
12.	628.3	97
13.	655.8	93
14.	686.2	87
15.	720.4	80
16.	760.9	70
17.	810.4	58
18.	877.8	44
19.	987.8	26

Table 4.40: Particle size with scattering intensity for 0.50% alumina and distilled water (75%) and ethylene glycol (25%) based nanofluids

Sr. No.	Particle size (nm)	Scattering intensity (%age)
1.	189.5	26
2.	220.2	44
3.	243.9	58
4.	264.3	70
5.	283.3	80
6.	301.4	87
7.	319.3	93
8.	337.2	97
9.	355.5	99
10.	374.5	100
11.	394.6	99
12.	415.9	97
13.	439.2	93
14.	465.2	87
15.	495.1	80
16.	530.7	70
17.	575.1	58
18.	636.8	44
19.	740.1	26

Table 4.41: Particle size with scattering intensity for 1.0% alumina and distilled water (75%) and ethylene glycol (25%) based nanofluids

Sr. No.	Particle size (nm)	Scattering intensity (%age)
1.	211.7	26
2.	244.0	44
3.	268.6	58
4.	289.8	70
5.	309.5	80
6.	328.2	87
7.	346.5	93
8.	364.9	97
9.	383.5	99
10.	402.8	100
11.	423.2	99
12.	444.7	97
13.	468.3	93
14.	494.5	87
15.	524.3	80
16.	559.9	70
17.	604.1	58
18.	665.1	44
19.	766.6	26

Alumina and distilled water (75%) and ethylene glycol (25%) based nanofluids

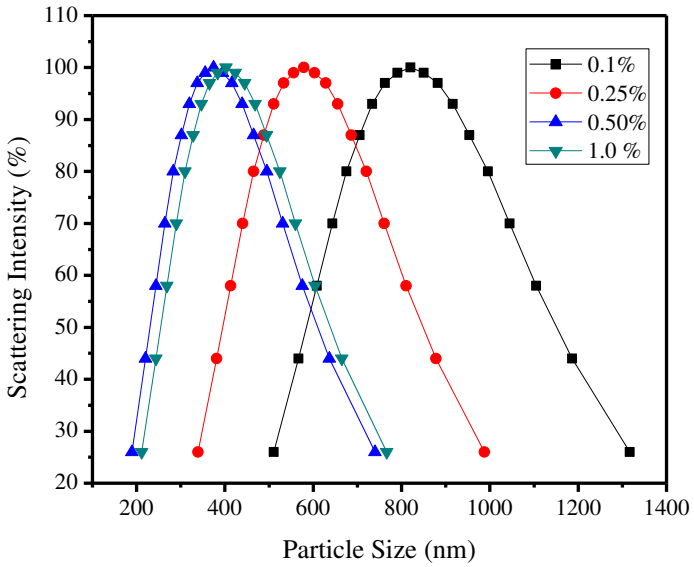

Fig. 4.14: Variation of particle size with scattering intensity

Table 4.42: Mean diameter of alumina and distilled water (75%) and ethylene glycol (25%) based nanofluids

Sr. No.	Volume fraction	Mean diameter (nm)
1.	0.1%	889.33
2.	0.25%	641.78
3.	0.5%	442.99
4.	1.0%	468.01

Alumina and distilled water (75%) and ethylene glycol (25%) based nanofluids

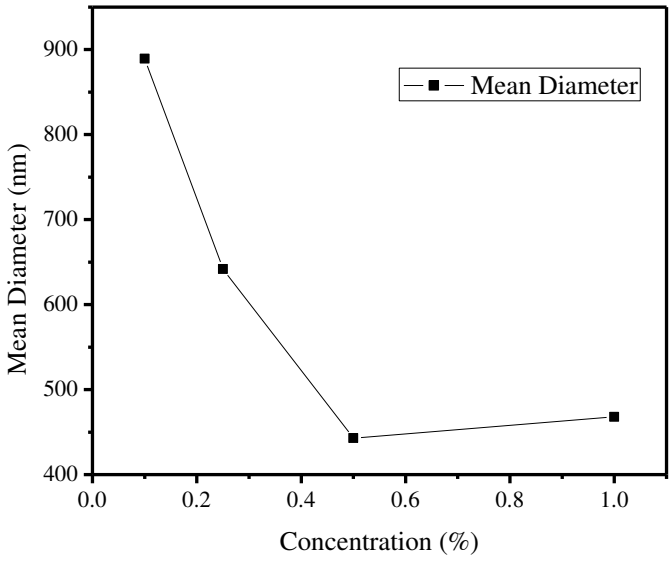

Fig. 4.15: Variation of mean diameter with concentration

Important Note:

The lower concentration (or when the dilution is more), particle agglomeration is more as shown in Fig. 4.11, Fig. 4.13 and Fig. 4.15. Therefore, a number of particles will acts as a giant particle having a large mean diameter. And cluster will form in the nanoparticle fluid suspension i.e. nanofluid, which results in larger particle size. Similarly, in higher concentration, particle agglomeration is less. Therefore, for higher concentration i.e. 1.0%, mean diameter is less than for lower concentration i.e. 0.1%. This is because, in lower concentration, dilution is more than higher concentration.

It can be seen from Fig. 4.11, for distilled water based nanofluids, this trend is not followed from 0.1% to 0.25%. But, from 0.25% to 1.0%, this trend is clearly followed, i.e. for 1.0% concentration; mean diameter is less than from 0.25% concentration.

It is observed from Fig. 4.13, for ethylene glycol based nanofluids, this trend is very nicely followed from 0.1% to 1.0%. Mean diameter falls sharply, as concentration increases.

It is found from Fig. 4.15, for distilled water (75%) and ethylene glycol (25%) based nanofluids based nanofluids, this trend is followed from 0.1% to 0.50%. But, at higher concentration of fluid mixture i.e. 1.0%, mean diameter get stabilized. Means, there is no remarkable change in the mean diameter. Also, in the fluid mixture distilled water (75%) and ethylene glycol (25%) based nanofluids, mean diameter value is very high than distilled water and ethylene glycol based nanofluids. It means that particle agglomeration is high in fluid mixture than pure fluid. Also, it may be because of dust in the sample.

4.6 Conclusion

This chapter discussed all the results coming from density, viscosity and thermal conductivity measurements. Results vary with the concentration as well as with the temperature. Density and viscosity increases with the nanoparticles concentration but they decreases with the temperature. Thermal conductivity increases with nanoparticles concentration as well as with the temperature. Particle size analysis shows that particle agglomeration is more in lower concentration.

Chapter – 5
Conclusions

This chapter explain the conclusions drawn from the work carried out are as follows:

1. Nanofluids, as a kind of new engineering materials consisting of nanometer sized particles and the base fluids, have attracted great attention of investigators for its superior thermal properties and many potential applications.

2. Nanofluids are prepared by two-step process i.e. dispersing the nanoparticles into base fluids. An ultra sonicator is also used to minimize particle agglomeration to get a uniform dispersion and stable suspension. Nanoparticles used are alumina (Al_2O_3) and the base fluids used are distilled water, ethylene glycol and a fluid mixture of distilled water and ethylene glycol. The volume fractions used are 0.1%, 0.25%. 0.50% and 1.0%.

3. Density is measured by pycnometer (specific gravity bottle). A hot plate is used for different temperatures. Results show that density increases with nanoparticles concentration and decreases with temperature. From 0.1 % to 1.0% volume fractions, density increases from 0.9% to 4.0%, 0.75% to 5.6% and 0.76% to 4.04% for alumina and distilled water, alumina and ethylene glycol and alumina and distilled water (75%) and ethylene glycol (25%) based nanofluids, respectively. There is 1% to 2% decreases in density from 30 °C to 90 °C.

4. Viscosity is measured by Ubbelohde viscometer. A hot plate is used for different temperatures. Results show that viscosity increases with nanoparticles concentration and decreases with temperature. From 0.1 % to 1.0% volume fractions, viscosity increases from 4.09% to 60%, 7.89% to 40.30% and 4.96% to 21.33% for alumina and distilled water, alumina and ethylene glycol and Alumina and distilled water (75%) and ethylene glycol (25%) based nanofluids respectively. There is a 58% to 76% decrease in viscosity from 30 °C to 90 °C.

5. Thermal conductivity is measured by KD2 pro thermal property analyzer. A water bath is used for different temperatures. Results show that thermal conductivity increases with nanoparticles concentration as well as with temperature. From 0.1 % to 1.0% volume fractions, thermal conductivity increases from 0.65% to 5.0%, 0.40% to 6.72% and 0.42% to 3.76% for alumina and distilled water, alumina and ethylene glycol and alumina and distilled water (75%) and ethylene glycol (25%) based nanofluids respectively. There is 6% to 12% increase in thermal conductivity from 25 °C to 60 °C.

6. Particle size analysis is done by Brookhaven particle size analyzer. Results show that, towards lower concentration, particle agglomeration is more. It means for higher concentration i.e. 1.0%, mean diameter is lower than for lower concentration i.e. 0.1%. This is because, in lower concentration, dilution is more. Therefore, a number of particles will acts as a giant particle having a large mean diameter. And cluster will form, resulting in large particle size. The variation of mean diameter (nm) with different volume fraction of alumina nanoparticles i.e. 0.1%, 0.25%, 0.50% and 1.0% is given in the following table:

Sr. No.	Volume fraction of alumina nanoparticles, %	Distilled water based nanofluids, nm	Ethylene glycol based nanofluids, nm	Distilled water (75%) and ethylene glycol (25%) based nanofluids, nm
1.	0.1	146.46	144.58	889.33
2.	0.25	160.79	141.71	641.78
3.	0.50	136.86	131.10	442.99
4.	1.0	106.02	100.14	468.01

Future scope of work

1. Few studies have been reported on surface tension of nanofluids with different volume fraction of nanoparticles and with different base fluids. So, work can also be done in this area.

2. Large increases in the critical heat flux of boiling heat transfer have been reported within the past years, and this phenomenon deserves thorough study.

3. Carbon nanotubes (CNT) have very high thermal conductivity around 3000 W/m-K. Therefore, even at very low concentrations of CNT, better results can be obtained. A very few study have been reported on thermophysical properties and convective heat transfer of carbon nanotubes and distilled water, carbon nanotubes and ethylene glycol based nanofluids having different volume fraction ranging from 0.01% to 1.0%. So, work should be done in this area.

Annexure – I

Professor Stephen U. S. Choi

Stephen U. S. Choi is a professor in the Department of Mechanical and Industrial Engineering at the University of Illinois at Chicago. He currently works as a Visiting Fellow at the Korea Institute of Energy Research. He joined Argonne National Laboratory in 1983 and has conducted research primarily in advanced fluids. His work on advanced fluids culminated in the invention of nanofluids. From 1993 to 2006, he led Argonne's nanofluids team as the principal investigator/team leader to develop stable nanofluids with high thermal conductivities. Prior to Argonne, he was a staff scientist at Lawrence Berkeley Laboratory. He received his doctorate in mechanical engineering from the University of California, Berkeley. Recently, Dr. Choi received the University of Chicago Distinguished Performance Award for pioneering scientific achievements and outstanding leadership in nanofluids research. He has published more than 100 technical papers. His current major research interests cover all aspects of nanofluids, including production, characterization, experiments in transport properties and single- and two-phase heat transfer, modelling, and theory.

Annexure-II

SAMPLE CALCULATIONS

Mass of nanoparticles for different concentrations:

For 50 ml of sample, $vol_{total} = 50\ ml$;

$$volume\ fraction = \frac{vol_{nanoparticles}}{vol_{total}} \times 100 \qquad (A)$$

$$volume\ fraction = \frac{\frac{mass_{Al_2O_3}}{\rho_{Al_2O_3}}}{50} \times 100 \qquad (B)$$

(At room temperature, $\rho_{Al_2O_3(99.5\%)} = 3.89\ \ gm/cm^3$)

So, from equation (3.2), for different volume fractions, $mass_{Al_2O_3}$ can be found out as:

For 0.1% volume fraction,

$$0.1 = \frac{\frac{mass_{Al_2O_3}}{3.89}}{50} \times 100$$

$$mass_{Al_2O_3} = 0.1945\ gm$$

For 0.25% volume fraction,

$$0.25 = \frac{\frac{mass_{Al_2O_3}}{3.89}}{50} \times 100$$

$$mass_{Al_2O_3} = 0.48625\ gm$$

For 0.50% volume fraction,

$$0.50 = \frac{\frac{mass_{Al_2O_3}}{3.89}}{50} \times 100$$

$$mass_{Al_2O_3} = 0.9725\ gm$$

For 1.0% volume fraction,

$$1.0 = \frac{\frac{mass_{Al_2O_3}}{3.89}}{50} \times 100$$

$$mass_{Al_2O_3} = 1.945\ gm$$